# Mobility and transport mechanisms of engineered nanoparticles in soils and water-saturated sediments

Vorgelegt von
M. Sc.
Laura Degenkolb

an der Fakultät VI – Planen, Bauen, Umwelt
der Technischen Universität Berlin
zu Erlangung des akademischen Grades

Doktor der Naturwissenschaften
- Dr. rer. nat. –

genehmigte Dissertation

Promotionsausschuss:

Vorsitzende: Prof. Dr. Eva Paton
Gutachter 1: Prof. Dr. Martin Kaupenjohann
Gutachter 2: Prof. Dr. Jan Siemens
Gutachter 3: Dr. Serge Stoll

Tag der wissenschaftlichen Aussprache: 12.11.2020

Berlin, 2021

## Table of contents

Table of contents ..... III
List of Figures ..... VI
List of Tables ..... VII
List of publications ..... VIII
Zusammenfassung ..... IX
Abstract ..... XII
1 General Introduction ..... 1
1.1 Nanoparticles- emerging anthropogenic pollutants ..... 1
1.2 Engineered nanoparticles in the environment ..... 3
1.3 Colloidal stability of nanoparticles in the environment ..... 4
1.4 The fate of nanoparticles in natural soils ..... 6
1.5 Transport and remobilization of nanoparticles in saturated sediment systems ..... 7
1.5.1 Transport and retention mechanisms ..... 7
1.5.2 Remobilization of nanoparticles retained in saturated porous media ..... 11
1.6 Aims of this thesis ..... 12
2 The Variable Fate of Ag and $TiO_2$ Nanoparticles in Natural Soil Solutions — Sorption of Organic Matter and Nanoparticle Stability ..... 14
2.1 Abstract ..... 14
2.2 Introduction ..... 15
2.3 Materials and methods ..... 19
2.3.1 Particle preparation ..... 19
2.3.2 Preparation of soil solutions ..... 20
2.3.3 FT IR analysis of soil solutions ..... 21
2.3.4 Sorption experiments with nanoparticles and soil solution ..... 22
2.4 Results ..... 25
2.4.1 Properties of soil solutions ..... 25
2.4.2 Sorption experiments of nanoparticles and NOM from soil solutions ..... 25
2.5 Discussion ..... 36
2.5.1 Sorption of soil organic matter to $TiO_2$ NP ..... 36
2.6 Conclusion ..... 42
3 Transport and retention of differently coated $CeO_2$ nanoparticles in saturated sediment columns under laboratory and near-natural conditions ..... 44
3.1 Abstract ..... 44
3.2 Introduction ..... 46
3.3 Material and methods ..... 50

3.3.1 Nanoparticles and coatings ..... 50
3.3.2 Properties of the water-saturated sediment system ..... 51
3.3.3 Laboratory column experiments ..... 53
3.3.4 Outdoor column experiments ..... 54
3.3.5 Analytical techniques ..... 56
3.4 Results and Discussion ..... 59
3.4.1 Nanoparticle properties ..... 59
3.4.2 Transport of differently coated $CeO_2$ NP in laboratory column experiments ..... 60
3.4.3 Comparison of laboratory experiments with experiments in a semi-technical scale ..... 70
4 Retention and remobilization mechanisms of environmentally aged silver nanoparticles in an artificial riverbank filtration system ..... 77
4.1 Abstract ..... 77
4.2 Introduction ..... 79
4.3 Material and Methods ..... 83
4.3.1 Nanoparticles ..... 83
4.3.2 Aging procedure ..... 83
4.3.3 Water-saturated sediment columns ..... 84
4.3.4 Design of near-natural column experiments ..... 86
4.3.5 Zeta potential and size of nanoparticles ..... 88
4.3.6 Remobilization experiments ..... 89
4.3.7 Analyses of remobilization samples ..... 90
4.4 Results ..... 97
4.4.1 Nanoparticle properties in the column supernatant ..... 97
4.4.2 Characteristics of the columns ..... 97
4.4.3 Silver breakthrough and retention ..... 98
4.4.4 Remobilization of Ag NP from sediments ..... 100
4.5 Discussion ..... 108
4.5.1 Transformation reactions of Ag NP in aging media and column water ..... 108
4.5.2 Retention mechanisms in riverbank filtration systems ..... 108
4.5.3 Remobilization mechanisms from sediments ..... 111
4.6 Conclusions ..... 116
5 The fate of silver nanoparticles in riverbank filtration systems- The role of biological components and flow velocity ..... 118
5.1 Abstract ..... 118
5.2 Introduction ..... 120
5.3 Material and Methods ..... 124
5.3.1 Experimental design ..... 124

5.3.2 Nanoparticle material ..... 126
5.3.3 Near-natural riverbank filtration experiment ..... 127
5.3.4 Laboratory column experiments ..... 128
5.3.5 Analyses ..... 130
5.4 Results ..... 136
5.4.1 Nanoparticle properties ..... 136
5.4.2 Comparison of pristine and aged sediment column properties ..... 137
5.4.3 Outdoor column experiment ..... 138
5.4.4 Lab column experiments ..... 140
5.4.5 Mass balance of column experiments ..... 143
5.5 Discussion ..... 144
5.5.1 The presence of biological components in aged sediments ..... 144
5.5.2 Nanoparticle reactions in the column system ..... 145
5.5.3 Effect of flow velocity on NP transport and retention ..... 145
5.5.4 The role of biomass for NP retention ..... 147
5.5.5 Nanoparticles in surface waters- a risk for potential drinking water reservoirs? ..... 150
5.6 Conclusions ..... 152
6 Synthesis and Conclusions ..... 153
6.1 Sorption of soil organic matter to nanoparticles ..... 153
6.1.1 Characteristics of natural organic matter ..... 153
6.1.2 Ionic composition ..... 154
6.1.3 The variable fate of nanoparticles in natural soil solutions ..... 155
6.2 Nanoparticle fate in riverbank filtration systems ..... 156
6.2.1 Transport and retention ..... 156
6.2.2 Remobilization potential ..... 161
6.2.3 Retention and remobilization mechanisms ..... 162
6.3 From lab scale to near-natural riverbank filtration systems ..... 164
6.4 Future Research ..... 165
7 References ..... 168
8 Danksagung ..... 183
Appendix ..... A-1

## List of Figures

Fig. 2. 1: Sorption of organic C of farmland soil solution to $TiO_2$ NP ..... 26
Fig. 2. 2: SUVA index of DOC of farmland soil solution before and after sorption to $TiO_2$ NP ... 27
Fig. 2. 3: E2/E4 ratio of DOC of farmland soil solution before and after sorption to $TiO_2$ NP ..... 28
Fig. 2. 4: Sorption of organic C of floodplain soil solution to Ag NP..... 32
Fig. 2. 5: SUVA index of DOC of floodplain soil solution before and after sorption to Ag NP .... 33
Fig. 2. 6: E2/E4 ratio of DOC of floodplain soil solution before and after sorption to Ag NP ..... 33
Fig. 2. 7: Zetapotential of Ag NP in floodplain soil solution ..... 35
Fig. 3. 1: Normalized cerium concentrations in the outflow of the laboratory columns as a function of pore volumes..... 61
Fig. 3. 2: Cerium content in filter sand of the lab columns..... 64
Fig. 3. 3: Cerium concentration in the pore water of two replicate columns (E1 and E2)..... 73
Fig. 3. 4: Cerium content in filter sand of the outdoor columns……74
Fig. 4. 1: Cross section of water-saturated sediment columns…… 86
Fig. 4. 2: Breakthrough of the differently aged Ag NP in 30 cm depth..... 98
Fig. 4. 3: Ag concentration in sand at various depths (0–10, 10–20, 20–30 cm) and for differently aged Ag NP.. ..... 99
Fig. 4. 4: Portion of Ag remobilized by UPW, soil extract, and SR-NOM from sediments applied in the riverbank filtration experiments..... 101
Fig. 4. 5: GFAAS absorbance signal for remobilization samples..... 104
Fig. 4. 6: Correlation of remobilized Al and Ag concentrations measured in the corresponding samples from remobilization experiments. ..... ……..106
Fig. 5. 1: Experimental design of the study..... 125
Fig. 5. 2: a) N concentration in pond water-aged sediments of outdoor lab column experiments and b) diatoms in the upper centimeter of the sediment of outdoor experiments..... 138
Fig. 5. 3: Erratic breakthrough events in a sampling depth of 15 cm in outdoor experiments... 139
Fig. 5. 4: $^{109}$Ag retention profile for the upper 30 cm of sediments for both columns.. ..... 140
Fig. 5. 5: Breakthrough of Ag NP in lab column experiments for both pristine and aged sediment..... 142
Fig. 5. 6: $^{109}$Ag NP retention profiles in pristine and aged sediments……....142
Fig. 6. 1: Schematic summary of transport, retention, and remobilization mechanisms of NP in near-natural saturated sediment systems……163

## List of Tables

Table 1. 1: Summary of flow velocities used in publications of NP transport experiments..... 11
Table 2. 1: Composition of inorganic elements of the soil solutions ..... 21
Table 2. 2: Overview about experimental conditions in the four sorption experiments ..... 23
Table 2. 3: Particle size and zetapotential of $TiO_2$ NP after equilibration with farmland soil solution..... 29
Table 2. 4: Particle size and zetapotential of $TiO_2$ NP after equilibration with floodplain soil solution..... 30
Table 2. 5: Particle size of Ag NP after equilibration with floodplain soil solutions..... 34
Table 3. 1: Nanoparticle properties before and after the experiment and ζ-potential values. .... 51
Table 3. 2: Composition of water used in laboratory column experiments..... 52
Table 4. 1: Remobilization procedure which includes applying mechanical forces and changing hydrochemical conditions……89
Table 4. 2: Atomization delay and average size of Ag NP in samples of remobilization experiment ..... 103
Table 4. 3: Results of SP-ICP-MS measurements of selected samples.. ..... 107
Table 5. 1: Background ion and NP concentration of the mobile phase of lab and outdoor column experiments ..... 125
Table 5. 2: Recovery of Ag in sediments of column experiments ..... 143
Table 6. 1: Transport, retention, and remobilization mechanisms occurring in near-natural, saturated sediment systems ..... 163

**List of publications**

Chapter 2: Degenkolb, L., Kaupenjohann, M., Klitzke, S., 2019. The Variable Fate of Ag and TiO2 Nanoparticles in Natural Soil Solutions—Sorption of Organic Matter and Nanoparticle Stability. Water, Air, & Soil Pollution 230. https://doi.org/10.1007/s11270-019-4123-z

Chapter 3: Degenkolb, L., Dippon, U., Pabst, S., Klitzke, S., 2019. Transport and retention of differently coated CeO2 nanoparticles in saturated sediment columns under laboratory and near-natural conditions. Environmental Science and Pollution Research 26, 15905–15919. https://doi.org/10.1007/s11356-019-04965-x

Chapter 4: Degenkolb, L., Metreveli, G., Philippe, A., Brandt, A., Leopold, K., Zehlike, L., Vogel, H.-J., Schaumann, G.E., Baumann, T., Kaupenjohann, M., Lang, F., Kumahor, S.K., Klitzke, S., 2018. Retention and remobilization mechanisms of environmentally aged silver nanoparticles in an artificial riverbank filtration system. Sci. Total Environ 645. 192-204. https://doi.org/10.1016/j.scitotenv.2018.07.079 0048-9697

Chapter 5: submitted to Science of The Total Environment, meanwhile published as: Degenkolb, L., Leuther, F., Lüderwald, S., Philippe, A., Metreveli, G., Amininejad, S., Vogel, H.-J., Kaupenjohann, M., Klitzke, S., 2020. The fate of silver nanoparticles in riverbank filtration systems — The role of biological components and flow velocity. Science of The Total Environment 699, 134387. https://doi.org/10.1016/j.scitotenv.2019.134387

## Zusammenfassung

Nanopartikel (NP) finden aufgrund ihrer vielversprechenden und einzigartigen Eigenschaften zunehmend in der Industrie und in Alltagsprodukten Einsatz. Diese speziellen Eigenschaften beruhen auf ihrer Größe von unter 100 nm und der damit verbundenen großen Oberfläche und hohen Reaktivität. Gelangen sie bei ihrer Herstellung oder Verwendung in die Umwelt, stellen sie gegebenenfalls ein Risiko für Ökosysteme und Lebewesen dar. Aus diesem Grund sollte ihr Eintrag in die Umwelt, stattfindende Transport- und Umwandlungsprozesse sowie daraus erwachsende Folgen für Ökosysteme detailliert untersucht werden, ehe höhere Umweltkonzentrationen auftreten.

Im Rahmen der vorliegenden Dissertation wurde die Umwandlung und Mobilität von Nanopartikeln im Boden und in wassergesättigten Systemen untersucht. Die wesentlichen physiko-chemischen Prozesse, die zur kolloidalen Stabilisierung von NP in diesen Systemen führen, wurden erforscht. Zudem stand die Untersuchung von Rückhaltemechanismen in Uferfiltrationssystemen im Vordergrund, da die Uferfiltration ein wichtiger Prozess in der Trinkwasseraufbereitung ist. Der Einfluss von Eigenschaften natürlicher Bodenlösungen wie Quantität und Qualität der organischen Substanz sowie Konzentration (multivalenter) Kationen auf die kolloidale Stabilität von Silber (Ag)- und Titandioxid ($TiO_2$) NP wurde anhand von Batchexperimenten erforscht. Die Untersuchung von wichtigen Retentionsmechanismen für den Rückhalt von Cerdioxid ($CeO_2$)- und Ag NP fand in kleinskaligen Laborsäulenversuchen statt. In naturnahen Uferfiltrationssystemen wurde die Wirksamkeit dieser Mechanismen dann in komplexeren Systemen und über längere Zeiträume überprüft.

Die Ergebnisse der Dissertation zeigen deutlich, dass Nanopartikel trotz ihrer gemeinsamen geringen Größe sehr unterschiedlichen Transformationsprozessen in der Umwelt unterliegen. Je nach Oberflächeneigenschaften unterscheidet sich Art und Menge der sorbierten organischen Substanz, die wiederum entscheidend für die kolloidale Stabilität und damit Mobilität der NP ist. Die Anwesenheit multivalenter Kationen, insbesondere Kalzium ($Ca^{2+}$), führt jedoch auch bei Anwesenheit unterschiedlicher organischer Coatings zur starken Aggregierung der NP. Kalzium und gelöste organische Substanz spielen auch für Transportprozesse in wassergesättigten porösen Medien eine wichtige Rolle: Während $Ca^{2+}$ zur verstärkten Anhaftung von NP an Sedimentoberflächen führt, fördern organische Coatings die sterische Abstoßung zwischen Partikeln und Oberflächen. Insbesondere NP mit (synthetischen) Coatings, die eine geringe Anfälligkeit für $Ca^{2+}$-Verbrückungen aufweisen, können in gesättigten Sedimenten über größere Distanzen transportiert werden. Neben diesen Eigenschaften der mobilen Phase sind aber auch hydrologische Faktoren und Eigenschaften der stationären Phase von Bedeutung. In abiotischen, definierten Laborsystemen sind vor allem Wechselwirkungen mit gegensätzlich geladenen Sorptionsplätzen der Festphase wie Eisenoxiden und Tonmineralen für den Rückhalt von NP verantwortlich In natürlichen Systemen dagegen bieten biologische Oberflächen wie Biofilme, Pflanzen und abgestorbene Organismen vielfältige Möglichkeiten für die Wechselwirkung mit NP. Hier kann auch eine Erhöhung der Fließgeschwindigkeit den Transport nicht verstärken. Dies führt zu einer geringen Wahrscheinlichkeit des NP-Transports in natürlichen wassergesättigten, porösen Medien wie Uferfiltrationssystemen. Stattdessen kommt es in den meisten Fällen zur Akkumulation von NP in oberflächennahen Sedimenten. Diese wiederum sind Änderungen von Umweltbedingungen ebenso wie hoher biologischer Aktivität ausgesetzt, was sowohl zu mechanischen als auch hydrochemischen Änderungen führen kann. In diesem Fall besteht das Risiko einer

Remobilisierung der zurückgehaltenen Nanopartikel, die vor allem durch Co-Mobilisierung mit natürlichen Kolloiden hervorgerufen und durch mechanische Scherkräfte sowie bei Anwesenheit organischer Makromoleküle verstärkt wird.

Die in der Dissertation erbrachten Ergebnisse weisen auf eine geringe Mobilität von NP in Böden und wassergesättigten Sedimenten hin. Durch die ubiquitäre Präsenz von Kationen aggregieren NP in Böden schnell. Nur in Bodenlösungen mit geringer Ionenstärke scheinen NP auch für längere Zeit stabil und damit mobil zu sein. Für Uferfiltrate als potenzielle Trinkwasserressource scheinen NP eine geringe Gefahr darzustellen, solange sie in den derzeit beobachteten niedrigen Konzentrationen vorliegen. Dennoch können stabile organische Coatings, höhere Fließgeschwindigkeiten und wachsende Mengen von eingetragenen NP zum verstärkten Transport in tiefere Sedimentschichten beitragen. Insbesondere wenn ein geschädigtes Ökosystem nicht ausreichend Retentionsplätze in Biofilmen und organischen Ablagerungen bietet, ist ein Durchbruch von NP möglich. Durch den Co-Transport von NP mit natürlichen Kolloiden wird zudem präferentiellen Fließwegen eine hohe Bedeutung im NP-Transport zukommen. Die bislang beobachtete starke Akkumulation von NP in oberflächennahen Sedimentschichten kann zu weiteren Gefahren für Ökosysteme führen wie die Aufnahme von NP durch Weidegänger und dadurch eine potentielle Akkumulation im Nahrungsnetz.

Alles in allem sollte der zunehmende Eintrag von NP in die Umwelt kritisch beobachtet werden und zukünftige Untersuchungen müssen vor allem auf naturnähere Systeme fokussiert sein, um bisher erforschte Prozesse und Mechanismen in komplexeren Systemen zu überprüfen.

**Abstract**

Due to their promising and unique properties, nanoparticles (NP) are increasingly being used in industry and in everyday products. Their special properties are based on their size of less than 100 nm and the associated large surface area and high reactivity. If released into the environment during production or use, they may pose a risk to ecosystems and living organisms. For this reason, their input into the environment, transport and transformation processes, and consequences for ecosystems should be studied in detail, before higher environmental concentrations will occur.

In this dissertation, the transformation and mobility of nanoparticles in soil and water-saturated systems were investigated. The main physico-chemical processes leading to colloidal stabilization of NP in these systems were uncovered. In addition, retention mechanisms in bank filtration systems were analyzed, as bank filtration is an important process in drinking water production. The influence of properties of natural soil solutions such as quantity and quality of organic matter and concentration of (multivalent) cations on the colloidal stability of silver (Ag) and titanium dioxide ($TiO_2$) NP was investigated by batch experiments. In small-scale laboratory column experiments, important mechanisms for the retention of cerium dioxide ($CeO_2$) and Ag NP were analyzed. In near-natural bank filtration systems, the effectiveness of these mechanisms was tested in more complex systems and over longer periods of time.

The results of this work clearly show that different nanoparticles, despite their common small size, are subject to very different transformation processes in the environment. Depending on their surface properties, the type and quantity of the sorbed organic substance differs, which in turn is decisive for the colloidal stability and thus mobility of the NP. Nevertheless, the presence of multivalent cations, especially calcium ($Ca^{2+}$),

leads to a strong aggregation of the NP, even if organic coatings differ. Calcium and dissolved organic matter also play an important role for transport processes in water-saturated porous media: While $Ca^{2+}$ leads to increased adhesion of NP to sediment surfaces, organic coatings promote steric repulsion between particles and surfaces. Especially NP with (synthetic) coatings, which are less susceptible to $Ca^{2+}$ bridging, can be transported over long distances in saturated sediments. In addition to these properties of the mobile phase, hydrological factors and properties of the stationary phase are important. In clean laboratory systems, interactions with the solid phase such as iron oxides and clay minerals are mainly responsible for the retention of NP. In natural systems, however, biological surfaces such as biofilms, plants, and dead biomass offer many possibilities for the interaction with NP. Here, even an increase in the flow velocity cannot increase the transport. This leads to a low probability of NP transport in water-saturated, porous media such as bank filtration systems. Instead, NP accumulate in surficial sediments in most cases. These may be exposed to changing environmental conditions as well as high biological activity, which can lead to both mechanical and hydrochemical changes. In this case, there is a risk of NP remobilization, caused mainly by co-mobilization with natural colloids under strong mechanical forces and the presence of organic macromolecules.

The results obtained in the dissertation indicate a low mobility of NP in soil and sediment ecosystems. Due to the ubiquitous presence of cations, NP aggregate rapidly in soils. Only in soil solutions with low ionic strength NP appear to be stable and thus mobile for a longer period of time. For riverbank filtrates as a potential drinking water resource, NP appear to be a low risk as long as they are present in the currently observed low concentrations. Nevertheless, stable organic coatings, higher flow velocities, and increasing amounts of introduced NP can contribute to increased transport into deeper sediment layers. Especially if ecosystems do not provide sufficient

retention sites in biofilms and organic matter, a breakthrough of NP is possible. The co-transport of NP with natural colloids leads to high importance of preferential flow paths for NP transport. The strong accumulation of NP in near-surface sediment layers observed so far may lead to further risks for ecosystems such as the uptake of NP by grazers and thus a potential accumulation in the food web.

All in all, the increasing input of NP into the environment should be critically observed and future investigations must focus on natural systems in order to test previously investigated processes and mechanisms in more complex environments.

# 1 General Introduction

## 1.1 Nanoparticles- emerging anthropogenic pollutants

With the industrialization in the end of the 19th century, the influence of anthropogenic activities on the environment increased. Large amounts of natural resources were used for industrial processes and by-products were released into the environment.

For example, the demand of heavy metals increased with the industrial revolution. Thus, heavy metals were emitted in the environment via mining activities, as particles from traffic or combustion processes, and by irrigation of agricultural fields with waste water. The pedosphere is an important sink for heavy metals which are - in contrast to organic contaminants - persistent so that they accumulate in soils (Han et al., 2001). With the growing use of pesticides to improve agricultural processes and the development of new medical products the number of chemicals reaching waste water and the environment further increased. Substances like DDT and organo-halogenes were spread over the entire globe and soon found even in ecosystems far from anthropogenic activities (Halsall et al., 1998; Pacyna and Oehme, 1988).

It took several decades to become clear that those anthropogenic pollutants do not only have negative impacts on the environment, but also on human health and ecosystem services. Until awareness for this problem reached people's minds and led to political decisions, a number of ecological catastrophes occurred in different areas of the world (e.g. DDT in birds, Carson, 2002). Anthropogenic contaminations may threaten the health of plants, phytoplankton communities, animals, and humans in future years (Hutchinson and Whitby, 1977; Rabinowitz and Wetherill, 1973; Yan, 1979).

In the 1970s, first attempts were developed to establish a precautionary environmental protection to avoid severe environmental consequences by anthropogenic pollutions (Harremoës et al., 2001). However, it was only in the late 1990s that the precautionary principle was used on a worldwide base. In Europe, new regulations, such as the REACH guideline, were formed to protect ecosystems and human health from the growing number of chemicals used in industrial processes.

Aside from pharmaceuticals and biocides as well as microbial contaminants, nanoparticles (NP) form a group of chemicals with unique and promising properties increasingly used in industrial processes (e.g. catalytic processes) and household applications (e.g. cosmetics, clothing, medicines). Exceptionally, these substances are not defined by their chemical nature, but by their size, being smaller than 100 nm in at least one dimension (National Research Council, 2014). The small size leads to very unique properties, such as high reactivity and quantum size effects, so that NP properties dramatically differ from the characteristics of a bulk material with similar chemical composition. For example, titanium dioxide ($TiO_2$) NP are used in sunscreens due to their photoactive properties. In contrast to bulk $TiO_2$, NP are transparent and offer a higher photocatalytic activity due to phase transformation from rutile to anatase in the nano-scale (Auffan et al., 2009).

Since the early 2000s, the fate of NP is increasingly studied by environmental researchers (Sani-Kast et al., 2017) as their production and therefore the risk for their release in the environment increase. Currently, engineered NP concentrations in soils are in the ng $kg^{-1}$ range (Gottschalk et al., 2013), far below any observed effect concentrations (Mueller and Nowack, 2008). The numerous attempts to investigate environmental fate of NP are therefore a positive example for precautionary environmental protection and may be the basis for an early regulation of NP

production and release to avoid any negative consequences on the environment and human health.

To evaluate the risk associated with the introduction of NP in the environment, the interdisciplinary research unit *Internano* was formed. Within this research group, hydrologists, chemists, soil scientists, and ecotoxicologists worked together to assess the fate and effects of NP in the environment. In this frame, my thesis comprises the investigation of NP fate in soils and saturated sediment systems.

## 1.2 Engineered nanoparticles in the environment

During production and use, engineered NP are released into the environment via different pathways that depend on the applications of NP. *Silver NP* for example, are one of the most frequently used nanomaterials (Vance et al., 2015). Due to their antimicrobial properties caused by the release of $Ag^+$ ions, they are included in wound dressings and sportswear (Rai et al., 2009). *Titanium dioxide NP* can be found in self-cleaning façade paints (Kaegi et al., 2008) and sunscreens (Popov et al., 2005). Both $TiO_2$ and Ag NP reach the environment predominantly via household effluents transporting them to waste water treatment plants (Gottschalk et al., 2009). There, the main fraction of NP accumulates in the sewage sludge which may be used as fertilizer for agricultural soils (Weggler-Beaton et al., 2003). A smaller part of NP reaches surface water directly with the waste water effluent. *Cerium dioxide NP* provide a high oxygen storage capacity and an easy transition between two oxidation states ($Ce^{3+}$ and $Ce^{4+}$) which makes them effective catalysts; further applications are the use as polishing agents in the electronic industry and in diesel fuels (Dahle and Arai, 2015). They reach the environment via both diffuse and point sources, such as

car exhausts, landfills and by the application of sewage sludge on soils (Cornelis et al., 2011; Keller and Lazareva, 2014).

As soon as NP are released into the environment they will interact with naturally present substances changing NP surfaces and therefore their colloidal stability. In addition, redox reactions on NP surfaces may change NP properties. For example, Ag NP tend to oxidize under environmentally relevant conditions which leads to (partial) NP dissolution and formation of a silver oxide layer on Ag NP surfaces. Furthermore, Ag as a chalcophile element gets sulfidized under anaerobic conditions (Kaegi et al., 2013). The coating with natural organic matter (NOM) is also well-known to change NP surfaces (Philippe and Schaumann, 2014). Those processes changing NP surface properties without complete loss of the original NP phase can be summarized as “aging processes” (Schaumann et al., 2015). Aging processes will depend on the environment NP get exposed to and result in a high heterogeneity of environmentally aged NP. To predict NP fate in soils and saturated sediments, it is crucial to understand the most relevant aging processes and their effects on NP stability and mobility.

### 1.3 Colloidal stability of nanoparticles in the environment

To understand NP mobility, general knowledge about nano-specific properties leading to colloidal stability of NP suspensions is fundamental. Nanoparticles in suspensions have a high free-energy potential and hence, tend to aggregate with each other or sorb to natural surfaces in the absence of a repulsive energy barrier (Everett, 1988a). Therefore, a low mobility of NP might be expected. However, in the presence of dominating repulsive forces NP can be colloidally stabilized. The

interaction energy between particles or particles and solid surfaces depends on intermolecular and interparticular forces such as (i) van-der-Waals, (ii) electrostatic, and (iii) steric forces (Everett, 1988b). (i) Intermolecular, van-der-Waals forces act only in close proximity of particles. In many cases, they are attractive and particles getting very close to each other will aggregate. (ii) Interparticular, electrostatic forces act on larger scales and are caused by particle surface charge. They lead to the formation of an electrical double layer (EDL) in which counter ions surround the particle surface. The thickness of the EDL is indirectly proportional to the ionic strength of the dispersion medium. (iii) Steric repulsion forces are caused by coating of NP surfaces with mostly organic molecules. They also influence van-der-Waal attraction forces by impeding the approximation of particle surfaces and lead to entropic repulsion by overlapping of coating molecules of different particles (Everett, 1988b).

The sum of attractive and repulsive electrostatic and steric forces induces NP stabilization or aggregation. By the DLVO theory, named after four people that were important for its development in the 1940s (Derjaguin, Landau, Verwey, and Overbeek), electrostatic interaction energies can be quantified. Steric and further electrostatic interaction forces (e.g., hydrogen bonding and entropic contributions) can be included in this quantification by the extended DLVO theory (Grasso et al., 2002).

Overall, the interaction energy between NP or between NP and available surfaces determines the stability of nanoparticle suspensions. This energy depends on intrinsic NP properties (i.e. chemical composition, particle size and shape), but also on characteristics of the surrounding medium (i.e. ionic strength and pH) and the presence of organic molecules adsorbed to particle surfaces.

## 1.4 The fate of nanoparticles in natural soils

To evaluate the risk of NP release into soils the fate of NP in soil environments is of high importance. In contrast to natural surface water, soils exhibit complex matrices which complicate the analysis of NP in these media. Therefore, knowledge about NP fate in soils is scarce. Already in 1990, Beckett illustrated that the surface charge of colloids in the environment is mainly controlled by natural organic matter (NOM) as well as the concentration of divalent cations (Beckett and Le, 1990). However, the interaction of NOM has been shown to cause very different effects on NP stability depending on various factors, such as NP surface charge, pH and ionic strength of the soil solution as well as properties of the adsorbed NOM (Gallego-Urrea et al., 2014; Liu et al., 2013).

Sorption mechanisms of NOM to NP have been extensively studied using model substances such as humic acids (HA) or fulvic acids (FA). Those studies pointed out, that small organic molecules are thermodynamically favored to adsorb first on NP surfaces. By time, they are replaced by larger molecules as those are entropically favored, so that medium- to large-sized molecules are expected to be primarily adsorbed onto NP surfaces (Vermeer et al., 1998). This may lead to enhanced NP stability as larger molecules add steric repulsion forces to NP surface energy. Nevertheless, there is a lack of studies using more realistic organic matter that could validate results gained by the use of model substances.

In a natural soil, not only NOM, but also inorganic ions are present to influence NP stability by compressing the EDL. Although stability studies consistently show the destabilizing effect of multivalent cations such as $Ca^{2+}$ and $Mg^{2+}$ to NP (Gmür et al., 2016) contrasting observations have been made in the presence of both cations and NOM. On the one hand, NOM mitigates the destabilizing effect of cations by steric stabilization; on the other hand, NOM-coated NP can be destabilized to larger

degrees when $Ca^{2+}$ is added, because of bridging complexation between coated NP (Akaighe et al., 2012; Chen et al., 2007). Furthermore, the ionic strength affects sorption processes of NOM to NP surfaces in various ways (Seijo et al., 2009): With increasing ionic strength, electrostatic repulsion between adsorbed organic molecules is lowered so that an increasing amount of NOM can adsorb to NP surfaces. At very high ionic strength, however, homoaggregation of NOM molecules competes with the sorption of NOM to NP surfaces, thereby reducing NOM available for sorption to NP.

Those observations highlight the complexity of processes affecting NP surface properties in natural soils. A prediction of NP fate is therefore challenging and gets even more complicated acknowledging that NP consist of a variety of core materials, industrial coatings, and size classes which might react differently in similar soils. The variable fate of different kinds of NP in soil solution with varying NOM and cation properties and the mechanisms of soil organic matter sorption are therefore still under debate.

## 1.5 Transport and remobilization of nanoparticles in saturated sediment systems

### 1.5.1 Transport and retention mechanisms

Saturated sediments serve as viable natural filters for surface waters, preventing the transport of various contaminants into groundwater. Due to this, induced bank filtration is used for the production of drinking water being cost-efficient and with low energy demand (Hoffmann and Gunkel, 2011). The potential for NP removal in these systems should be well-known to estimate the risk of NP for potential drinking water reservoirs. The cleaning capacity of bank filtration systems for colloidal entities depends mainly on the pore size of sediment systems responsible for mechanical

filtration or straining processes, and the availability of retention sites for physico-chemical interactions of colloids with the stationary phase. By column experiments conducted with different kinds of NP, the following main factors governing NP transport and retention in saturated porous systems were identified (e.g., by Bradford et al., 2011, 2006, 2002; Cornelis et al., 2013; Sagee et al., 2012)

(I) Intrinsic NP properties:

As the definition of NP is based on particle size instead of material properties, a wide range of chemical substances can be included in this definition. Therefore, surface properties and, hence, NP transport depend on the chemistry of the nanomaterial itself (Ben-Moshe et al., 2010; Lecoanet et al., 2004). Additionally, NP size determines the transport and retention of particles (Tripathi et al., 2012): the smaller the particles the more they are affected by Brownian motion and hence diffusion instead of advection processes. The surface charge of NP not only influences NP colloidal stability, but also their interaction with the stationary phase of a porous system. Therefore, also particle coatings- whether of industrial or natural origin- are of high importance for the transport of NP (Zhang and Zhang, 2014).

(II) The mobile phase of the saturated porous medium:

Hydrochemical properties such as pH and ionic strength affect adsorption processes of NP to solid surfaces. For example, increasing ionic strength of the surrounding medium compresses the EDL and therefore induces NP aggregation followed by sedimentation or NP adsorption to sediments, reducing the transport of NP. In addition, NOM which is ubiquitously present in the environment has been observed to enhance NP transport in column experiments by steric repulsion between NP and the stationary phase (Chen et al., 2012). The flow velocity of the mobile phase is another

important parameter affecting NP transport in the porous system: at low flow rate, NP residence time in the pore space increases, hence offering more possibilities for NP interaction with the stationary phase and diffusion in small pores. Therefore, retention increases with decreasing flow rate.

(III) The properties of the stationary phase:

When transported through a water-saturated porous system, NP interact with the solid-water-interface (SWI). Nanoparticles can be adsorbed to sediment grains in a stable primary energy minimum or might be reversibly attached in a secondary energy minimum (Franchi and O'Melia, 2003; Hahn and O'Melia, 2004). Reversible attachment leads to slow NP transport through the column potentially resulting in a retarded breakthrough (Zhang et al., 2016). Interaction in a primary minimum might not be reversible and leads to retention of NP in the sediment systems (Tufenkji and Elimelech, 2004). Aside from physico-chemical interactions, mechanical filtration and straining can retain NP. In the former case, NP or NP aggregates have a higher diameter than the pores so that infiltration is blocked. In the latter case, NP are retained in dead pore ends or in sediment-sediment contact zones. Chemical and physical surface heterogeneities also increase NP retention as they offer favorable attachment sites even in the presence of overall repulsive forces and lead to particle entrapment (Shen et al., 2010).

These parameters affecting NP transport in saturated sediment systems have mainly been identified by well-defined laboratory experiments (e.g., Braun et al., 2015; Petosa et al., 2013; Sagee et al., 2012). Studies in riverbank filtration systems, however, are lacking in the literature. Several authors pointed out that in more complex systems, NP transport differs from what is found in the lab. For example,

Emerson et al. (2014) stated that NP transport might be overestimated in the lab after conducting medium-scale experiments in soils. Furthermore, biological retention mechanisms play an important role in the bank filtration process (Hoffmann and Gunkel, 2011), but are not often considered in NP transport experiments. Tripathi et al. (2012) observed the importance of biofilms on NP retention in sand columns, and mesocosm studies support these findings as NP accumulate in biological components, such as microorganisms and plants (Avellan et al., 2018; Nevius et al., 2012). Although it will be of high importance for NP risk assessment, knowledge about the role of biological material for NP transport in near-natural riverbank filtration systems is still insufficient.

As another important factor for NP retention in saturated sediments, different flow velocities were identified to result in different NP breakthrough (Braun et al., 2015). At high flow rates (e.g., 3 m $d^{-1}$, Braun et al., 2015) NP were transported almost unretarded comparable to a conservative tracer, whereas reducing flow velocities led to partial NP retention on sediment surfaces. Applied flow velocities for most NP studies are generally between 3 and 20 m $d^{-1}$ (Table 1. 1), while flow rates in saturated fine sand range between 0.5 and 1.5 m $d^{-1}$ (Kunkel and Wendland, 1997) and flow rates for riverbank filtration at the river Rhine were observed to be 0.25-3.5 m $d^{-1}$ (Schubert, 2002). In the lower flow range, however, NP transport studies are rarely conducted. Nevertheless, NP transport mechanisms might vary significantly when flow rates decrease. For example, NP transport will be strongly affected by diffusion processes instead of advection. This might cause significant changes in NP transport in the lower flow regime (i.e. <1 m $d^{-1}$; Chang and Chan, 2008), which has not sufficiently been investigated, experimentally.

**Table 1. 1:** Summary of publications of NP transport experiments: Darcy flux is mostly larger than 1 m $d^{-1}$.

| Publication | Darcy-Flux [m $d^{-1}$] | Medium | NP material | NP concentration [mg $L^{-1}$] |
|---|---|---|---|---|
| Sagee et al. (2012) | 9.504 | soil | Ag | n.d.[1] |
| | 2.448 | | nm300 | |
| Braun et al. (2015) | 0.04752 | loamy sand | Ag | 60 |
| | 2.88 | | | |
| | 0.0216 | soil | | |
| Cornelis et al. (2013) | 8.1 | soil | Ag | 1.7 |
| El Badawy et al. (2013) | 15.2 | quartz sand | Ag | 10 |
| Lin et al. (2011) | 17.28 | glass beads | Ag | 1.35 |
| Taghavy et al. (2013) | 14.4 | sand | Ag | 3 |
| Petosa et al. (2013) | 2.9 | quartz, loamy sand | $CeO_2$ | 100 |
| Sun et al. (2015) | 12 | silica sand | ZnO | 34-430 |
| | 3.6-4.6 | soil | | |
| Li et al. (2013) | 55.7 | dirty and clean sand | Ag, $CeO_2$, $TiO_2$, ZnO | Ag: 45 |

[1] n.d. = not defined

### 1.5.2 Remobilization of nanoparticles retained in saturated porous media

While transport and retention mechanisms in near-natural saturated sediment systems have not been studied in detail, so far, an accumulation of NP in upper soil layers and aquatic sediments was observed in several studies (Espinasse et al., 2018; Geitner et al., 2018; Lowry et al., 2012). On the one hand, this reduces the possibility of a translocation of NP in deeper soil or sediment layers. On the other hand, surficial soils and sediments are exposed to environmental changes such as increased flow velocities in rivers, bioturbation, or heavy rain events, which might lead to changing hydrochemical and physical conditions. This may affect the stability of NP retained in these upper sediments and potentially lead to a remobilization of originally retained NP. By mimicking heavy rain events, Makselon et al. (2018) observed only minor remobilization of Ag NP in soils. Also, Hoppe et al. (2015) did not observe remobilization of Ag NP in farmland soils. However, laboratory studies by

Metreveli et al. (2015) illustrated that NP disaggregation is induced by reducing ionic strength and addition of NOM when strong mechanical forces are present. For NP attached to sediments of a riverbank filtration system, the remobilization potential has not yet been studied.

## 1.6 Aims of this thesis

The main drivers for an environmental risk associated with NP release into soils and saturated sediments are NP mobility (i.e. the possibility to be transported over large distances and between environmental compartments) as well as NP toxicity (i.e. ecotoxicity and toxicity to humans). Mobility is connected to NP stability which is strongly related to NP surface properties (e.g. surface charge and coating). Stable NP might be transported over large distances whereas aggregation and sedimentation immobilize NP. While ecotoxicity studies were conducted in other work packages of the *Internano* project, this thesis assesses the stability and transport of NP in soils and saturated sediments to evaluate the possibility of NP exposure in different environmental compartments, such as soils and the saturated zone (i.e. riverbank filtrates). Therefore, the study focuses on the following two main questions:

### I) How do natural soil solutions affect the stability of different NP?

As stability is predominantly influenced by natural organic matter as well as the presence of inorganic ions in soils, chapter 2 focuses on sorption processes of soil organic matter from different natural soil solutions and their effect on the stability of Ag and $TiO_2$ NP.

II) Which factors are responsible for NP retention in saturated sediments and how can NP be remobilized?

This question was answered by transport studies under laboratory as well as near-natural conditions. The effect of different environmental media in the presence of synthetic and natural organic coatings on $CeO_2$ NP transport was investigated (chapter 3). Furthermore, retention and remobilization mechanisms of environmentally aged Ag NP were analyzed in chapter 4. To gain detailed information on two important retention mechanisms (i.e. the role of dead and living organic matter, and the effect of flow velocity) Ag NP transport in saturated sediments under lab scale and near-natural conditions was evaluated (chapter 5).

Experiments were undertaken in batch studies and lab-scale columns. In addition, the facility for the simulation of riverbank and slow sand filtration (SIMULAF) of the Federal Environment Agency, Berlin, was used to value results from lab experiments in the context of a more complex, environmentally relevant system. Overall, this thesis adds knowledge about NP fate in soils and saturated sediments and evaluates the effectiveness of riverbank filtration in retaining NP under a set of different conditions (i.e. different flow velocity, ionic strength, and NP materials and organic coating).

# 2 The Variable Fate of Ag and $TiO_2$ Nanoparticles in Natural Soil Solutions — Sorption of Organic Matter and Nanoparticle Stability

Authors: Laura Degenkolb, Martin Kaupenjohann, Sondra Klitzke

Post-print, published in “Water, Air and Soil Pollution”, original publication can be found under https://doi.org/10.1007/s11270-019-4123-z

## 2.1 Abstract

Engineered nanoparticles (NP) like Ag and $TiO_2$ offer unique properties for various applications. Thus, the entry of the NP in soil environments is expected to increase in the future due to their growing industrial use. To avoid potential hazards due to these anthropogenic products, NP behavior in the environment should be well understood. In natural soil solutions, we investigated NOM adsorption onto Ag and $TiO_2$ NP and its influence on NP colloidal stability.

Therefore, we extracted soil solutions from a floodplain soil (Fluvisol) and a farmland soil (Cambisol) differing in NOM quality and inorganic ion concentration. We measured the amount of adsorbed organic carbon as well as changes in aromaticity and molecular weight of NOM upon adsorption onto NP. Additionally, the size and zetapotential of NP in both soil solutions were investigated.

We observed that the highly hydrophilic NOM of floodplain soil solution rich in inorganic ions strongly adsorbed to Ag but not to $TiO_2$ NP. Instead, sorption to $TiO_2$ NP was observed for the more hydrophobic NOM of the farmland soil with low ionic strength which did not sorb to Ag NP. These differences had a strong effect on NP stability, leading to Ag NP destabilization in case of floodplain soil solution and $TiO_2$ NP stabilization in the presence of farmland soil solution.

Our results point out the necessity of studies in more complex systems and suppose that oxic and metallic NP might show very different fate depending on the environment they are exposed to.

## 2.2 Introduction

The use of engineered inorganic nanoparticles (NP) has been growing over the last decades because of the unique physical, chemical and optical properties of nano-sized materials (Auffan et al. 2009). Applications vary from electronic devices over medical use to cosmetic products. This leads to an increased exposure of those materials in the environment where adverse effects on ecosystems or human health may be expected making it necessary to study the behavior of NP in more detail.

Two of the industrially most widely used NP are silver (Ag) and titanium dioxide ($TiO_2$) NP due to their antimicrobial properties as well as high refractive index and UV resistance, respectively (Gottschalk et al. 2013). Several studies about NP showed that they enter soils via flooding events, irrigation activities or application of sewage sludge (Gottschalk et al. 2009; Lecoanet et al. 2004; Wigger et al. 2015). In soils especially pH, natural organic matter (NOM) and (divalent) cations have a strong influence on the fate and stability of particles (Philippe und Schaumann 2014; Thio et al. 2012; Van Hoecke et al. 2011).

One of the main questions regarding nanoparticles' fate in soils is whether the particles remain colloidally stable and keep acting as NP or whether they aggregate and sediment on soil particles. In this context, NOM often acts as stabilizing agent for NP as it sorbs to particle surfaces and enhances steric and electrostatic repulsion forces between particles themselves or between NP and soil particles reducing homo- and heteroaggregation (Klitzke et al. 2015; Stankus et al. 2011). Contrarily, cations in the soil solution are known to compress the electrostatic double layer of colloids, thereby reducing the energy barrier between the particles which leads to aggregation (for example French et al. 2009). Especially calcium (Ca) and other divalent cations specifically interact with nanoparticles forming bridges between

particles and soil surfaces (Baalousha et al. 2013; Stankus et al. 2011). Both of these effects lead to colloidal destabilization and aggregation of NP.

Numerous research studies focused either on NOM or Ca affecting NP in the environment. Under natural conditions, however, both act in combination making it difficult to predict NP behavior. Additionally, when investigating the effect of NOM, model substances such as humic and fulvic acids are often used as representatives for soil organic matter (Sani-Kast et al. 2017). This of course, helps to mechanistically understand the processes taking place between organic molecules and NP, but does not provide any information on natural systems. One general assumption of these studies is that short-chained, low molecular weight (LMW) organic matter (OM) is kinetically favored to adsorb first. Over time, it is replaced or covered by high molecular weight (HMW) OM as this is thermodynamically favored because of entropic reasons (Vermeer et al. 1998). In total, this observation is assumed to lead to a preferential sorption of medium- or large-sized OM on NP surfaces. For $TiO_2$ NP it was shown that organic matter rich in aromatic compounds is sorbed to a larger degree than non-aromatic molecules (Y. Li et al. 2015). The HMW organic matter also seems to have stronger stabilizing effects against aggregation than LMW organic matter (Louie et al. 2015). Most likely, this is due to the stronger steric stabilization effect of these molecules, as it becomes more relevant in solutions with higher ionic strength when electrostatic stabilization plays a minor role.

The presence of cations also affects the adsorption of organic matter on colloid surfaces. In a model study by Seijo et al. (2009), it has been shown that a higher amount of fulvic acid (FA) molecules adsorbs to colloids at higher ionic strength while monolayer adsorption is often observed for low ionic strength. This is caused by reduced electrostatic repulsion between adsorbed molecules with increasing ionic strength. But when ionic strength exceeds a certain number, the formation of FA

homoaggregates competes with the adsorption process of FA onto colloids. This reduces the amount of FA available for adsorption. Additionally, the conformation of adsorbed organic matter depends on ionic strength: Small, coil-shaped molecules are adsorbed directly on colloid surfaces at low IS while bulky aggregates of organic molecules are formed at higher IS which hinders the adsorption of single molecules (Buffle et al. 1998; Seijo et al. 2009). As ions are ubiquitous in soil systems they will strongly influence the adsorption of organic matter on NP and should therefore be taken into account in sorption studies.

As an example, Klitzke et al. (2015) investigated the influence of soil solution on Ag NP in a more complex system. Surprisingly, they found that short-chained, non-aromatic compounds were sorbed preferentially over long-chained, aromatic components, contradicting most previous studies. The authors attributed this to combined effects of cations and organic molecules and thereby showed the necessity of studies in more complex systems. Our study therefore investigates the effect of natural soil solution on Ag as well as $TiO_2$ NP.

Despite of the numerous studies with different NP, researchers still struggle in making general assumptions on the fate of NP in the environment. Therefore, each NP system has to be studied and described on its own. Our study investigates the influence of soil solution on one metallic (Ag) and one oxic ($TiO_2$) nanomaterial. Two soil solutions differing especially in organic matter and Ca content, originating from a farmland and a floodplain soil (Fluvisol and Cambisol, respectively), were used to study the sorption of organic matter onto NP surfaces. The following hypotheses were tested in batch experiments:

I) Larger dissolved organic carbon (DOC) concentrations will lead to more pronounced preferential sorption of favorable NOM fractions than lower DOC concentrations because sorption-induced fractionation predominantly takes place when the concentration of sorbates exceeds the amount of available sorption sites.

II) Aromatic and medium to high MW OM will be preferentially sorbed over non-aromatic, LMW OM because of larger thermodynamic stability.

III) An increase in ionic strength in soil solution decreases the stabilizing effect of NOM, especially when hydrophilic or LMW OM is adsorbed. The electrostatic hindrance of LMW OM is less effective at high Ca concentrations than the steric stabilization of HMW OM. Hydrophilic NOM has a high charge density which leads to enhanced formation of Ca-bridges between coated NP and therefore destabilization.

We conducted experiments with two soil solutions strongly differing in organic matter quality and inorganic ion concentration. The adsorbed amount of OM from soil solution was quantified by DOC measurements after equilibrating NP in natural soil solution. The aromaticity and molecular weight of adsorbed OM was estimated by UV adsorption analyses. With these measurements we investigated the effect of soil solution (i.e. ionic strength, and quality and quantity of adsorbed OM) on NP stability.

## 2.3 Materials and methods

### 2.3.1 Particle preparation

Silver nanoparticles

Uncoated Ag NP were used for all sorption experiments to avoid interferences of organic coating agents with DOC measurements. Those particles were obtained as powder of 35 nm particles from iolitec nanomaterials, produced by plasma-chemical vapor deposition. Detailed information about Ag NP characteristics are reported by Abraham et al. (2013). To prepare NP suspensions, 40 mg of the powder were dispersed by ultrasonication with an ultrasonic probe (Branson© Sonifier 250) in 40 mL of Millipore water for 68 min with a power of 700 J $mL^{-1}$ (calibrated before each sonication). To remove large particles still undispersed or aggregated, suspensions were filtered through a 0.22 µm polyether sulfone membrane (Syringe filters, Rotilabo®). The concentration of total Ag in the suspensions was measured by inductively coupled plasma- optical emission spectroscopy (ICP-OES, iCAP 6300 duo, Thermo Fisher Scientific) following 24 h of dissolution of particles with 5% $HNO_3$ and shaking on a horizontal shaker. As particle suspensions of uncoated Ag NP are hardly stable, suspensions had to be freshly prepared prior to each sorption experiment and stored for short time scales at 4 °C. The method of powder dispersion leads to variable and very low silver concentrations. Therefore, the applied Ag concentrations in the sorption experiments differ from each other. The amount of sorbed DOC was then re-calculated to mass of silver present in the batches enabling the comparison of the experiments.

Titanium dioxide nanoparticles

Titanium dioxide nanoparticles (P25, Evonik) were prepared at the Institute of Particle Technology in Braunschweig by stirred media milling in an HCl solution. Using a milling time of 8 h followed by ultrasonic bath treatment and centrifugation a primary particle size of 79 nm with a concentration of 2.18 g $L^{-1}$ was produced. Those particles were stored in HCl solution at pH 3.5 in the dark at 4 °C. For batch experiments, they were diluted in HCl of the same pH to a stock concentration of 100 mg $L^{-1}$ after sonication in an ultrasonic bath for 10 min.

### 2.3.2 Preparation of soil solutions

To compare the effect of soil solutions with different characteristics on NP, two soils were chosen with widely varying Ca concentrations and DOC properties. A clayey silt soil (Fluvisol) was received from the upper 5-15 cm of a floodplain soil of the river Rhine near Karlsruhe (Germany, GPS: N49°08′13.62″ E008°21′39.6″), and a well aggregated silty sand (Cambisol described in Sänger et al. 2017) was obtained from a plowed farmland topsoil in Berge (Germany, GPS: N52°30′58.25″ E13°22′36.97″). Soil solutions were prepared freshly before each experiment. They were obtained by 16 h of shaking soil in Millipore water in a soil to water ratio of 1:5 and 1:2.5 for farmland and floodplain soil, respectively. Afterwards, the solid phase was removed by centrifugation (1,050 *x g*, 7 min, Sigma 2D) and filtration through 0.45 µm cellulose nitrate membranes (Sartorius Stedim biotech GmbH, 37070 Göttingen, Germany). To remove colloids already present in the soil solution, an ultracentrifugation step followed this procedure (125,000 *x g*, 4 h, Beckman Optima TL). For this centrifugation step, a colloid density of 1.2 g $cm^{-3}$ and a cut-off-size of 16 nm were applied. The soil solution was stored at 4 °C for no longer than one week.

Elemental analyses of soil solutions were conducted by ICP-OES measurements; pH was analyzed by a pH meter (761, Knick) and electric conductivity (EC) measured by an electrode (pH/Cond Level 1, inoLab). Results are summarized in Table 2. 1.

**Table 2. 1:** Composition of inorganic elements of the soil solutions measured by ICP-OES, pH and EC.

| Element | C in Farmland soil solution (in mg $L^{-1}$) | C in Floodplain soil solution soil (in mg $L^{-1}$) |
|---|---|---|
| **Al** | 0.1 ± 0.0 | 0.0 ± 0.0 |
| **Ca** | 9.1 ± 0.6 | 83.5 ± 1.2 |
| **Fe** | 0.2 ± 0.0 | 0.0 ± 0.0 |
| **K** | 6.3 ± 0.1 | 1.1 ± 0.1 |
| **Na** | 1.0 ± 0.1 | 4.7 ± 0.0 |
| **Mg** | 1.4 ± 0.2 | 7.6 ± 0.1 |
| **Mn** | 0.0 ± 0.0 | 0.0 ± 0.0 |
| **F** | 1.1 ± 0.0 | 0.5 ± 0.0 |
| **Cl** | 3.2 ± 0.0 | 2.6 ± 0.0 |
| **$NO_3$** | 6.7 ± 0.0 | 183.5 ± 0.0 |
| **$PO_4$** | 3.4 ± 0.3 | n.d. |
| **$SO_4$** | 5.9 ± 0.0 | 27.0 ± 0.0 |
| **DOC** | 16.4 ± 0.3 | 9.2 ± 0.0 |
| **pH [-]** | 7.0 | 8.1 |
| **EC [µS $cm^{-1}$]** | 82.5 | 540 |

### 2.3.3 FT IR analysis of soil solutions

Undiluted soil solutions were analyzed by FT IR spectroscopy to obtain information about differences in main functional groups occurring in DOC of soil solutions. The soil solution samples were analyzed with a Bio- Rad FTS 135 using the KBr technique (Capriel et al. 1995; Celi et al. 1997) to obtain absorption spectra of organic matter in a range of wavelength numbers between 3900 and 40 $cm^{-1}$. In our study, the soil solution was mixed with 80 mg KBr using a volume of soil solution such that after freeze drying (Christ Alpha 2-4, 48 h) each sample contained 0.5 mg of organic carbon. Afterwards the mixture was dried for 12 h over silica gel in a desiccator to standardize the water content, finely ground in an agate mortar, and compressed to KBr pellets. From these pellets, FT IR spectra were recorded using a

resolution of 1 $cm^{-1}$ and an average of 16 replicate scans and corrected against ambient air ($H_2O$ and $CO_2$) as background (Haberhauer und Gerzabek 1999). The spectra were smoothed (boxcar moving average algorithm, factor 55), and corrected for baseline shifts using WIN-IR Pro 3.4 software (Digilab, Massachusetts, USA).

Information about the hydrophobicity of the NOM was gained from the C-H:C=O ratio that is larger when NOM is more hydrophobic (Ellerbrock et al. 2001). This ratio was calculated from the intensity of absorption (peak height) at 2934 and 2857 $cm^{-1}$ (originating from symmetric and asymmetric stretching of C-H bonds, Capriel et al. (1995)) and the absorption intensity at 1710 and 1624 $cm^{-1}$ (known for stretching vibrations of C=O bonds; Celi et al. (1997)). The height of adsorption bands was calculated using WIN-IR Pro 3.4 software after baseline and background signal subtraction.

### 2.3.4 Sorption experiments with nanoparticles and soil solution

Nanoparticles were equilibrated with soil solution of farmland or floodplain soil on a horizontal shaker (KS501 digital, IKA Labortechnik) at 130 rpm for 24 h as previous experiments had shown that equilibrium sorption was reached after this time interval (data not shown). The soil solution was used in five concentrations (100 % (i. e. undiluted) and diluted with Millipore water to 75 %, 50 %, 25 % and 0 % of the initial soil solution) to study the effect of different soil solution concentrations on NP stability and adsorption of DOC on NP. Diluted soil solutions contained lower quantities of DOC and ions but had a constant DOC-to-ion ratio. Each concentration step was studied in triplicates. Nanoparticles were added in final concentrations of 3 mg $L^{-1}$ and 38-260 µg $L^{-1}$ for $TiO_2$ and Ag NP, respectively. The conditions of the four batch experiments are summarized in Table 2. 2. For floodplain soil solution, the pH was

adjusted to 7.8 ± 0.2 and for farmland soil solution to 7.5 ± 0.0 using 0.075 M KOH. It should be noted that results of the batch experiment of Ag NP with floodplain soil solution were already published by Klitzke et al. (2015). As the current publication deals with other questions and compares different soil solutions and nanoparticles, those results are shown again for reasons of comparison. The reader should be aware that the floodplain soil of the current study originates from the same site, but from a later sampling campaign than the soil used by Klitzke et al. (2015). This is why SUVA index and E2/E4 value are higher in the current experiments than in the study by Klitzke et al. (2015). All parameters given for floodplain soil solution here (e.g. ion concentrations, FT IR spectra) refer to the soil sample taken for the current study. A description of the soil solution used by Klitzke et al. (2015) can be found in their publication.

**Table 2. 2:** Overview about experimental conditions in the four different sorption experiments.

| **Batch experiment** | **Ag NP – floodplain**[2] | **Ag NP – farmland** | **$TiO_2$ NP – floodplain** | **$TiO_2$ NP – farmland** |
|---|---|---|---|---|
| **$c_{(NP)}$ [mg/l]** | 0,038 | 0,264 | 3 | 3 |
| **$d_{(NP)}$ [nm]**[1] | 76.3 ± 1.9 (Pk1) | 64.6 ± 4.32 | 73 ± 14.8 | 73 ± 14.8 |
| **ζ- potential**[1] **[mV]** | -31.6 ± 1.5 | -31.6 ± 1.5 | 38.8 ± 1.4 | 38.8 ± 1.4 |
| **pH** | 7.8 ± 0.2 | 7.7 ± 0.1 | 7.5 ± 0.0 | 7.5 ± 0.1 |

[1] d and ζ- potentials measured in initial media, i.e. HCl solution for $TiO_2$ NP and Millipore water for Ag NP

[2] obtained from Klitzke et al. (2015)

After 24 h of shaking, samples were centrifuged (15 min at 7,000 *x g* and 30 min at 11,000 *x g* for Ag NP and TiO2 NP, respectively, Beckman Optima TL) to remove nanoparticles together with adsorbed organic matter (OM). In the supernatant, DOC concentrations as well as optical density at 254 and 410 nm of the remaining DOC were measured with a TOC analyzer (TOC — 5050 A Shimadzu) and a UV/vis

spectrometer (Lambda 20, Perkin Elmer), respectively. To characterize molecular weight and aromaticity of DOC in the supernatant the specific UV absorption index at 254 nm (SUVA) and the absorption ratio at 254 and 410 nm (E2/E4 ratio) were calculated. An increasing SUVA value in solution indicates increasing aromaticity of the organic matter in solution (Weishaar et al. 2003). The E2/E4 ratio gives an estimation of the average molecular weight of NOM molecules suggesting rising molecular weight with decreasing ratios (Andersen und Gjessing 2002; Spencer et al. 2007).

The effect of soil solution on NP stability was investigated by measurements of size and zetapotential before and after equilibration in soil solution by a Zetasizer Nano ZS (Malvern Instruments, UK). The hydrodynamic diameter of NP was analyzed based on measurements of the intensity-weighed diffusion coefficient, calculating the size with the Stokes-Einstein equation. If not otherwise mentioned, size data are given as Z-Average acknowledging that at larger polydispersity index (PdI > 0.3) this value does not reflect the true particle diameter but rather illustrates the change in particle size. Size data from fairly monodisperse initial suspensions were used to calculate the surface area available for sorption of DOC assuming spherically shaped particles. With these data the amount of sorbed DOC per m² of NP was calculated.
Zetapotential of NP as an estimation of the surface potential was measured in a folded capillary cell (DTS1070) by a Zetasizer Nano ZS (Malvern) and calculated from the electrophoretic mobility using the Helmholtz-Smoluchowski equation.

## 2.4 Results

### 2.4.1 Properties of soil solutions

Floodplain soil solution contained nine times more Ca and 26 times more $NO_3$ than farmland soil solution (Table 2. 1). The ionic strength of floodplain soil solution was 10-fold higher than the one of farmland soil solution.

The spectral data obtained in FT IR measurements showed clear differences between the C-H:C=O ratio of both soil solutions (Online Resources, Fig. S 2. 2. 1 and S 2. 2). While the NOM of floodplain soil solution had a ratio of 0.0049, NOM of farmland soil solution showed a more than 10 fold higher ratio of 0.074. This illustrates that both soil solutions contain highly hydrophilic NOM which is caused by the extraction in water and subsequent centrifugation of undissolved particles. However, the extracted NOM of floodplain soil solution is relatively more hydrophilic while NOM of farmland soil solution is relatively more hydrophobic.

### 2.4.2 Sorption experiments of nanoparticles and NOM from soil solutions

Titanium dioxide nanoparticles

a) NOM of farmland soil solution

**Sorption of organic matter**

After equilibration of $TiO_2$ NP with farmland NOM the concentration of DOC in the supernatant decreased, indicating the sorption of OM onto NP. With increasing soil solution concentration more OM was adsorbed reaching a maximum of C at NP surfaces at an equilibrium DOC concentration of 14.5 ppm (Fig. 2. 1). At this soil

solution concentration 0.52 ± 0.07 and 0.029 ± 0.004 mg C was sorbed per mg and m² NP, respectively. At the largest DOC concentration of 17.6 ppm (i.e. in undiluted soil solution) less DOC was removed from solution (0.31 ± 0.03 mg DOC $mg^{-1}$ $TiO_2$ NP).

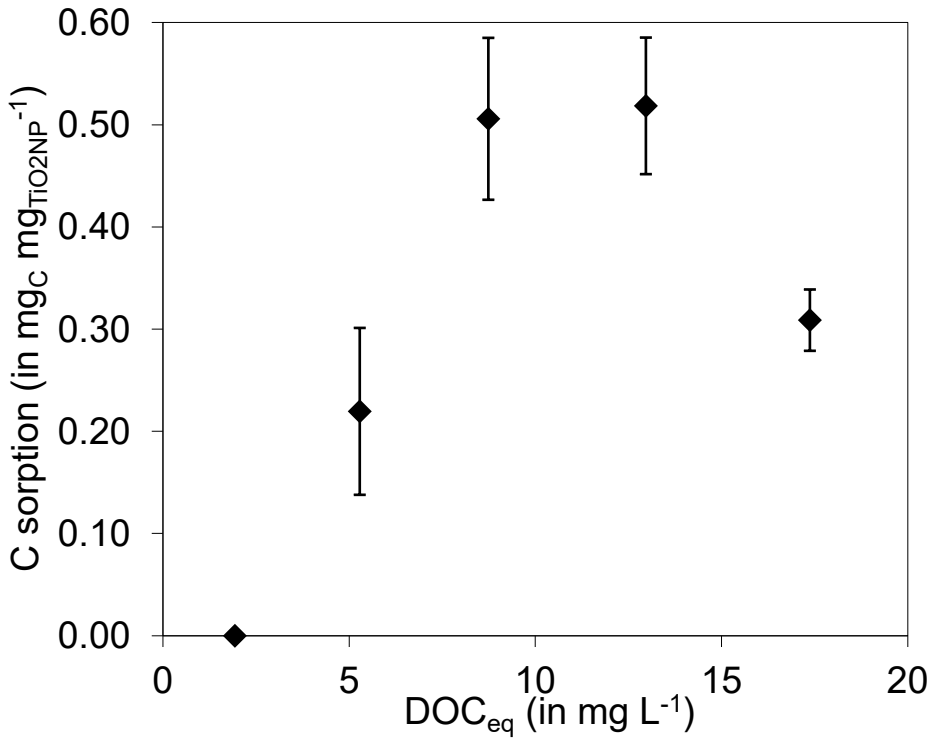


**Fig. 2. 1:** Sorption of organic C of farmland soil solution to $TiO_2$ NP as a function of DOC equilibrium concentration.

**Quality changes of NOM**

After centrifugation of coated NP, SUVA index and E2/E4 ratio were measured in the supernatant. Due to the low amounts of sorbed OM, changes were small for both parameters (Fig. 2. 2 and Fig. 2. 3). For the SUVA index a small difference of DOC properties before and after equilibration with $TiO_2$ NP was measured (Fig. 2. 2). The SUVA showed a tendency to increase upon adsorption of OM to $TiO_2$ NP indicating a preferred sorption of non-aromatic OM.

The E2/E4 index was larger after adsorption of the OM on NP surfaces for the lowest equilibrium DOC concentration of 5.3 ppm (Fig. 2. 3). This means that LMW organic matter remained in solution indicating that more long-chained, HMW organic matter sorbed to $TiO_2$ NP. The preference vanished when larger concentrations of DOC were in solution and the difference in E2/E4 ratio between DOC before and after sorption was reduced with increasing equilibrium DOC concentration.

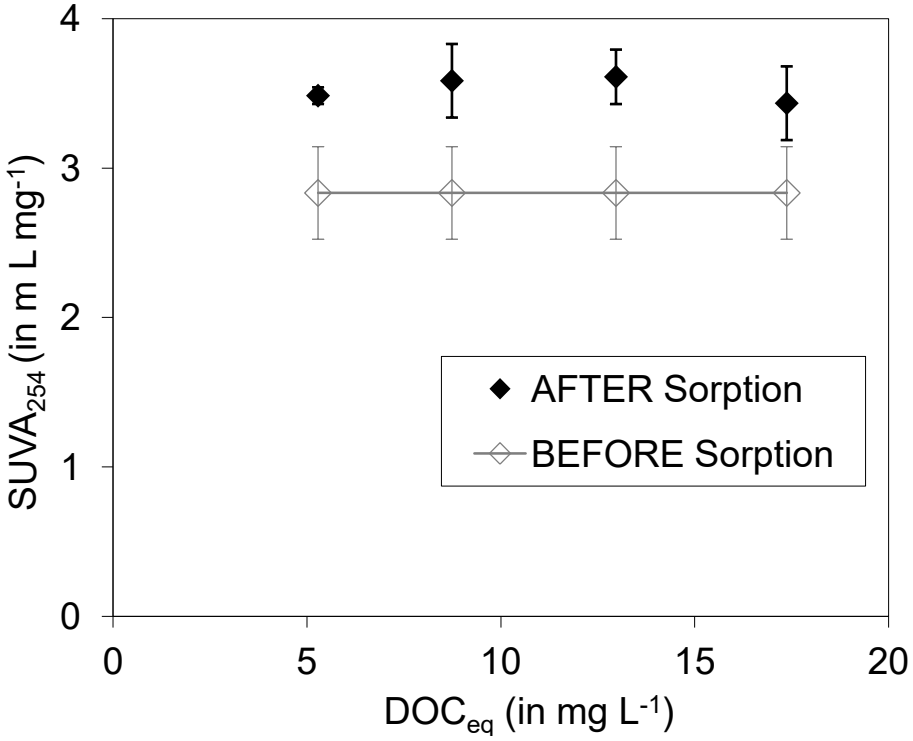


**Fig. 2. 2:** SUVA index of DOC of farmland soil solution in the supernatant before and after sorption to $TiO_2$ NP as a function of DOC equilibrium concentration.

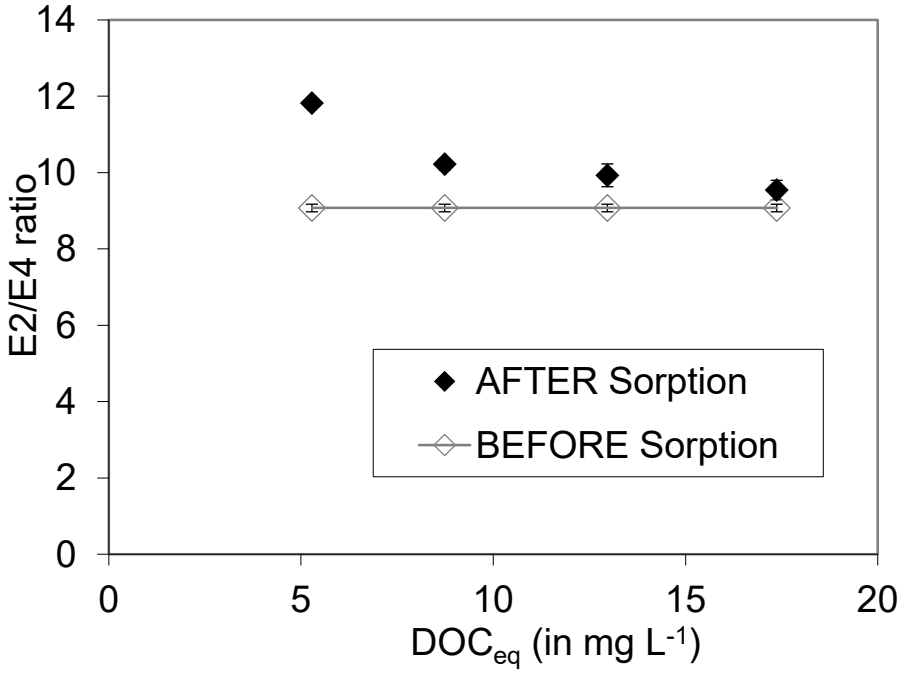


**Fig. 2. 3:** E2/E4 ratio of DOC of farmland soil solution in the supernatant before and after sorption to $TiO_2$ NP as a function of DOC equilibrium concentration.

**Colloidal stability of NP**

The colloidal stability of NP was analyzed by DLS and zetapotential measurements (Table 2. 3). The size of $TiO_2$ NP during the experiment was larger than that of primary particles. This is because $TiO_2$ NP were diluted in water at pH 7 where NP are not stable. Equilibrating $TiO_2$ NP with farmland soil solution did not change the zetapotenial of the NP surfaces, probably due to similar charge of the original surface of the nanoparticles and the NOM (both -20 mV). Nevertheless, a decrease in particle diameter in DLS measurements following the addition of farmland soil solution suggests NP stability to be predominantly affected by farmland NOM. This might be due to an increased steric hindrance through HMW organic substances adsorbed to the NP surface that adds to the electrostatic repulsion forces between the particles. However, increasing amounts of NOM of soil solution did not enhance the stability of the NP, even though further adsorption of OM took place (Fig. 2. 1).

**Table 2. 3:** Particle size (Z-Average and Peak 1) and zetapotential (ZP) of $TiO_2$ NP after equilibration with NOM of farmland soil solutions of different concentrations.

| DOC [ppm] | Z-Ave [nm] | Pk1 [nm] | ZP [mV] |
|---|---|---|---|
| **0** | 275 ± 133 | 129 ± 11 | -21.1 ± 4.2 |
| **5.3** | 120 ± 44 | 74 ± 17 | -21.4 ± 1.4 |
| **8.7** | 109 ± 18 | 82 ± 20 | -18.7 ± 0.2 |
| **13.0** | 112 ± 21 | 89 ± 41 | -19.0 ± 0.9 |
| **17.4** | 113 ± 15 | 88 ± 30 | -19.1 ± 1.4 |

b) NOM of floodplain soil solution

**Sorption of organic matter**

Equilibration of $TiO_2$ NP with NOM of floodplain soil solution did not change the amount of DOC in the supernatant (Online Resources, Fig. S 2. 3). This means that no adsorption of this kind of OM occurred on the $TiO_2$ NP.

**Quality changes of NOM**

As no adsorption of OM on the NP surfaces occurred no changes in the SUVA of the NOM were detected (Online Resources, Fig. S 2. 4). However, it remains unclear why the E2/E4 ratio increased at low DOC concentrations (Online Resources, Fig. S 2. 5). The effect could be related with a narrow $TiO_2$-DOC ratio as the trend is comparable to the results at lowest soil solution concentration in farmland soil solution.

**Colloidal stability of NP**

The presence of floodplain soil solution led to a strong aggregation of $TiO_2$ NP up to diameters of more than 500 nm (Table 2. 4). With increasing soil solution concentration an increased aggregation of $TiO_2$ NP was observed due to the

increasing ionic strength. At DOC concentrations higher than 5 no additional NP destabilization was observed. As $TiO_2$ NP were not coated by organic matter they were not additionally stabilized (neither sterically nor electrostatically) against aggregation. Therefore, the high ionic strength and especially Ca concentration of floodplain soil solution and, hence, the decreased Debye-Hueckel-length, led to dominant electrostatic attraction forces between particles. The zetapotential did not change with addition of soil solution supporting the observation that no OM sorbed onto $TiO_2$ NP.

**Table 2. 4:** Particle size (Z-Average and Peak 1) and zetapotential of $TiO_2$ NP after equilibration with DOC of floodplain soil solutions of different concentrations.

| DOC [ppm] | Z-Ave [nm] | Pk 1 [nm] | ZP [mV] |
|---|---|---|---|
| **0** | 275 ± 133 | 129 ± 11 | -15 ± 3 |
| **2.7** | 122 ± 9 | 121 ± 15 | -15 ± 1 |
| **5.0** | 763 ± 125 | 417 ± 93 | -14 ± 0 |
| **6.9** | 905 ± 226 | 486 ± 115 | -14 ± 0 |
| **9.0** | 768 ± 155 | 497 ± 70 | -14 ± 0 |

Silver nanoparticles

a) NOM of farmland soil solution

**Sorption of organic matter**

With the addition of Ag NP to farmland soil solution the DOC concentration did not change (Online Resources, Fig. S 2. 6). Therefore, it is concluded that no adsorption of NOM of farmland soil solution took place during the experiment.

**Quality changes of NOM**

As expected from the DOC measurements the quality of NOM in the soil solution did not change as a consequence of the equilibration with Ag NP (Online Resources, Fig. S 2. 7 and S 8).

**Stability of NP**

Due to very low Ag NP concentrations DLS and zetapotential measurements showed very poor results (data not shown). Even though measured count rates were below 100 kcps, repeated size measurements with reproducible results did not show any destabilization of particles through the addition of farmland soil solution. This is probably because of the low ionic strength and low Ca concentration in this soil solution. Results of the zetapotential measurements were not reliable and could therefore not be interpreted.

b) NOM of floodplain soil solution

The experiments of sorption of floodplain NOM on Ag NP have been conducted and published by Klitzke et al. (2015). As they complement the picture of NOM sorption on different kinds of NP surfaces they are summarized in the context of this work.

**Sorption of organic matter**

A maximum sorption of 0.17 ± 0.02 mg C per µg Ag NP (22.55 ± 2.94 mg C $m^{-2}$ Ag NP) was estimated at a DOC concentration of 11.8 ppm (Fig. 2. 4). At a larger soil solution concentration (15.8 ppm DOC) the sorbed amount was slightly lower (0.16 ± 0.02 mg C $\mu g^{-1}$ Ag NP).

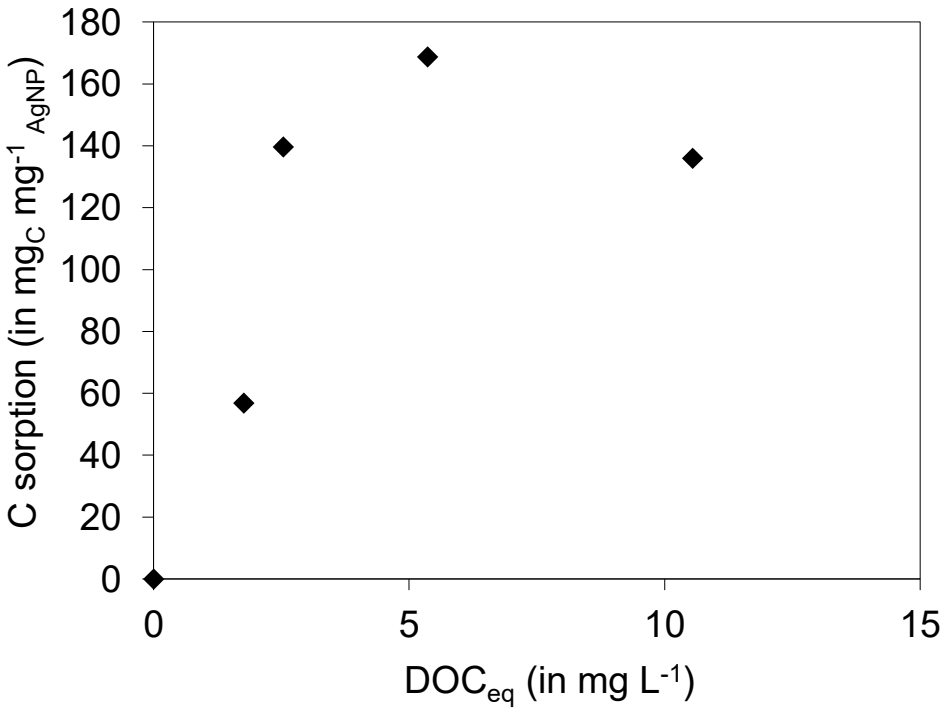


**Fig. 2. 4:** Sorption of organic C of floodplain soil solution to Ag NP as a function of DOC equilibrium concentration (data from Klitzke et al. 2015).

**Quality changes of NOM**

The SUVA index measured in the supernatant of the soil solution after sorption experiments increased compared to the one before equilibration with Ag NP (Fig. 2. 5). This relative increase in aromaticity shows that non-aromatic substances were preferentially removed from solution and adsorbed on NP. With increasing DOC concentration of the soil solution the differences between DOC before and after sorption diminished.

The E2/E4 ratio showed only minor changes at low equilibrium DOC concentrations (Fig. 2. 6). At the largest DOC concentration of 15.8 ppm (i.e. in undiluted soil solution) the value decreased notably showing preferential adsorption of short-chained, LMW organic matter as HMW organic matter remained in solution.

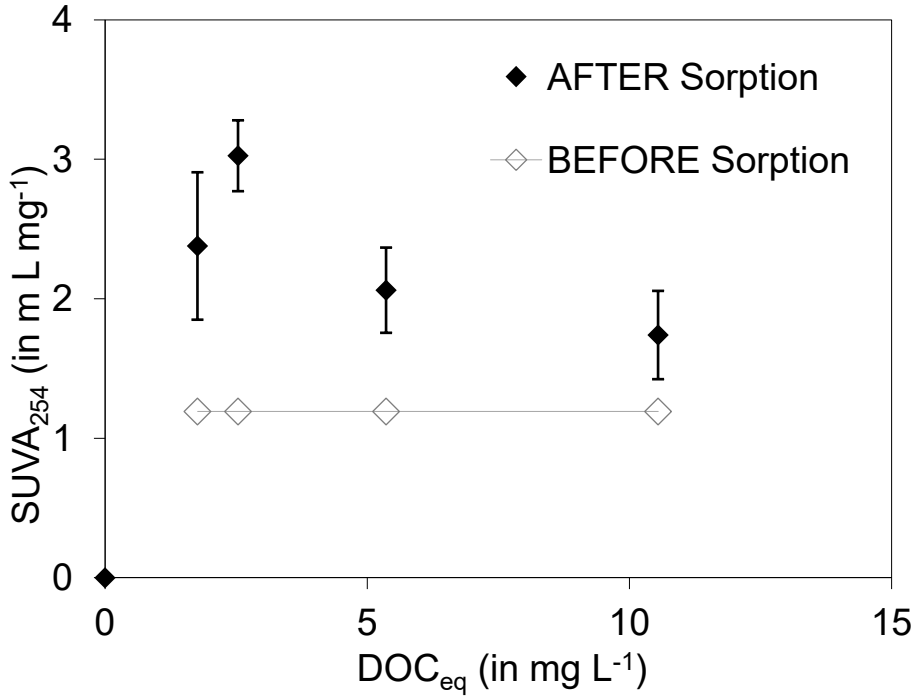


**Fig. 2. 5:** SUVA index of DOC of floodplain soil solution in the supernatant before and after sorption to Ag NP as a function of DOC equilibrium concentration (data from Klitzke et al. 2015).

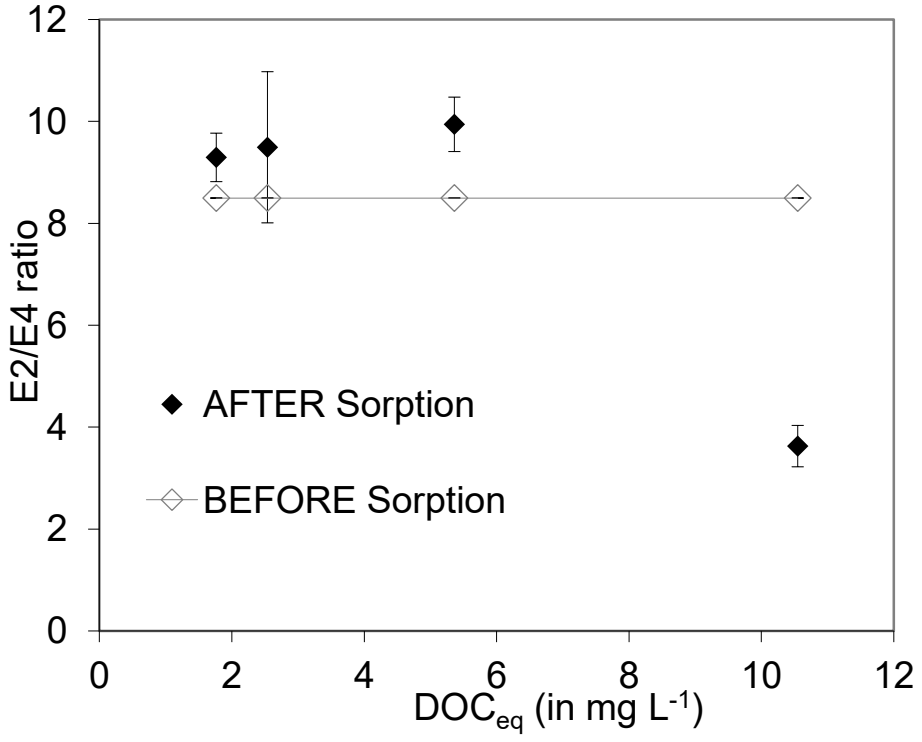


**Fig. 2. 6:** E2/E4 ratio of DOC of floodplain soil solution in the supernatant before and after sorption to Ag NP as a function of DOC equilibrium concentration (data from Klitzke et al. 2015).

## Colloidal stability of NP

Because of the low Ag NP concentrations that led to low count rates during DLS measurements, size data should be handled carefully. Still, it is visible that the contact to floodplain soil solution led to increased diameters of Ag NP (Table 2. 5) and, hence, a destabilization of colloidal Ag NP. The Z-Average particle diameter was largest in the soil solution with equilibrium DOC concentrations of 2.5 ppm but Peak 1 increased constantly with increasing soil solution concentration due to the increasing ionic strength (Table 2. 5). Especially at the largest soil solution concentration most particles seem to be aggregated as also Peak 1 was larger than 200 nm and PdI smaller compared to lower soil solution concentrations. This may have led to a decreased surface area available for DOC adsorption and may explain the decreased amount of adsorbed DOC at largest DOC concentrations.

**Table 2. 5:** Particle size of Ag NP (Z-Average and Peak 1) after equilibration with DOC of floodplain soil solutions of different concentrations (Klitzke et al., 2015).

| DOC [ppm] | Z-Ave [nm] | Pk1 [nm] | % Pk1 | PdI |
|---|---|---|---|---|
| **0** | 45 ± 18 | 57 ± 12 | 85 | 0.3 |
| **1.8** | 199 ± 64 | 71 ± 31 | 95 | 0.4 |
| **2.5** | 545 ± 384 | 97 ±26 | 92 | 0.7 |
| **5.4** | 348 ± 159 | 131 ± 42 | 84 | 0.6 |
| **10.6** | 306 ± 79 | 202 ± 90 | 84 | 0.5 |

Zetapotential measurements could not be analyzed due to poor data quality in the experiments of Klitzke et al. (2015). Therefore, measurements with larger Ag NP concentrations and a more sensitive instrument were conducted during the present study. Those results show that the presence of floodplain soil solution reduced the absolute value of the zetapotential of Ag NP explaining the lower stability of the colloidal system (Fig. 2. 7).

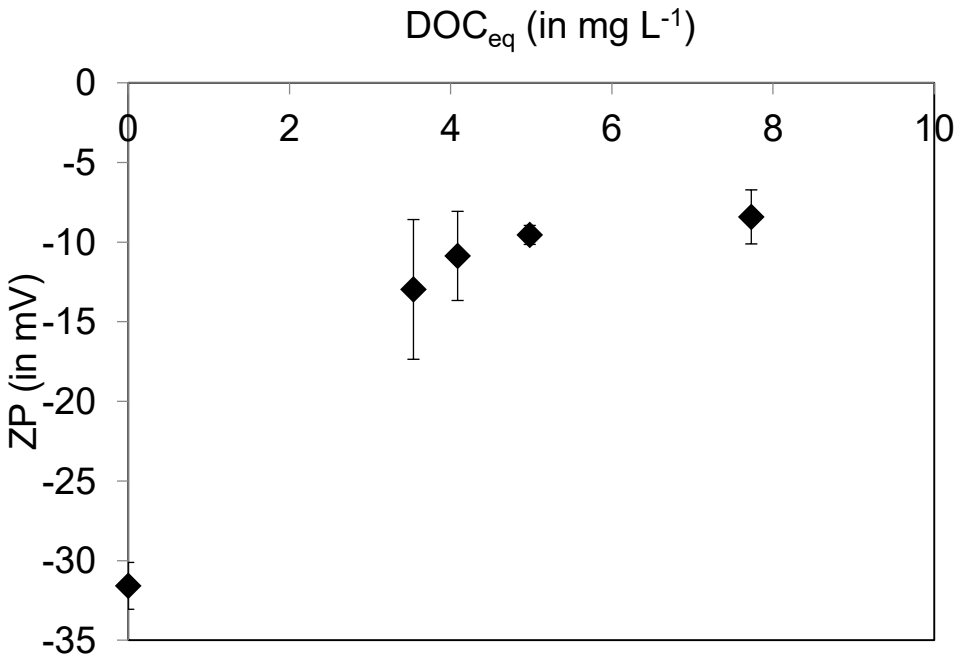


**Fig. 2. 7:** Change of zetapotential of Ag NP in floodplain soil solution as a function of equilibrium DOC concentration.

## 2.5 Discussion

### 2.5.1 Sorption of soil organic matter to $TiO_2$ NP

$TiO_2$ NP were equilibrated in two different natural soil solutions, one originating from a floodplain soil with more hydrophilic NOM and another one from a farmland soil with more hydrophobic NOM. The different NOM quality is in accordance with the common observation that aquatic NOM is more hydrophilic than terrestrial NOM (Thurman und Malcolm 1981; Thurman 2012). We observed no adsorption of the water-borne floodplain OM onto $TiO_2$ NP while the terrestrial OM of farmland soil solution sorbed to the NP. Similarly, Gu et al. (1994) and Luo et al. (2016) observed preferential adsorption of hydrophobic NOM on iron oxides and $TiO_2$ NP, respectively. Hydrophobic interactions are considered important processes for OM interactions on oxic NP (Yang et al. 2009). This might explain why strongly hydrophilic OM did not sorb to $TiO_2$ NP. Beside the different NOM quality of both soil solutions, adsorption might also be influenced by the presence of different inorganic compounds in solution: A high ionic strength with dominating Ca and $NO_3$ concentration in floodplain soil solution might have inhibited sorption of organic matter due to a competition for sorption sites (Ali und Dzombak 1996; Geelhoed et al. 1998) or cross-linking of NOM (Philippe und Schaumann 2014).

In the environment of farmland DOC and low ionic strength, 0.03 mg C $m^{-2}$ $TiO_2$ NP were adsorbed. This is significantly lower than values in the literature, observing maximum sorption of 0.46 mg $m^{-2}$ on $TiO_2$ NP and 0.1-0.4 mg $m^{-2}$ on iron oxides (Z. Li et al. 2018; Yang et al. 2009). Due to the low amounts, the formation of a single layer of OM on $TiO_2$ NP surfaces can be assumed, which is in line with observation for iron-oxides (Vermeer et al. 1998).

In case of $TiO_2$ NP, our second hypothesis proposing HMW and aromatic organic matter preferentially sorbing to NP seems to be only partially supported: From the farmland soil solution a HMW OM fraction was adsorbed (Fig. 2. 3) although the difference might be partially caused by the presence of $TiO_2$ NP as a comparable effect was seen when no adsorption took place in case of floodplain soil solution (Fig. S 2. 5). Sorption of HMW OM to oxic particle surfaces is in agreement with a study from Davis and Gloor (1981), where HMW OM was preferentially adsorbed on Fe-oxides. In contrast to our hypothesis, we observed slightly preferential adsorption of non-aromatic OM on $TiO_2$ NP. This is also contradictory to observations by Erhayem and Sohn (2014) and Y. Li et al. (2015) measuring preferential adsorption of aromatic compounds. The low amount of adsorbed OM as well as the sorption of the more hydrophobic DOC in our study could be an evidence for the dominance of weaker hydrophobic interactions between $TiO_2$ NP and farmland NOM.

We further hypothesized that sorption-induced fractionation becomes more pronounced when larger DOC concentrations are in solution due to competition for sorption sites (Hypothesis I). In contrast to this, the E2/E4 ratios (i.e. reference for molecular weight of organic matter) before and after sorption rather approximated each other with increasing DOC concentration (Fig. 2. 3) and at highest equilibrium values no difference in molecular weight of DOC before and after sorption was visible. Decreasing differences between unsorbed and initial DOC with increasing equilibrium DOC concentration have also been observed for C-sorption on iron oxides and minerals (Hur und Schlautman 2003; Li et al. 2018). The decreasing difference of the E2/E4 ratio before and after sorption might be attributed to the low amount of sorbed OM: As only a small portion of OM of farmland soil solution (0.03 mg C $m^{-2}$ $TiO_2$) was adsorbed, the amount of non-sorbed DOC in solution strongly

increased with rising equilibrium DOC concentrations. In this case the difference of E2/E4 ratio before and after sorption vanishes at larger DOC concentrations. However, the preferential sorption of HMW OM as observed for low equilibrium DOC concentrations may continue with increasing DOC concentrations in solution. This is supported by the constant values of the zetapotential of $TiO_2$ NP independent from increasing DOC concentration which suppose similar kinds of OM on the NP surfaces at all DOC concentrations. Li et al. (2018) hypothesized that sorption-induced fractionation becomes only visible when more than 50 % of OM is removed from solution by adsorption processes. As this amount is far from being reached in our experiments, we cannot observe preferential adsorption in the experiments. Thus, our results do not disprove our hypothesis and we still presume that preferential adsorption of HMW OM might be more pronounced at larger DOC concentrations as observed by other studies (Gu et al. 1994; Vermeer et al. 1998). However, adsorbed organic matter concentrations were too low to measure differences between unsorbed and initial DOC.

The sorption of farmland OM to $TiO_2$ NP led to a stabilization of the NP which was confirmed by DLS measurements showing reduced particle diameters (Table 2. 3). This supports Hypothesis III expecting HMW OM and low ionic strength to stabilize NP in soil environments. Our findings are in line with results of Nason et al. (2012) observing larger humic acid molecules to have stronger stabilizing effects than smaller fulvic acid molecules for Au NP as well as with results from Louie et al. (2015) proving better stabilization of Au NP by molecules with MW >100 kg $mol^{-1}$. In contrast, the more hydrophilic NOM of floodplain soil did not stabilize $TiO_2$ NP which led to NP destabilization in the presence of elevated Ca concentrations.

### 2.5.2 Sorption of soil organic matter to Ag NP

As opposed to $TiO_2$ NP, Ag NP adsorbed the more hydrophilic, water-borne organic matter of floodplain soil solution that contained high amounts of $NO_3$ and Ca ions (Fig. 2. 4), while NOM from farmland soil solution was not adsorbed. The adsorption of floodplain NOM to Ag NP was already investigated by Klitzke et al. (2015). The soil used in our study was taken two years later and differed in some properties. To compare the results of Klitzke et al. (2015) for Ag NP in floodplain soil solution with $TiO_2$ NP in floodplain soil solution this should be taken into account.

The preferential adsorption of more hydrophilic floodplain OM on Ag NP is in line with Metreveli et al. (2016), who also observed larger adsorption of hydrophilic NOM on the hydrophilic Ag NP surfaces. Additionally, more than 700 times more organic matter sorbed to Ag NP compared to $TiO_2$ NP. Possibly, this is caused by the bridging effect of Ca ions (Baalousha et al. 2013; Stankus et al. 2011) with hydrophilic NOM in the Ca-rich floodplain soil solution that allowed multiple layers of organic molecules to be sorbed on the NP. The adsorbed amount of 22.55 mg C $m^{-2}$ is also 10-100 times larger than values commonly presented in the literature (Hur und Schlautman 2003; Li et al. 2018; Yang et al. 2009). Potentially, this can be explained by the very high C-to-NP- ratio in the experiments of our study in combination with the high Ca concentration in floodplain soil solution. At high ionic strength, Vermeer and Koopal (1998) as well as Nason et al. (2012) observed increasing sorption of OM to NP which was explained by changes in the conformation of organic molecules: At high ionic strength the intramolecular repulsion is reduced leading to denser layers of adsorbed organic matter enhancing the amount of sorbed OM. As environmental NP concentrations are expected to be in the µg $L^{-1}$ range (Gottschalk et al. 2013) and inorganic ions are ubiquitous, we hypothesize that the adsorbed amount might be underestimated in studies using lower C-to-NP- ratios and low ionic strength.

The results of the quality of sorbed OM (i.e. SUVA and E2/E4 ratio in Fig. 2. 5 and Fig. 2. 6) were unexpected as other studies mostly show a preferential sorption of HMW and aromatic OM (for example Louie et al. (2013) for Au NP, Yin et al. (2015) for Ag NP). Instead, non-aromatic and short-chained organic matter from floodplain soil solution was adsorbed by Ag NP contradicting our Hypothesis II. This might be a result of the presence of inorganic ions. De Laat and van den Heuvel (1995) showed that adsorption of HMW OM is often retarded by LMW OM or small ions adsorbing on NP surfaces, forming an electrostatic barrier. This barrier is, amongst others, a function of the salt concentration in solution. In the floodplain soil solution the high ionic strength might therefore be responsible for the preferential adsorption of LMW OM as HMW OM compounds are repelled by the energy barrier. Additionally, Hur und Schlautman (2003) observed that the exchange of LMW OM against HMW OM plays a larger role when hydrophobic interactions are predominant. As NOM of the floodplain soil was very hydrophilic, hydrophobic interactions might be subsidiary. Another possible explanation mentioned by Klitzke et al. (2015) is that the small organic molecules are enlarged by bridging with divalent cations and therefore act as larger molecules. In either case, the presence of inorganic ions such as Ca seems to have a crucial effect on the adsorption of organic matter on Ag NP and the colloidal stability of the particles.

Even though adsorption of OM on NP surfaces often leads to steric and/or electrostatic stabilization of NP, Ag NP aggregated in floodplain soil solution, as shown by DLS measurements (Table 2. 4). Especially when short-chained organic matter with low steric stabilization potential is adsorbed, high ionic strength can cause destabilization of NP followed by aggregation (Louie et al. 2015; Yin et al. 2015). This destabilization was also a result of the decreased absolute values of the zetapotential (-32 compared to -10 mV as shown in Fig. 2. 7) followed by decreased

electrostatic repulsion together with the bridging effect of Ca ions, as assumed in Hypothesis III.

The preferential adsorption of non-aromatic OM on Ag NP was more pronounced at lower equilibrium DOC concentrations contradicting hypothesis I. It might be explained by increasing amounts of non-sorbed OM with increasing DOC concentration in solution blurring the results of the UV-vis absorption measurement (as mentioned for $TiO_2$ NP). Anyhow, this explanation becomes less probable taking into account that extremely large amounts of organic matter are adsorbed. In contrast to aromaticity, molecular weight- dependent preferential sorption of organic matter was only observed at highest carbon concentrations supporting our first hypothesis. LMW organic matter was preferentially adsorbed while HMW substances remained in solution. Due to the high ion concentration in undiluted soil solution, an almost complete aggregation of Ag NP was observed. This may have limited the surface area available for DOC adsorption and promoted preferential adsorption due to the limitation of sorption sites. In this situation smaller and faster molecules adsorbed predominantly.

## 2.6 Conclusion

The variable fate of nanoparticles in natural soils

Bringing these divers results together several essential conclusions can be drawn.

1. It is a widely accepted assumption that NP in natural soils are promptly coated by organic molecules due to their high surface area - volume ratio. In our study it became clear that not all organic molecules will sorb to nanoparticles suggesting that the formation of a natural organic coating is strongly dependent on the environment nanoparticles are exposed to. In our study, the highly hydrophilic NOM of a floodplain soil solution rich in inorganic ions strongly sorbed to Ag NP but not to $TiO_2$ NP. Instead, sorption to $TiO_2$ NP was observed for the more hydrophobic organic matter of a farmland soil with low ionic strength which did not sorb to Ag NP. Hence, sorption of organic matter seems to be strongly dependent on the NP material and the difference between oxic and metallic NP is clearly visible.

2. Our results contradict the common assumption that aromatic and HMW OM sorbs preferentially to NP (for example Davis and Gloor 1981; Erhayem and Sohn 2014). We could show that this generalization is not applicable to all types of NP. For $TiO_2$ NP this hypothesis can be supported in case of molecular weight by the results of our study but Ag NP in a solution with high ionic strength showed a contrasting behavior preferring non-aromatic, LMW OM. This clearly shows, that what holds true for simplified systems using pure model substances can be contrary in more complex situations i.e. the combination of organic matter and inorganic ions. Taking into account that real soil solutions also contain natural colloids the situation might become even more complex.

3. Besides the complementing insights in sorption processes on NP surfaces, our study can also add information on the stability of NP in soil systems. Often organic substances are thought to be main drivers of the colloidal stability (Chowdhury et al.

2012) but our results point out that the role of inorganic ions must not be neglected. When LMW OM sorbs to particles in systems with high ionic strength (here: Ag NP in floodplain soil solution) a destabilization of the NP takes place. Stabilization is predominant when HMW OM sterically stabilizes NP and ionic strength is lower (here: $TiO_2$ in farmland soil solution).

Altogether, our findings suggest that $TiO_2$ and Ag NP entering similar environments may undergo different pathways. While Ag NP in floodplain soils might be coated by hydrophilic OM and therefore stabilized against aggregation, $TiO_2$ NP might immediately undergo aggregation and immobilization due to the missing organic coating in the same environment. In farmland soils, the opposite might be observed. This will also affect the ecotoxicological risk of NP. Hence, it is important for the industrial use and risk assessment of NP to classify NP depending on their fate in the environment. This study could show that there are great differences between the fate of oxic and metallic NP when comparing $TiO_2$ and Ag. Therefore, the role of natural organic matter on NP behavior in a soil environment must not be considered uniform.

# 3 Transport and retention of differently coated $CeO_2$ nanoparticles in saturated sediment columns under laboratory and near-natural conditions

Authors: Laura Degenkolb, Urs Dippon, Silke Pabst, Sondra Klitzke

Post-print, published in “Environmental Science and Pollution Research”, original publication (open-access) can be found under https://doi.org/10.1007/s11356-019-04965-x

## 3.1 Abstract

Where surface-functionalized engineered nanoparticles (NP) occur in drinking water catchments, understanding their transport within and between environmental compartments such as surface water and groundwater is crucial for risk assessment of drinking water resources. The transport of NP is mainly controlled by i) their surface properties, ii) water chemistry and iii) surface properties of the stationary phase. Therefore, functionalization of NP surfaces by organic coatings may change their fate in the environment.

In laboratory columns, we compared the mobility of $CeO_2$ NP coated by the synthetic polymer polyacrylic acid (PAA) with $CeO_2$ NP coated by natural organic matter (NOM) and humic acid (HA), respectively. The effect of ionic strength on transport in sand columns was investigated using deionized (DI) water and natural surface water with 2.2 mM $Ca^{2+}$ (soft) and 4.5 mM $Ca^{2+}$ (hard), respectively. Furthermore, the relevance of these findings was validated in a near-natural bank filtration experiment using HA-$CeO_2$ NP.

PAA-$CeO_2$ NP were mobile under all tested water conditions, showing a breakthrough of 60% irrespective of the $Ca^{2+}$ concentration. In contrast, NOM-$CeO_2$ NP showed a lower mobility with a breakthrough of 27% in DI and <10% in soft surface water. In hard surface water, NOM-$CeO_2$ NP were completely retained in the

first 2 cm of the column. The transport of HA-$CeO_2$ NP in laboratory columns in soft surface water was lower compared to NOM-$CeO_2$ NP with a strong accumulation of $CeO_2$ NP in the first few centimetres of the column. Natural coatings were generally less stabilizing and more susceptible to increasing $Ca^{2+}$ concentrations than the synthetic coating. The outdoor column experiment confirmed the low mobility of HA-$CeO_2$ NP under more complex environmental conditions. From our experiments, we conclude that the synthetic polymer is more efficient in facilitating NP transport than natural coatings and hence, $CeO_2$ NP mobility may vary significantly depending on the surface coating.

## 3.2 Introduction

Cerium dioxide nanoparticles ($CeO_2$ NP) are used in various industrial applications, e.g., in diesel fuels, catalytic converters, and polishing agents (Garcia et al., 2005; Reed et al., 2014). As a result, increasing concentrations of these engineered nanoparticles (NP) in the environment can be expected. In surface waters, $CeO_2$ NP are predicted to reach concentrations in the range of $10^{-2}$ µg $L^{-1}$ (Gottschalk et al. 2013). The presence of $CeO_2$ NP in the environment was repeatedly shown to cause negative effects on organisms such as ammonia oxidizing bacteria (García et al. 2012) or earthworms (Collin et al. 2014). Damage of human lung cells as well as oxidative stress can also be caused by $CeO_2$ NP (Lin et al. 2006). An exposure to humans for example via drinking water should therefore be avoided. As riverbank filtrates are an important source for drinking water (Sprenger et al. 2017) it must be ensured that $CeO_2$ NP entering the environment will be retained in these systems by natural filtration mechanisms, e.g., straining, adsorption, and attachment to biofilms. To understand the likelihood for transport of NP into environmental compartments such as groundwater, studies on the stability and the transport of NP in natural systems are important.

Many studies are currently undertaken on this topic elucidating the main factors governing NP transport in porous systems. Those factors include intrinsic NP properties (e.g., shape and size: Tiraferri und Borkovec 2015), hydrochemical properties of the mobile phase (e.g., pH and ionic strength: Praetorius et al. 2014) as well as characteristics of the pore system itself (e.g., pore size and connectivity: Cornelis et al., 2013; Fang et al., 2016; Lv et al., 2016; Troester et al., 2016). Additionally, organic molecules adsorbed to NP surfaces are of high importance for their colloidal stability: while bare $CeO_2$ NP do commonly aggregate in most surface

waters, the coverage of their surface with either synthetic or natural organic coating agents can stabilize $CeO_2$ NP to different degrees (Booth et al. 2015; Dippon et al. 2018; Sehgal et al. 2005). A very effective manufactured stabilization agent is polyacrylic acid (PAA) as it exhibits a high negative surface charge stabilizing NP by electrostatic repulsion (Sehgal et al. 2005). Authors showed that PAA-coated $CeO_2$ NP were stable even at $Ca^{2+}$ concentrations up to 6 mM which could potentially result in high transport of NP in column experiments (Chanteau et al. 2009; Petosa et al. 2013). In contrast, natural coating agents such as humic acid (HA) and fulvic acid (FA) seem to stabilize $CeO_2$ NP in a broad pH range but the presence of divalent cations such as $Ca^{2+}$ can cause bridging effects and strong aggregation of NP (Oriekhova und Stoll 2016a; Stankus et al. 2011).

Nanoparticles released in the environment will most likely be coated with natural organic matter (NOM), synthetic coatings might be replaced or covered by NOM (Louie et al. 2016) which may change NP stability (Davis und Gloor 1981; Tipping und Higgins 1982).In comparison to uniform, synthetic coatings used to stabilize NP suspension in industrial processes, natural organic matter consists of a variety of macromolecules that form a heterogeneous coating on NP surfaces. This will most likely lead to different stability and therefore mobility of naturally and synthetically coated NP. However, the different influence of synthetic compared to natural occurring polymers on $CeO_2$ NP transport has not been studied in detail so far. Laboratory column experiments investigating the influence of one or more of the before-mentioned factors, showed that a transport of NP through sediments or soils takes place when NP are colloidally stable, but NP will be retained in systems with high ionic strength (e.g., Liang et al., 2013; Petosa et al., 2013). Organic matter concentrations and ionic strength affect NP attachment to sediment surfaces: increasing ionic strength enhances the attachment, while the presence of organic

matter reduces it (Geitner et al. 2017). Therefore, we tested the influence of waters with different ionic strength on NP transport comparing different organic matter coatings on $CeO_2$ NP. We hypothesize that polyacrylic acid-coated $CeO_2$ NP will be more stable in natural surface water as they are less susceptible to enhanced $Ca^{2+}$ concentrations than natural organic matter coated $CeO_2$ NP. Thus, a higher transport of PAA-$CeO_2$ NP is expected to occur in saturated sediment columns.

In addition, processes determining the transport behavior of NP can vary significantly from lab studies to environmental systems. As an example, Markus et al. (2015) stated that the aggregation processes taking place differ in lab experiments compared to environmentally relevant systems. The importance of heteroaggregation on NP fate in natural surface water of a mesocosm experiment has been shown by Espinasse et al. (2018). Furthermore, biological activity in environmental systems may lead to more versatile attachment sites than present in well-defined laboratory systems. We expect that this increased complexity will cause a stronger retention in natural systems compared to lab studies and should therefore be taken into account when assessing a potential risk of NP transport.

In the first part of our study, we compared the mobility of PAA-coated $CeO_2$ NP (PAA-$CeO_2$ NP) with $CeO_2$ NP coated by NOM or HA (NOM-$CeO_2$ NP and HA-$CeO_2$ NP) in laboratory sand columns under saturated conditions. The experiments were conducted in deionized water as well as natural surface water with different $Ca^{2+}$ concentrations to account for different types of water. In the second part, the transport of HA-$CeO_2$ NP was investigated in a more complex bank filtration system in semi-technical scale and these results were compared to the results of laboratory column experiments. With this approach our study aimed at identifying differences in the transport of synthetically and naturally coated $CeO_2$ NP in sandy sediments in the

presence of different surface waters. The relevance of findings from laboratory studies was validated by an outdoor bank filtration experiment.

## 3.3 Material and methods

### 3.3.1 Nanoparticles and coatings

Polyacrylic acid-coated $CeO_2$ NP (Partikular GmbH, Germany) with a hydrodynamic diameter (HDD) of 74 nm were produced by laser ablation from bulk material directly within PAA solution (Sigma Aldrich, $M_w$ = 2100). Therefore, particle surface modifications due to intermediate synthesis steps or residues from synthesis chemicals can be excluded.

Pristine $CeO_2$ NP for coating with NOM and Humic acid (HA) were purchased from Nyacol Inc. (USA). The uncoated particles with a HDD of 80 nm were stabilized in acetic acid at pH 2. These particles were coated prior to experiments with either NOM or HA using the following procedures: a) Nordic reservoir-NOM was purchased from IHSS (International humic substance society, USA, Nordic reservoir organic matter, batch 1R108N) as powder with 1 g NOM containing 0.31 g $C_{org}$. For stock solutions, 0.02 g NOM powder was dissolved in 100 mL ultrapure water. Pristine $CeO_2$ NP were coated by adding 10 mL of a 500 mg $L^{-1}$ $CeO_2$ NP suspension into 90 mL of 200 mg $L^{-1}$ NOM solution and subsequent stirring for 48 h at 4°C in the dark. Finally, the pH of the suspension was adjusted to pH 7 using dilute KOH (analytical grade, Merck, Germany). b) HA sodium salt (Sigma Aldrich) solutions were prepared like the NOM solution but filtered (0.45 µm, regenerated cellulose) before addition of the NP. For the bank filtration experiment, HA was prepared in shares of 4 g per 4.8 L water and centrifuged before filtration (Schleicher & Schuell filter paper).

Prior to the experiments, the differently coated NP suspensions were diluted in the target water to 4 mg $L^{-1}$ of $CeO_2$ leading to different particle properties depending on

hydrochemical conditions (Table 3. 1). All solutions containing NOM or HA were stored at 4°C in the dark and used within one week.

**Table 3. 1:** Nanoparticle properties (hydrodynamic diameter (HDD) before and after the experiment and ζ-potential values; mean and standard deviation from 3 replicates) and water conditions (electrical conductivity (EC) and pH) of the laboratory column experiments.

| **Medium** | **DI water** | | **Soft surface water** | | | **Hard surface water** | |
|---|---|---|---|---|---|---|---|
| **Coating** | **PAA** | **NOM** | **PAA** | **NOM** | **HA** | **PAA** | **NOM** |
| **HDD (Z-Ave) before [nm]** | 74 | 79 | 76 | 64 | 105 | 87 | 590 |
| **SD** | 1 | 1 | 0 | 1 | 5 | 2 | 37 |
| **HDD (Z-Ave) after [nm]** | 70 | 78 | 73 | 88 | 156 | 87 | >3000[a] |
| **SD** | 1 | 0 | 1 | 1 | 1 | 2 | 699 |
| **HDD (Vol-Pk 1) before [nm]** | 55 | 55 | 57 | 45 | 86 | 54 | 70 |
| **SD** | 3 | 6 | 2 | 5 | 14 | 15 | 22 |
| **HDD (Vol-Pk 1) after [nm]** | 56 | 49 | 52 | 64 | 75 | 53 | -[b] |
| **SD** | 2 | 6 | 2 | 2 | 30 | 3 | -[b] |
| **ζ-potential [mV]** | -48.1 | -34.8 | -22.2 | -21.6 | -18.0 | -18.7 | -17.9 |
| **SD** | 3.0 | 12.0 | 0.8 | 2.1 | 0.9 | 1.0 | 1.1 |
| **EC [µS cm$^{-1}$]** | 0.31 | 0.31 | 527 | 786 | 505 | 995 | 1001 |
| **pH** | 7.5 | 6.5 | 7.6 | 7.9 | 6.9 | 7.8 | 7.9 |

[a] PdI > 0.7, therefore DLS data not reliable
[b] Not evaluated due to particle sedimentation

### 3.3.2 Properties of the water-saturated sediment system

The transport of $CeO_2$ NP was investigated under water-saturated conditions in quartz sand columns. As mobile phase, we used natural pond water from a sand filtration pond located at the property of the Federal Environment Agency, Berlin. For laboratory column experiments, the water was sampled from the pond and filtered (<0.45 µm, Nylon, Whatman, GE Healthcare) prior to each experiment and the main ion concentrations were measured and found to be constant during all sampling time points (Online Resources, Fig. S 3. 3. 1). To investigate the influence of the water hardness on NP transport, we used differently hard water: deionized (DI) water ($Ca^{2+}$ concentration 0 mM), soft surface water (DI water-diluted pond water with a $Ca^{2+}$ concentration of 2.2 mM), and hard surface water (pond water with a $Ca^{2+}$

concentration of 4.5 mM). In the context of this study, the terms “soft” and “hard” were chosen to differentiate between the two $Ca^{2+}$ concentrations and do not correspond to any classification system. Columns of the outdoor experiments were located in the sand filtration pond and flushed with surface water throughout the year. For our study, we diluted the surface water to soft water conditions ($Ca^{2+}$ concentration 2.2 mM) using deionized (DI) water.

**Table 3. 2:** Composition of water used in laboratory column experiments. In the outdoor column experiment, the water composition roughly matched the soft surface water, but fluctuations in concentrations were caused by changing weather conditions. Ion concentrations were measured by ion chromatography (Metrohm, Germany).

| Parameter | DI water | Soft surface water / Outdoor columns[b] | Hard surface water |
|---|---|---|---|
| **Electrical conductivity (µS cm$^{-1}$)** | 0.055 | 520 / 250-520 | 850-950 |
| **pH** | -[c] | 7.7 | 7.7 |
| **Al (mM)** | b.d.l.[a] | 0.00 | 0.00 |
| **Ca (mM)** | b.d.l.[a] | 2.2 | 4.5 |
| **Fe (mM)** | b.d.l.[a] | 0.00 / 0.11 | 0.00 |
| **K (mM)** | b.d.l.[a] | 0.06 | 0.1 |
| **Mg (mM)** | b.d.l.[a] | 0.34 | 0.7 |
| **Na (mM)** | b.d.l.[a] | 1.25 | 2.5 |
| **Cl (mM)** | b.d.l.[a] | 1.19 | 2.4 |
| **$SO_4$ (mM)** | b.d.l.[a] | 1.30 | 2.6 |
| **$NO_3$ + $NO_2$ (mg L$^{-1}$)** | b.d.l.[a] | 0.03 | 0.05 |
| **$NH_4$ (mg L$^{-1}$)** | b.d.l.[a] | 0.01 | 0.01 |

[a] below detection limit. [b] Average values for dry weather conditions. Where lab and outdoor column experiments differed from each other noteworthy, two numbers are given (lab/outdoor). [c] not measurable due to low conductivity

All columns were filled with medium grain-sized sand ($d_{50}$: 1.8 mm; grain size distribution Fig. S 3. 2 in the Online Resources). For lab experiments, the sand was washed with DI water and then filled into columns under water-saturated conditions to avoid trapping of air bubbles. Subsequently, the columns were equilibrated with particle-free water for 48 hours prior to particle injection to ensure constant boundary conditions for all sand columns. The outdoor columns were filled with sediment 3 months prior to the start of the experiment and then flushed with natural, undiluted pond water. Therefore, a well-established ecological community can be expected in

the outdoor columns, which was confirmed by microscopy images showing a high number of diatoms (Degenkolb et al. 2018). Two days prior to the NP transport experiments, the flushing water was changed to soft surface water to adjust the desired hydrochemical conditions.

### 3.3.3 Laboratory column experiments

The laboratory columns were made of glass, equipped with Polytetrafluoroethylene (PTFE) end pieces and had a length of 18 cm and a diameter of 4.3 cm. They were operated in upward flow to reduce the possibility of air entrapments. The flow rate was set to 0.5 mL $min^{-1}$, equivalent to a pore water velocity (Darcy velocity) of 1.3 m $day^{-1}$ using peristaltic pumps. A tracer experiment with NaCl was done prior to each NP transport experiment measuring the electric conductivity (TetraCon, WTW, Germany) in the column outflow. From this, an effective porosity ($\eta_{eff}$) between 0.35 and 0.38 was calculated which was used to normalize the sampling time to the unit of "pore volumes" (PV).

The NP transport experiments were conducted in duplicates at room temperature. A $CeO_2$ NP suspension with a final Ce concentration of 4.0 ± 0.6 mg $L^{-1}$ was added to the desired water (DI, soft or hard surface water) one hour before start of the experiment. After this time, the suspension was injected at a constant flow velocity (0.5 mL $min^{-1}$) for 3 PV. It should be noted that the pH of the added particle suspensions slightly differed between the experiments (Table 3. 1). This was mainly caused by the different pH values of the NOM-, PAA- and HA-$CeO_2$ NP stock suspensions and the buffering capacity of the applied water. After NP addition flushing was done with the respective NP-free water for 13 PV. The outflow of the columns was sampled in intervals of 40 min in glass tubes. Aliquots of the water

samples were used for cerium and total organic carbon (TOC) quantification (vario TOC cube, Elementar, Germany). As the TOC concentration showed the same transport behavior as the NaCl tracer (i.e. similar retention under identical flow velocity), this value can be interpreted as a tracer measured parallel to the NP injection indicating whether NP transport was retained or not. Upon termination of the experiment, the sand from the columns was sampled in 1 cm sections and analyzed for cerium content.

### 3.3.4 Outdoor column experiments

To assess the transferability of results about $CeO_2$ NP transport from laboratory columns to more complex environmental conditions, the facility for the simulation of riverbank and slow sand filtration (SIMULAF) located at the German Environment Agency in Berlin was used. This facility is described in more detail in Degenkolb et al. (2018). In brief, we used two water-saturated columns filled with the same medium grain-sized sand as used in laboratory column experiments. For experiments with NP, we diluted the water to an electric conductivity (EC) of 250-520 µS $cm^{-1}$ by adding DI water equivalent to soft surface water conditions in the lab. Fluctuations in the conductivity were caused by heavy rain events. Physico-chemical parameters of the diluted pond water are summarized in Table 3. 2. In contrast to the lab experiments, the pond water was not filtered and therefore, the presence of natural colloids larger than 0.45 µm can be expected which is demonstrated by larger Fe concentrations in the mobile phase of outdoor columns (Table 3. 2). The columns with a length of 1.5 m and a surface area of 1 $m^2$ had sampling ports in 15, 30, 50, and 90 cm depth as well as at the outflow (Online Resources, Fig. S 3. 3). In 15, 30, 50, and 90 cm depth, water was sampled continuously with a pump rate of 0.5 L $h^{-1}$.

Samples were taken with an autosampler every 30 min for the first 24 h. Afterwards the sampling interval was increased stepwise to 60 min (day 2), 90 min (day 3-4) and 6 h (day 5-30). The samples were collected in glass vessels and subsequently stored in plastic tubes at 10°C until analysis. Additionally, samples from the outflow were taken manually once or twice a day directly into plastic tubes as the possibility for breakthrough in this depth was lowest. Electric conductivity and temperature were monitored over the whole experimental period in the column supernatant and EC also in the outflow (Online Resources, Fig. S 3. 4).

The outdoor experiment was conducted from 26$^{th}$ of June until 25$^{th}$ of July 2017. A filter velocity of 0.5 m day$^{-1}$ (i. e. Darcy velocity ≈ 1.45 m day$^{-1}$) was kept constant over the entire experiment as well as during the tracer experiment. We used NaCl solution (EC in the supernatant: 2.5 mS cm$^{-1}$) as a tracer and measured EC in all depths of the columns.

Prior to NP injection, samples of the water head of the sediment columns were collected as blank samples and to describe hydrochemical characteristics of the mobile phase. Cerium dioxide NP were injected into 100 L of diluted pond water in the column supernatant with a final Ce concentration of 4.3 mg L$^{-1}$. After gentle stirring, 3 replicates were taken from each column supernatant. We waited until complete infiltration of the NP dispersion before adding diluted pond water as the mobile phase of the transport experiment. Sampling was conducted over a period of 30 days. During this time, two intense rainfall events significantly reduced the EC of the mobile phase (Online Resources, Fig. S 3. 4) but did not affect the flow velocity due to the constant pumping. This phenomenon was expected to influence the colloidal stability and thus the transport behaviour of $CeO_2$ NP and was therefore included in the evaluation of the experiment.

After termination of the experiment, sand samples were taken from 0-30 cm depth in 5 cm intervals and from 40-90 cm depth in 10 cm intervals measured from the sand surface. Cerium dioxide NP were extracted and quantified as described below.

### 3.3.5 Analytical techniques

Particle size and ζ-potential of $CeO_2$ NP were measured by dynamic light scattering (DLS) with a Zetasizer Nano ZS (Malvern Instruments, UK) and ζ-potentials were calculated based on the electrophoretic mobility of the NP (using the Helmholtz-Smoluchowsky equation). The NP size in different media was investigated in batch experiments prior to and at the end of column experiments (Table 3. 1). All NP sizes indicated in this study are intensity-weighted least square sum Z-average values with PdI ≤ 0.3 which corresponds to a broad monodisperse distribution. These values are suitable to observe changes in NP size (e.g., caused by aggregation). However, as they are biased to larger particle sizes, the volume-weighted largest peak is also given in Table 3. 1.

.

Digestion of Ce in aqueous samples: Aqueous suspensions taken from the column outflow of laboratory experiments and different depths of the outdoor columns, respectively, were sampled in 10 mL aliquots and dried at 40°C for 12 h. The residues were then digested in the microwave using a modified aqua-regia digestion with $HNO_3$ and HCl in a ratio of 3:1 (v/v). In detail, 6 mL of 65 % $HNO_3$ and 2 mL of 32 % HCl were added to the dried sample and digested for 20 min at 160°C in the microwave (Mars 5x, CEM GmbH) in PTFE or tetrafluorethylene-perfluorether copolymer (PFA) pressure vessels. Digested samples were filtered (Whatman filter paper) to remove possible quartz particles.

Digestion of Ce in sediment samples: Sediment samples of the columns were analyzed for Ce content to measure the amount of retained $CeO_2$ NP. Acid digestion of the complete sediments yielded high background Ce concentrations with a large standard deviation, exceeding the cerium concentration applied in the form of NP (Online Resources, Fig. S 3. 5). Therefore, we developed a selective extraction technique based on established methods for the extraction of exchangeable ions (Filgueiras et al. 2002). An amount of 5 g wet sand was weighted into vials and a volume of 12 mL ultrapure water was added. These samples were sonicated for 60 min in an ultrasonic bath, and subsequently, 10 mL of the supernatant were pipetted for digestion as described for aqueous suspensions. The recovery of cerium by this method was 80% (Online Resources, Fig. S 3. 5).

Cerium quantification: All digested samples were analyzed for Ce concentrations by inductively coupled plasma optical emission spectroscopy (ICP-OES, PerkinElmer Optima 8300) in duplicates. Quantification limits, determined according to DIN 32645, were 2 µg $L^{-1}$ in the measurement solution using the wavelengths 413.764 nm, 418.660 nm and 401.239 nm. The measurement procedure followed the recommendation of ISO 11885 standard using 5% $HNO_3$ in the matrix. As lab internal standard, Ytterbium was used.

For all experiments, a mass balance was calculated from the mass of cerium broken through the column and the mass retained in the sediment (Online Resources, Eq. 3. 1). The mass in aqueous samples of lab experiments was calculated by multiplying the sampling volume with the measured concentrations. As we collected the complete outflow and measured every second sample, we multiplied the mass of

each sampling point by 2, assuming equal concentrations in neighboring samples. For calculation of the mass in sediments, the effective porosity of $\eta_{eff}$ = 0.35 was used for all calculations and the measured values were corrected by the recovery rate of the digestion method.

## 3.4 Results and Discussion

### 3.4.1 Nanoparticle properties

Polyacrylic acid-coated $CeO_2$ NP had a HDD of <90 nm in all tested water conditions (i.e. deionized, soft surface, and hard surface water) and were stable over the course of the experiments (Table 3. 1). In contrast, NOM-$CeO_2$ NP had a stable HDD of <80 nm in DI water and soft surface water but aggregated in hard surface water (>500 nm). In DI water, PAA-$CeO_2$ NP had a more negative ζ-potential than NOM-$CeO_2$ NP (-48 compared to -35 mV). In soft and hard surface water, ζ-potentials of NOM- and PAA- $CeO_2$ NP were comparable (-22.2 and -21.6 mV in soft surface water and -18.7 and -17.9 mV in hard surface water, respectively, Table 3. 1). For PAA- $CeO_2$ NP, this decrease in ζ-potential did not change NP size. Polyacrylic acid is well known as effective stabilizing coating agent maintaining particle stability in $Ca^{2+}$ concentrations up to 10 mM (Chanteau et al. 2009) which was confirmed by our measurements. However, the decreasing ζ-potential with increasing ionic strength suggests that not only electrostatic, but also steric stabilization mechanisms might be responsible for the high stability of PAA-$CeO_2$ NP. In contrast to PAA- $CeO_2$ NP, NOM-$CeO_2$ NP size increased in hard surface water. Probably, the bridging effect of $Ca^{2+}$ between NOM-coated NP surfaces increased the aggregation process (Philippe und Schaumann 2014). As ζ-potentials seem to be not the determining parameter for NP stabilization, we conclude that different degrees of $Ca^{2+}$ bridging were responsible for the different stability of synthetically and naturally coated NP. The stabilization of $CeO_2$ NP in our study by PAA may be supported by high amounts of access PAA in NP suspension as described below (chapter 3.2.1).

The surface properties of HA-$CeO_2$ NP in soft surface water which were injected into laboratory as well as the artificial bank filtration columns were measured in the beginning and at the end of the lab column experiment. The HDD of HA-$CeO_2$ NP slightly increased during column experiments from 105 to 156 nm and the ζ-potential (-18 mV) was less negative compared to PAA- and NOM-$CeO_2$ NP (Table 3. 1). Due to the presence of natural inorganic and organic colloids in the pond water of outdoor columns, DLS measurements were not applicable in the large-scale experiments.

### 3.4.2 Transport of differently coated $CeO_2$ NP in laboratory column experiments

Different organic coatings as well as varying hydrochemical conditions played an important role in the transport of $CeO_2$ NP in saturated sediment columns (Fig. 3. 1, error bars depict observed maximum and minimum value). Synthetically coated PAA-$CeO_2$ NP showed more breakthrough (50-60 %) and lower retention than NOM-coated $CeO_2$ NP (0-27 %; Online Resources, Table S 3.1). Furthermore, the influence of $Ca^{2+}$ was generally more pronounced for NOM-$CeO_2$ NP compared to PAA-$CeO_2$ NP.

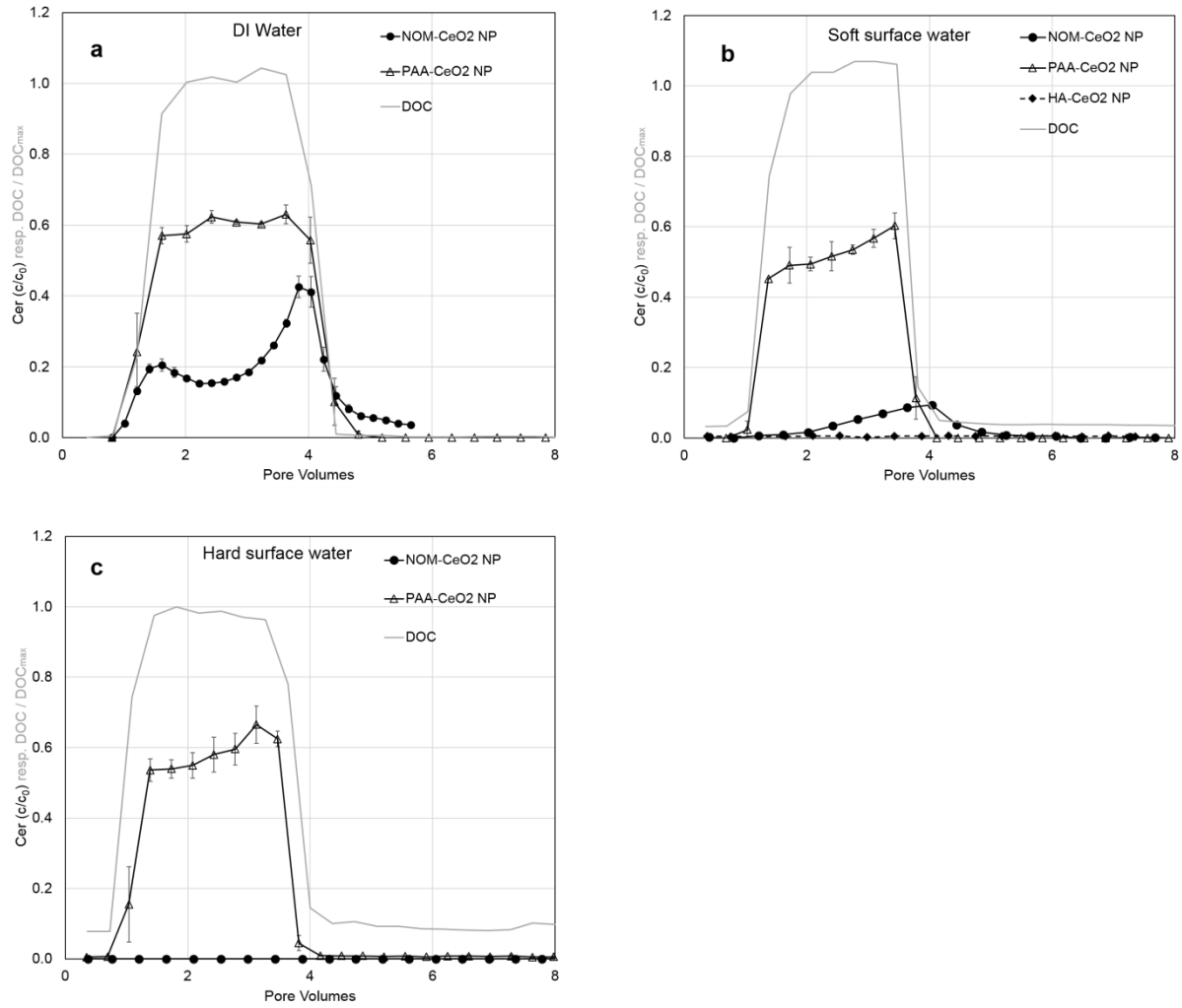


**Fig. 3. 1:** Normalized cerium concentrations in the outflow of the laboratory columns as a function of pore volumes. Circles represent NOM-$CeO_2$ NP, triangles PAA-$CeO_2$ NP and diamonds HA-$CeO_2$ NP; the mobile phase was DI water (a), soft surface water (b) and hard surface water (c). The grey line represents the TOC concentration which can be interpreted as conservative tracer in this context. Errorbars depict the range (maximum and minimum values) of duplicate columns.

Transport in deionized water

Breakthrough in DI water was observed for both PAA - and NOM-$CeO_2$ NP (Fig. 3. 1a). The strongly negative ζ-potentials and colloidal stability of the NP in this medium favored their transport. Nevertheless, both kinds of $CeO_2$ NP were partly retained at the sediment-water-interface (SWI), with retention being stronger for NP coated with NOM. While NP coated with PAA showed a breakthrough of 60% of the initially

injected Ce, only 27% of the NOM-$CeO_2$ NP broke through (Online Resources, Table S 3.1).

Polyacrylic acid-coated $CeO_2$ NP showed almost no retardation in comparison to the tracer (TOC-concentration, Fig. 3. 1a). This transport behavior is similar to the constant breakthrough of PAA-coated $CeO_2$ NP observed by Petosa et al. (2013) in quartz sand columns. In contrast to this steady-state behavior, NOM-$CeO_2$ NP showed a dynamic breakthrough increasing over the course of the experiment (Fig. 3. 1a) which suggests the blocking of attachment sites with increasing NP injection (Bradford et al. 2011). Nevertheless, a decrease in NP concentration after approximately 1.5 PV was observed in our study for NOM-$CeO_2$ NP in DI water. Decreasing breakthrough over time is commonly interpreted as a consequence of mechanical filtration processes leading to pore clogging (Petosa et al. 2013). However, aggregation of $CeO_2$ NP in DI water was not observed (Table 3. 1) suggesting that this explanation might not be valid for our experiment as particles are considerably smaller than the pore system. Therefore, surface attachment processes must play a dominating role for the reduced breakthrough and transport of $CeO_2$ NP through our columns, comparable to observations in other studies with $CeO_2$ NP (e.g., Geitner et al. 2017). The dynamic breakthrough profile of NOM-$CeO_2$ NP is more similar to curves observed for systems with a higher variety of attachment sites as described in the study by Petosa et al. (2013). In our study, a higher variety of functional groups is expected for the NOM coating compared to the PAA coating as PAA has only carboxyl groups while Nordic reservoir-NOM consists of various molecules with different functional groups (Ritchie und Perdue 2003). This enhanced variability of NP led to more possibilities for particle-sediment interactions, hence increasing retardation processes, an effect that has already been described by Bolster et al. (1999). Furthermore, NOM-$CeO_2$ NP showed a tailing after 5 PV which

suggests that NOM-$CeO_2$ NP were reversibly attached in a secondary energy minimum under low ionic strength conditions. In contrast to our results, Geitner et al. (2017) observed a generally lower steric stabilization effect for linear and more uniform coating molecules (such as PVP) compared to larger, more heterogenic structures (such as HA and NOM). This underlines that steric stabilization alone might not be the prevailing stabilizing mechanism for PAA coating, but electrostatic effects are also relevant.

Another factor that might have increased the transport of the PAA-$CeO_2$ NP was the higher background TOC concentration in PAA-$CeO_2$ compared to NOM-$CeO_2$ NP suspension (115 ppm compared to 17 ppm) which might have enhanced the repulsion between sediment surfaces and NP and led to competition for sorption sites. In a study by Chen et al. (2012), the addition of humic acids (1-10 mg $L^{-1}$) to sand columns led to increased $TiO_2$ NP elution, which also suggests an influence of higher TOC concentrations in our study.

The stronger retention of NOM-$CeO_2$ NP was further demonstrated by the retention profiles (Fig. 3. 2a): higher Ce contents in the sediments were measured in the case of NOM-coated NP compared to PAA-$CeO_2$ NP. Our extraction method which included the separation of $CeO_2$ NP from the sediment by ultrasonic bath treatment had a recovery of only 80%. Hence, the Ce contents cannot be interpreted as absolute concentrations, but a clear trend for the distribution of Ce in the columns is visible. Interestingly, NOM-$CeO_2$ NP seem to accumulate in the upper part of the column close to the outflow. This is evidence of detachment processes which are also indicated by the tailing of the breakthrough curve. Typically, particles attached in a shallow secondary energy minimum are detachable for example by hydrochemical changes and are then slowly transported through the column (Braun et al. 2015).

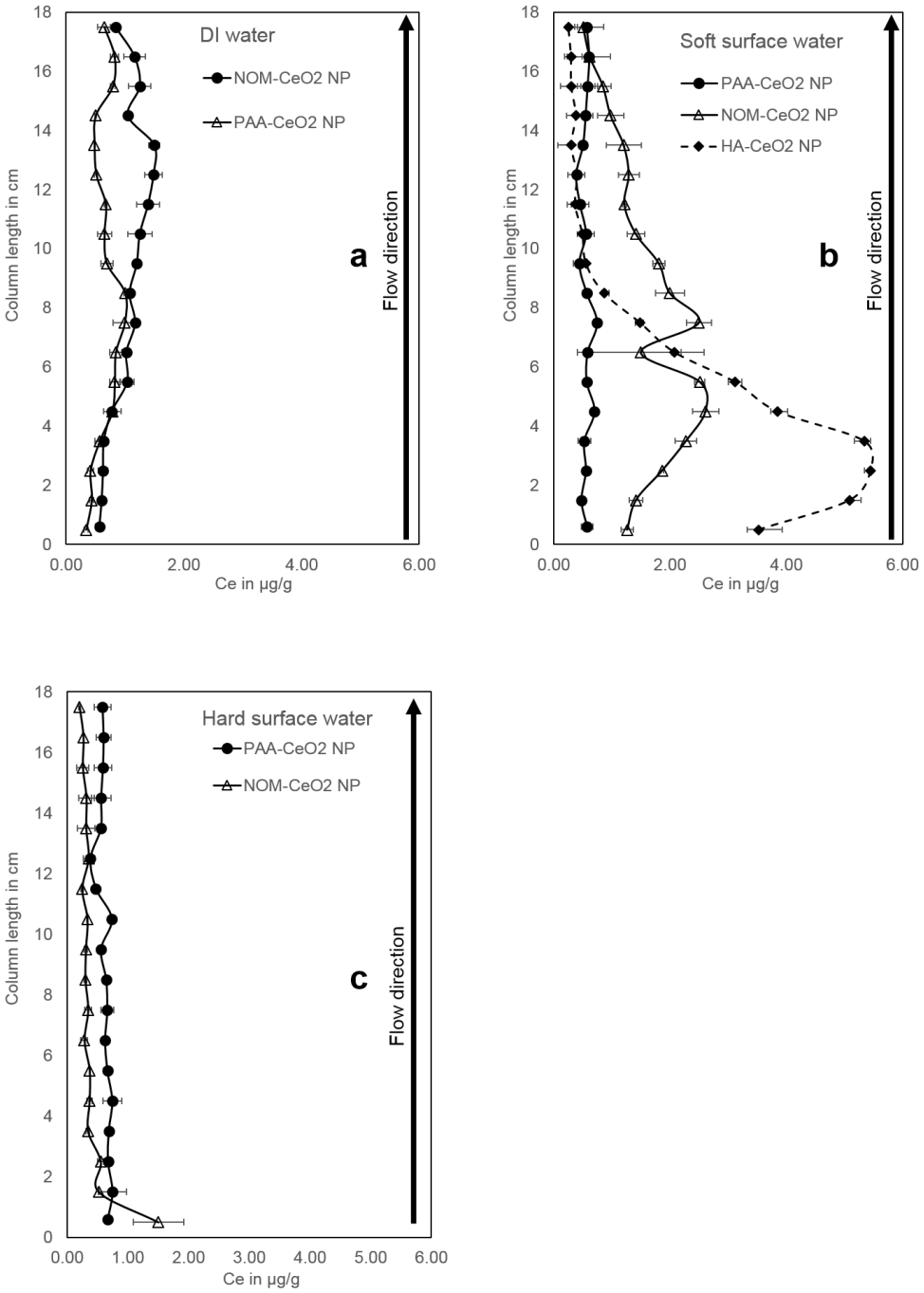


**Fig. 3. 2:** Cerium content in filter sand of the lab columns flushed with DI water (a), soft surface water (b), and hard surface water (c) for PAA- $CeO_2$ NP (circles), NOM-$CeO_2$ NP (triangles), and HA-$CeO_2$ NP (diamonds). Errorbars depict the range (maximum and minimum values) of duplicate columns.

## Transport in soft surface water

In soft surface water (i.e. $Ca^{2+}$ concentration of 2.2 mM) PAA-$CeO_2$ NP broke through without any retardation (Fig. 3. 1b) and with a recovery of 50% of initially injected NP (Online Resources, Table S 3.1). The slight increase of breakthrough over time

indicates saturation of attachment sites. In contrast, NOM-coated NP showed a total breakthrough of less than 10% which appeared obviously retarded. The shift in breakthrough compared to the tracer (TOC concentration) can be explained by equilibrium sorption processes while the tailing of the breakthrough curve indicates non-equilibrium retardation processes typically occurring at the SWI (Kumahor et al. 2016). Enhanced retention as shown by the low recovery in the effluent might be a result of enhanced $Ca^{2+}$ concentrations in soft surface water compared to DI water. Calcium is highly effective in screening the surface charge of NP as well as of sediment surfaces, and this reduces electrostatic repulsion, thus increasing the likelihood of deposition processes (Derjaguin und Landau 1941; Verwey und Overbeek 1948). Petosa et al. (2013) observed no effect of $Ca^{2+}$ on PAA-$CeO_2$ NP for concentrations below 6.7 mM which is in line with the unaffected transport behavior of PAA-$CeO_2$ NP in our study. Instead, NOM-$CeO_2$ NP were already affected by a $Ca^{2+}$ concentration of 2.2 mM. This supports the hypothesis of a higher stability of the synthetic coating agent PAA compared to natural coatings. In the presence of monovalent cations, Li et al. (2013) found a complete breakthrough of NOM-coated $CeO_2$ NP up to NaCl concentrations of 3 mM. This underlines the strong effect of divalent cations on NP stability as present in the water phase of our study.

While the retention of PAA-$CeO_2$ NP was equally distributed over the whole length of the column, NOM-$CeO_2$ NP were mainly retained between 3 and 8 cm depth (Fig. 3. 2b). Compared to the experiments in DI water, NOM-coated $CeO_2$ NP were transported over a shorter distance in soft surface water, due to their lower stability and stronger interaction with the sediment surfaces in the presence of higher ionic strength. This is in line with the low Ce concentrations in the outflow of the column. The NP accumulation at a distance from the column inlet demonstrates that non-

equilibrium sorption and detachment of NP retained in a secondary energy minimum caused a slow NP transport through the column.

As both $CeO_2$ NP showed a similar HDD of <80 nm under soft surface water conditions before application to the column, retention is not expected to be caused by physical straining processes (i.e. deposition of NP aggregates in small pore spaces, e.g., in grain-grain-contact zones). Straining is dependent on the ratio of colloid to median grain size diameter ($d_{50}$). Bradford et al. (2002) found that colloid transport was not influenced by straining in sand columns with a $d_{50}$ as large as 0.71 mm and a colloid size smaller than 0.45 µm. As we have a larger $d_{50}$ (i.e. 1.88 mm) and smaller initial particle sizes (i.e. 75 nm) straining processes are unlikely to occur for non-aggregated NP. Instead, attachment of $CeO_2$ NP to the sediment surfaces supported by the bridging effect of $Ca^{2+}$ were responsible for NP retention. Those effects have been observed for example by Wang et al. (2015) for the transport of PVP-coated Ag NP in soils. Bridging, however, seemed to play a minor role for PAA-$CeO_2$ NP. Chanteau et al. (2009) explained the high stability of those NP with the formation of anionic adlayers on the NP surfaces leading to both electrostatic *and* steric stabilization (Sehgal et al., 2005). In contrast, Torkzaban et al. (2012) observed deposition of PAA-coated quantum dots on sand for $Ca^{2+}$ concentrations as low as 1 mM. The authors explained this by bridging complexation of the carboxylic group of PAA forming bridges between NP and solid surfaces. They used lower particle concentrations ($1.4*10^{11}$ NP $L^{-1}$ compared to $6.1*10^{13}$ NP $L^{-1}$ in our study) which might partially explain the different results. A recent study by Dippon et al. (2018) compared the colloidal stability of NOM- and PAA-coated $CeO_2$ NP in batch experiments, finding a stronger stabilizing effect for NOM compared to PAA. Their experiments were conducted with lower PAA background concentrations (77 ppm compared to 115 ppm in our study). This would lead to the conclusion that the

destabilization of PAA-$CeO_2$ NP by $Ca^{2+}$ might be dependent on the ratio between $Ca^{2+}$ and PAA in the system. Probably, free PAA can remove $Ca^{2+}$ from the solution by reactions with the carboxylic groups, thereby preventing a destabilization of $CeO_2$ NP by $Ca^{2+}$. Additionally, PAA as a manufactured polymer, can have different chain lengths which might be crucial for the occurrence of steric stabilization processes (Ghosh et al. 2011). Therefore, it is difficult to compare the results of studies that used different PAA-coated NP when information about background TOC and chain length is not provided.

In soft surface water we investigated the transport of $CeO_2$ NP with a second kind of natural coating agent, namely Humic Acids (Fig. 3. 1b). Due to the availability of large quantities of this coating agent we chose it for the experiments in the large-scale artificial bank filtration system. Therefore, this laboratory experiment provides a reference to the situation applied in the outdoor columns. Cerium concentrations in the outflow of the column were in the range of the limit of quantification, thus the transport of HA-$CeO_2$ NP below 20 cm was very low. This demonstrates that a coating with HA was less stabilizing against aggregation and sedimentation than NOM indicating that different natural organic coatings vary in their stabilizing properties. This has also been shown by Li et al. (2017) who compared the stabilization of $CeO_2$ NP by NOM of the Ohio River (OR) and Suwannee River-HA and found a stronger stabilization by OR-NOM. A recovery of 96 ± 8 % of Ce in the sediment proved the low transport of HA-$CeO_2$ NP under soft surface water conditions (Online Resources, Table S 3.1). The main part of the NP was retained in the column already between 2 and 5 cm depth (Fig. 3. 2b). The enhanced ionic strength in soft surface water compared to DI water caused a slight aggregation of HA-$CeO_2$ NP (185 nm at the end of the experiment, Table 3. 1). However this particle

size is too low to explain NP retention by mechanical filtration or straining processes (Bradford et al. 2002). It is more likely that chemical attachment processes, such as $Ca^{2+}$ bridging or attachment in a deeper energy minimum were responsible for NP retention. As particles are mainly retained close to the column inlet the reversibility of attachment seems lower compared to NOM-$CeO_2$ NP. However, highest Ce contents were not detected in the very first section of the column which suggests that HA-$CeO_2$ NP are transported through the column very slowly following attachment and detachment processes. Such a bell-shaped retention profile has also been observed by Tong et al. (2005) for bacteria transport in quartz sand. The authors attributed this to detachment processes which are more pronounced at the column inlet due to the collision of attached and mobile colloids.

During our experiments, the colloidal stability of HA-$CeO_2$ NP was confirmed by DLS measurements for a time period of 10 h. However, as shown by the column experiment, this cannot be directly related with a high potential for NP transport in sediment columns. Despite their high colloidal stability, HA-$CeO_2$ NP transport was very low. An important reason for this is the presence of the sediment surfaces offering a high number of interaction sites for NP. Those SWI can lead to non-equilibrium attachment and therefore retention of NP as observed by Kumahor et al. (2016).

Transport in hard surface water

Breakthrough of NOM-$CeO_2$ NP was completely prevented in water with a $Ca^{2+}$ concentration of 4.5 mM (Fig. 3. 1c). Under these hydrochemical conditions, increased aggregate sizes were observed (Online Resources, Fig. S 3. 6). Potentially, this enhanced aggregation caused by NP destabilization led to physical straining processes, an additional retention mechanism besides adsorption to

sediment surfaces. This can explain the accumulation of Ce in the upper 2 cm of the column (Fig. 3. 2c). As demonstrated by Bradford et al. (2006) increasing ionic strength promotes straining and this process is most relevant close to the column inlet where particle aggregates enter small or dead pores and get retained. At a greater distance from the inlet, advection, dispersion, and size exclusion lead to flow focusing and therefore minimization of straining processes so that attachment is the determining retention process in deeper sediment layers.

Contrarily, PAA-$CeO_2$ NP exhibited a total breakthrough of 58% under hard surface water conditions showing almost no retardation, which is comparable to the results in DI and soft surface water (Online Resources, Table S 3.2). As for soft surface water conditions, a trend for increasing breakthrough over time is visible suggesting the saturation of attachment sites. The retention profile is also comparable to the one observed in soft surface water (compare Fig. 3. 2b and c). These results prove the strong stabilizing effect of the synthetic coating agent.

For the transport experiment of NOM-$CeO_2$ NP in hard surface water, we observed a very low recovery in sediment and water of only 18% of initially injected Ce. This might be attributed to the strong aggregation of the NP under high $Ca^{2+}$ concentrations which was observed immediately after mixing NP with the water (Online Resources, Fig. S 3. 6). Although the suspension was stirred over the whole experimental duration, not all NP may have reached the column due to sedimentation or aggregation in the tubes. Another possibility is that large $CeO_2$ NP aggregates were caught in the glass frit (pore size 50 µm) at the bottom of the column. This would lead to a much lower input concentration of $CeO_2$ NP than in the other experiments which might have reduced NP breakthrough. However, the complete amount of NP was immobilized at the beginning of the column due to the low colloidal stability of NOM-$CeO_2$ NP. Therefore, we expect that even larger concentrations of

$CeO_2$ NP added to the column would have been retained in the very first part of the column.

Generally, our experiments showed a lower stabilization of $CeO_2$ NP with natural organic coatings that consist of many different molecules leading to variable functional groups on NP surfaces, compared to PAA forming a layer of similar coating molecules on NP surfaces. A study by Geitner et al. (2017) showed contrary results with stronger stabilization provided by HA and NOM than by PVP. This was explained by the better steric stabilization by large, heterogeneous macromolecules than by uniform, linear molecules. However, PAA may have a very strong electrostatic stabilization potential that effectively stabilizes $CeO_2$ NP as shown by Sehgal et al. (2005). Our results have important implications for the fate of NP in the environment. As industrial coatings are replaced or covered by natural organic molecules, their mobility might change dramatically (Louie et al. 2016). According to our results, a lower stability and hence, mobility can be expected when natural coatings replace industrial ones, but this will depend on characteristics of both the industrial coating and the NOM present in the environment.

### 3.4.3 Comparison of laboratory experiments with experiments in a semi-technical scale

In the outdoor sediment columns (SIMULAF), the insights from laboratory column experiments were compared with a system of conditions closer to a real-world-scenario to value the relevance of data gained in small–scale and well-defined laboratory experiments. Besides the larger size of the experiment at semi-technical scale, the presence of natural colloids in the mobile phase and biological activity

(e.g., presence of algae and biofilms) in the outdoor system represent major differences between lab and outdoor experiments.

The injection of HA-$CeO_2$ NP to the laboratory column led to a very low breakthrough suggesting a low risk for HA-$CeO_2$ NP transport through sediment systems (Fig. 3. 1b). This observation was confirmed in the outdoor bank filtration columns: only low amounts of Ce were quantified in the aqueous phase until a depth of 15 cm; in 30 and 50 cm depth most concentrations were below the quantification limit, and in a depth of 90 cm no Ce was detected except for one sampling point (Fig. 3. 3). Thus, the main part of added HA-$CeO_2$ NP was retained in the upper 15 cm.

In the sediments, highest Ce contents were found between a depth of 0 and 5 cm (Fig. 3. 4) which is comparable to our findings in the laboratory (i.e. highest Ce contents between 2 and 5 cm depth, Fig. 3. 2b). Even after an exchange of more than 400 PV in the upper 15 cm most Ce was located in the top sediment layers which indicates a very low mobility and an irreversible attachment of HA-$CeO_2$ NP on sediments of the artificial bank filtration system. In contrast to the lab columns, the calculation of a mass balance in the outdoor columns resulted in unrealistically high recoveries of 200-300 % (Table S 3.2). Due to the larger complexity of the outdoor system, $CeO_2$ NP might have been more heterogeneously distributed in the sediment so that sampling was not representative. Additionally, the upper centimeters of the outdoor columns which retained the main part of the NP contained layers of organic deposits. They can reduce the bulk density of the upper sediment layers leading to an overestimation of total amounts of particles (Online Resources, Eq. 1). Detailed explanations can be found in the Online Resources. Overall, the accumulation and strong retention of $CeO_2$ NP in the upper sediment layers was clearly visible from our experiment and confirmed lab-scale findings.

The accumulation of HA-$CeO_2$ NP in the top sediment layers of outdoor columns was most likely attributed to the attachment of NP to solid surfaces. Straining is unlikely to occur as the NP were shown to be stable under the used hydrochemical conditions and therefore colloid sizes were too small to cause straining (Table 3. 1). Instead, the interactions of NP with sediment surfaces (Kumahor et al. 2016) as well as with biofilms and plants (as shown by Ikuma et al., 2015; Tripathi et al., 2017) were probably important processes in the present experiment. Additionally, the presence of natural colloids is expected to play a central role in NP immobilization (Degenkolb et al. 2018; Hoppe et al. 2015). With a large surface area, colloids offer important attachment sites for NP in soils and are expected to reduce NP transport. However, the NP transport and retention behavior was comparable in both lab (i.e. absence of natural colloids) and outdoor (i.e. presence of natural colloids) experiments considering, that the spatial resolution of sampling in the outdoor experiment was lower than in lab experiments. Hence, natural colloids were not determining for $CeO_2$ NP retention in our study, although they may have interacted with the NP.

The Ce concentrations in the water of the bank filtration system at a depth of 15 cm differed considerably between the two sediment columns, which underlines the challenge of replicating tests in heterogeneous natural systems. Still, the trend in both columns was similar with a Ce breakthrough between 3.5 and 10 h in 15 cm depth, and no breakthrough below.

Changing weather conditions during the 3 weeks of the experiment did not influence NP breakthrough. Even a heavy rain event between day 6 and 8 which reduced the ionic strength in the water did not lead to NP remobilization and enhanced breakthrough (Online Resources, Fig. S 3. 4). In natural systems, heavy rain events may additionally cause enhanced flow velocities depending on the geological setting. As shown by Makselon et al. (2018) this can remobilize NP, but this factor was not

included in our experiments as the pump rate was kept constant and saturated conditions were maintained at all times.

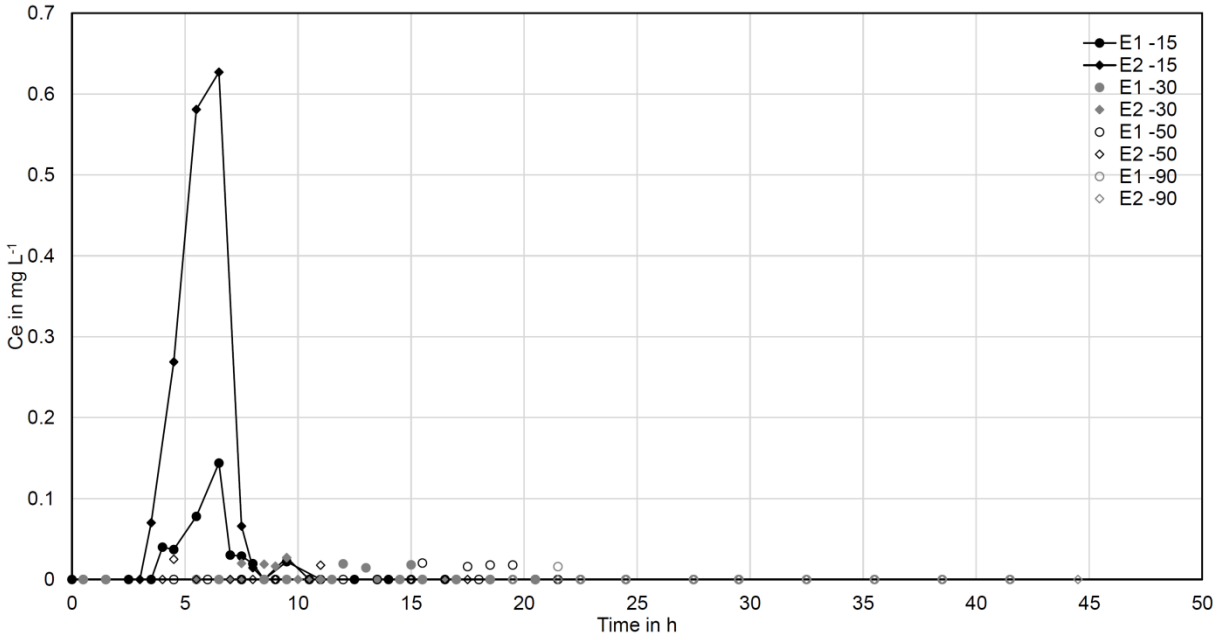


**Fig. 3. 3:** Cerium concentration in the pore water of two replicate columns (E1 and E2) at various sampling depths (15, 30, 50 and 90 cm) of outdoor experiments with HA-$CeO_2$ NP. Breakthrough is illustrated over time and not pore volumes as pore volumes differ between the sampling depths while this graph demonstrates the time-shifted breakthrough in different depths.

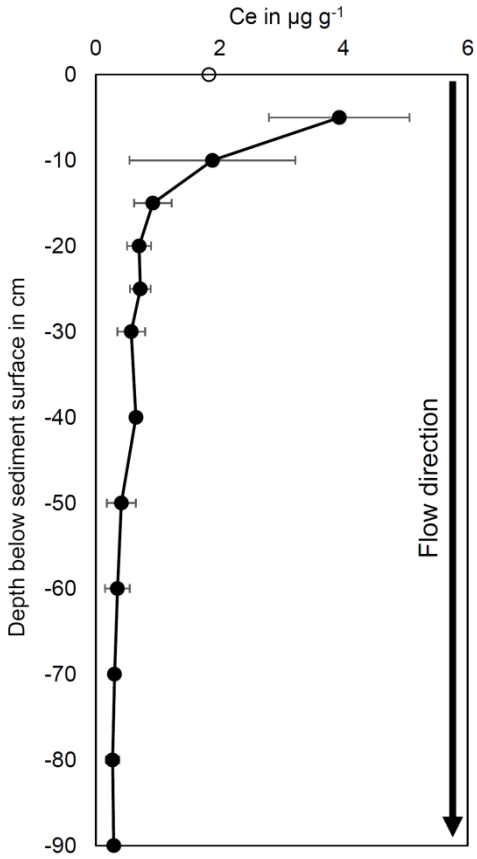


**Fig. 3. 4:** Cerium content in filter sand of the outdoor columns flushed with soft surface water for HA-$CeO_2$ NP. Errorbars depict the range (maximum and minimum value) of 4 replicates (depth 0-30 cm) and 2 replicates (depth 40-90 cm) per column, respectively.

### 3.5 Conclusions

With the laboratory column experiments, we could clearly observe differences between the transport of synthetically, PAA-coated $CeO_2$ NP and natural organic matter-coated $CeO_2$ NP: Changes in solution chemistry did not influence the breakthrough of the NP in the former case where generally a high breakthrough was observed. Instead, NP retention was strongly dependent on the water chemistry in the latter case where higher ionic strength and especially the presence of $Ca^{2+}$ reduced the breakthrough of NOM-$CeO_2$ NP and led to an accumulation of Ce already in the first centimeters of the column. We suggest that for both particles the main retention process was chemical and electrostatic interaction with the solid phase instead of physical retention, such as straining or mechanical filtration. However, the NOM coating caused a strong sensitivity of $CeO_2$ NP to hydrochemical changes leading to enhanced retention at higher ionic strength and $Ca^{2+}$ concentration. In contrast, the PAA coating was less susceptible to increasing ionic strength and added colloidal stability to the NP and, thus, enhanced transport in water-saturated sediment systems. This is in line with our hypothesis that synthetically coated NP will be more mobile than naturally coated particles. However, the stabilizing manufactured coating might decompose or be exchanged against NOM in natural systems (Lau et al. 2013). Most likely this would lead to a reduced transport in the environment.

The comparison of NOM-$CeO_2$ NP with HA-$CeO_2$ NP shows that different natural coating agents have different effects on the colloidal stability and transport of NP. Additionally, an important transport mechanism of PAA-coated $CeO_2$ NP seems to be attributed to the high concentrations of excess PAA in suspension, which is not attached to NP surfaces. Entering the environment, a strong dilution of this

background DOC is expected which would lead to lower NP transport than observed in our study. Therefore, future studies should exclude the effect of excess PAA by removing non-bound molecules before addition to the column.

Breakthrough of HA-$CeO_2$ NP proved to be very low in both small-scale laboratory as well as large-scale near natural experiments. In our experimental setup, changing weather conditions such as intense rain events were not the driving factor for NP transport. Furthermore, the presence of biological activity and natural colloids did not significantly change the transport behavior of HA-$CeO_2$ NP. These results contradict our expectation of a stronger NP retention in more complex systems. Instead, we can conclude that important transport mechanisms for organically coated metal-oxide NP can already be described with less work-intensive but simplified laboratory experiments. In future studies, this should also be tested for a higher number of NP (e.g., PAA-$CeO_2$ NP).

From the results of our study, we can conclude that an accumulation of naturally coated $CeO_2$ NP in surficial sediment layers of bank filtration systems can be expected. These upper sediment layers might be exposed to shear forces, water turbulences and changing hydrochemical conditions when in contact with the river bed. Possibly, this might lead to remobilization of $CeO_2$ NP when physico-chemical conditions change, a mechanism which was already demonstrated for Ag NP by Degenkolb et al. (2018).

# 4 Retention and remobilization mechanisms of environmentally aged silver nanoparticles in an artificial riverbank filtration system

Authors: Laura Degenkolb, George Metreveli, Allan Philippe, Anja Brandt, Kerstin Leopold, Lisa Zehlike, Hans-Jörg Vogel, Gabriele E. Schaumann, Thomas Baumann, Martin Kaupenjohann, Friederike Lang, Samuel Kumahor, Sondra Klitzke

Post-print, published in “Science of the Total Environment”, original publication (open-access) can be found under https://doi.org/10.1016/j.scitotenv.2018.07.079
0048-9697

## 4.1 Abstract

Riverbank filtration systems are important structures that ensure the cleaning of infiltrating surface water for drinking water production. In our study, we investigated the potential risk for a breakthrough of environmentally aged silver nanoparticles (Ag NP) through these systems. Additionally, we identified factors leading to the remobilization of Ag NP accumulated in surficial sediment layers in order to gain insights into remobilization mechanisms.

We conducted column experiments with Ag NP in an outdoor pilot plant consisting of water-saturated sediment columns mimicking a riverbank filtration system. The NP had previously been aged in river water, soil extract, and ultrapure water, respectively. We investigated the breakthrough in different depths and retention of NP. In subsequent batch experiments, we studied the processes responsible for a remobilization of Ag NP retained in the upper 10cm of the sediments, induced by ionic strength reduction, natural organic matter (NOM), and mechanical forces. We determined the amount of remobilized Ag by ICP-MS and differentiated between particulate and ionic Ag after remobilization using GFAAS. The presence of Ag-containing heteroaggregates was investigated by combining filtration with single-particle ICP-MS.

Single and erratic Ag breakthrough events were mainly found in 30cm depth and Ag NP were accumulated in the upper 20cm of the columns. Soil-aged Ag NP showed the lowest retention of only 54%. Remobilization was induced by the reduction of ionic strength and the presence of NOM in combination with mechanical forces. The presence of Calcium in the aging- as well as the remobilizing media reduced the remobilization potential. Silver NP were mainly remobilized as heteroaggregates with natural colloids, while dissolution played a minor role.

Our study indicates that the breakthrough potential of Ag NP in riverbank filtration systems is generally low, but the aging in soil increases their mobility. Remobilization processes are associated to co-mobilization with natural colloids.

Keywords: heteroaggregation, nanoparticle transformation, breakthrough, mobility, reversibility

## 4.2 Introduction

Riverbank filtration systems are natural systems that may ensure the cleaning of surface water for recharging groundwater. Due to their natural cleaning capacity, i.e. through mechanical filtering, sorption, and biodegradation processes, these systems have become increasingly important for drinking water production (Sprenger et al., 2017). The effectiveness of riverbank filtration in removing microorganisms such as pathogens (i.e. bacteria and viruses) from infiltrating surface water has long been recognized in Germany (Schmidt et al., 2003). Nowadays, there is a much larger number of potential pollutants in anthropogenically influenced water bodies which need to be removed before drinking water usage (Schmidt et al., 2003). One example are nanoparticles (NP) which are included in many industrial applications and consumer products (“Danish Consumer Council. The Nanodatabase.” 2018). Amongst synthetic inorganic NP, silver nanoparticles (Ag NP) were the most frequently used nanomaterials in consumer products until 2015 (Vance et al., 2015).

After being released into rivers and lakes (Cleveland et al., 2012), Ag NP can undergo various transformation processes. In the following manuscript, the processes leading to the transformation of NP in the environment without complete loss of the original NP phase are termed “aging processes” (Schaumann et al., 2015). Surface oxidation, coating with natural organic matter (NOM), and cation-induced bridging between NP are aging phenomena which significantly influence the surface properties of NP (Darlington et al., 2009; Nel et al., 2006; Schaumann et al., 2015). Aging in different environmental media therefore has a strong impact on the fate of NP and their colloidal and chemical stability in natural surface water and porous systems. However, the fate of these environmentally modified NP is still underrepresented in the literature (Selck et al., 2016).

Recent studies conducted in complex aqueous systems suggest that unaged Ag NP mainly accumulate in upper sediment layers due to (hetero)aggregation processes and sorption to the solid phase (Coleman et al., 2013; Furtado et al., 2015). Additionally, an accumulation of NP in biofilms is often observed (Ferry et al., 2009; Nevius et al., 2012). Studies investigating the fate of Ag NP in soils have shown that horizontal and vertical translocation is very limited (Schlich et al., 2017) and a remobilization of Ag NP from the solid phase is negligible (Hoppe et al., 2015). Although there are experiments investigating the transport of NP in laboratory sediment columns (such as Zhang and Zhang, 2014 for Ag NP, Lv et al., 2016 for $TiO_2$, Fang et al., 2016 for $CeO_2$) and aquifers (Adrian et al., 2018), main retention mechanisms of riverbank filtration systems (such as filtration by biofilms or retention on clay minerals) are not taken into account in most of them. Studies that consider more environmentally relevant conditions suggest that the transport potential of engineered NP in the real environment will be much lower than predicted by laboratory experiments (Emerson et al., 2014). This highlights the need for more complex and realistic outdoor experiments. Therefore, the aim of our study was to investigate the breakthrough and retention of aged Ag NP in riverbank filtration systems and to understand the mechanisms that lead to their remobilization by answering the following questions:

1*) Does the aging of Ag NP in soils or rivers before reaching riverbank filtration systems affect their breakthrough and retention in natural sediments?* Recent studies about NP stability clearly show that a coating with NOM can enhance the colloidal stability of NP (Philippe and Schaumann, 2014). In our study, we focused on aging processes in rivers and soils, leading to the the coating of NP with NOM and cation-induced aggregation, two important processes affecting NP stability and fate. Additionally, the dominating process in natural surface waters is heteroaggregation

due to the high concentration of natural colloids in environmental systems compared to NP concentrations (Lowry et al., 2012; Praetorius et al., 2014). This might also lead to the co-transport of NP with natural colloids in porous systems (Makselon et al., 2017; Neukum et al., 2014). To account for this process, we used natural, colloid-containing pond water as mobile phase for the transport experiment.

2) *Which mechanisms can induce the remobilization of Ag NP retained in surficial sediment layers?* Long-term mesocosm studies show that the majority of NP in aquatic ecosystems is accumulated in upper soil and sediment layers (i.e. Lowry et al., 2012). Therefore, we hypothesized that a large part of Ag NP would be accumulated in the surficial sediment layers of riverbank filtration systems. In natural systems, these upper sediments are exposed to varying shear forces caused by turbulence in rivers and to changing hydrochemical conditions. While heavy rain falling could dilute river water and reduce ionic strength, flooding might transport a large amount of NOM from floodplain soils into rivers. Both ionic-strength reduction and enhanced NOM concentrations in combination with shear forces have been shown to cause disaggregation of Ag NP homoaggregates (Metreveli et al., 2015). Based on these findings, we aimed at identifying conditions that may cause a remobilization of Ag NP immobilized in the surface sediments of an artificial riverbank filtration system. To detect the main remobilization mechanisms, the properties of remobilized Ag were characterized. This included the differentiation between dissolved and particulate Ag as well the analysis of the aggregation state of Ag NP. Both characteristic are of high importance for a prediction of the fate of remobilized Ag and potential consequences of Ag remobilization.

Our study was undertaken in two parts:

1. The breakthrough and retention of Ag NP, aged in river water, soil extract, and ultrapure water respectively, were studied in a near-natural, water-saturated porous system. The experiments were conducted in an outdoor artificial riverbank filtration system. Compared to laboratory studies as used in the literature (i.e. El Badawy et al., 2013; Liang et al., 2013; Sagee et al., 2012) our system had larger dimensions and was influenced by atmospheric changes. The biological activity was driven by the surrounding pond water conditions.

2. In laboratory batch experiments, we systematically studied the effect of ionic strength, NOM, divalent cations, and mechanical forces on the extent of Ag remobilization. To gain a more mechanistic process understanding, those experiments were conducted under less realistic conditions, but had a stronger focus on analytics including the use of a high amount of analytical tools. In order to measure dissolved Ag we used a novel interpretation strategy of Graphite Furnace Atomic Absorption Spectrometry (GFAAS) which allowed $Ag^+$ to be distinguished from Ag NP also when $Ag^+$ ions were adsorbed to natural colloids or complexed by organic ligands (Feichtmeier and Leopold, 2014). The presence of Ag NP-containing heteroaggregates was tested by combining 1 µm-filtration and Single-Particle Inductively Coupled Plasma- Mass Spectrometry (SP-ICP-MS). With the multiplicity of analyses, we were able to not only identify important remobilization mechanisms, but also characterize the properties of remobilized Ag NP. For some less common analyses, the theoretical background is described in the Supporting Information (SI).

## 4.3 Material and Methods

### 4.3.1 Nanoparticles

We used citrate-stabilized Ag NP that were produced according to the method of Turkevich et al. (1951) modified for Ag which is described in more detail in Klitzke et al. (2015). Transmission electron microscopy (TEM) images can be found in the SI of Metreveli et al. (2015). Particles had a diameter (z-average, determined by dynamic light scattering) of 34 ± 1 nm, a polydispersity index of 0.34 ± 0.01 (both obtained from six replicate measurements) and a ζ-potential of − 60.8 ± 0.9 mV (obtained from three replicate measurements).

### 4.3.2 Aging procedure

In order to apply Ag NP at more environmentally relevant state, Ag NP were aged in soil extract, and river water (Table S 4. 1). Additionally, Ag NP equilibrated in ultrapure water (UPW) were used as a reference for un-aged Ag NP.

Ultrapure water was prepared by an Ultrapure Water System (Evoqua, Water Technologies) and had an electrical conductivity (EC) of 0.055 µS/cm.

Soil extract was prepared from samples of a Fluvisol taken from a meadow close to the River Rhine near Leimersheim, Germany (GPS: N49°08’13.62’’ E008°21’39.6’’).

The soil was sieved (2 mm), homogenized and stored field-moist in the refrigerator (4 °C) before use. Soil samples were mixed with water (1:10 mass ratio), shaken on a horizontal shaker (130 rpm, KS501 digital, IKA Labortechnik) for 16 h, and subsequently filtered over a 1.2 µm cellulose nitrate membrane (Type 11303–047 N, Sartorius). To remove suspended soil colloids (d > 30 nm, ρ = 1.2 g $cm^{-3}$) the extract was ultracentrifuged (Optima TL, Beckmann) at 156,990 x *g* for 1.5 h at 10 °C. The method, adopted by Klitzke et al (2015), extracts both soluble and colloidal

components of the soil. However, in the subsequent centrifugation step we removed colloidal particles in order to study the effect of dissolved soil components only.

River water was sampled from the River Rhine close to the soil-sampling site (GPS: N49°07'26.4'' E008°21'48.3''). Water was filtered (0.1 µm cellulose-nitrate membrane, Whatman) to remove all micron-sized particles.

Soil extract and river water were characterized for pH, dissolved organic carbon (DOC) concentration (TOC-5050 A Shimadzu) and the concentration of main elements (K, Mg, Ca, Na, Al, Fe, and Mn) measured by ICP- optical emission spectrometry (OES), iCAP 6000, Thermo Scientific, Table S 4. 1).

Aging of NP was done by shaking (8 rpm, end-over-end shaker GFL 3040) of a suspension of citrate-stabilized Ag NP (final concentration in the suspension 20 mg $L^{-1}$ Ag NP) in the respective medium for 24 h. Previous experiments showed that this time is sufficient for the sorption process of NOM to NP surfaces to reach equilibrium. The shaking procedure was carried out in ambient light but without any direct sunlight. The ζ-potential of the Ag NP was determined directly after the aging procedure.

### 4.3.3 Water-saturated sediment columns

The experimental setting of the artificial riverbank filtration system and the applied analytical methods are summarized in Fig. 4. 1.

The transport experiments were conducted on the German Environment Agency's facility for the simulation of riverbank and slow sand filtration (SIMULAF) located in Berlin, Germany. We used three large-scale, water-saturated sediment columns (diameter 1.13 m, filter area 1 m², filter length 1.5 m; followed by a supporting layer of

0.2 m) with a water head of 10 cm, which are embedded in a slow sand filtration pond and are flown through by surrounding pond water extracted on-site from a quaternary aquifer (Fig. 4. 1). This offers the possibility to study a near-natural system where biological processes including biofilm formation take place and natural colloids are present. The columns were filled with coarse-grained medium sand 12 months before the start of the experiment ($d_{50}$: 0.38 mm, bulk density in the top 10 cm: 1.76 g $cm^{-3}$; $Fe_{tot}$: 1.143 ± 0.094 g $kg^{-1}$, $Al_{tot}$: 0.869 ± 0.135 g $kg^{-1}$ draining/supporting layer: coarse-grained sand, $d_{50}$: 1.8 mm; grain size distribution of both sands see Fig. S 4. 1). For the experiment, they were fed with a mixture of the pond water (pH 7.0, ionic strength 18.4 mM), and reverse osmosis water (mixing ratio v/v = 1:4). The pH value, EC as well as cation and anion concentrations of this mixture were determined (Table S 4. 2 and Table S 4. 3).

We collected water samples from sampling ports in various depths (30 cm, 50 cm, and 90 cm). The sampling ports consisted of perforated PVC tubes (horizontally installed across the filter area) connected via a stainless steel section to PTFE tubing, leading to a vacuum pump. Additionally, samples were taken at the outflow (i.e. after 1.5 m of sediment passage). Probes were installed at the outflow for the recording of hydrochemical parameters such as EC (Tetracon 325, WTW), pH (SenTix 41, WTW), oxygen content (CellOx 325, WTW), and redox potential (SenTix ORP, WTW, values were corrected for the standard potential of the redox probe relative to the hydrogen normal electrode at 20 °C, i.e. + 211 mV). In addition, EC was monitored in the supernatant.

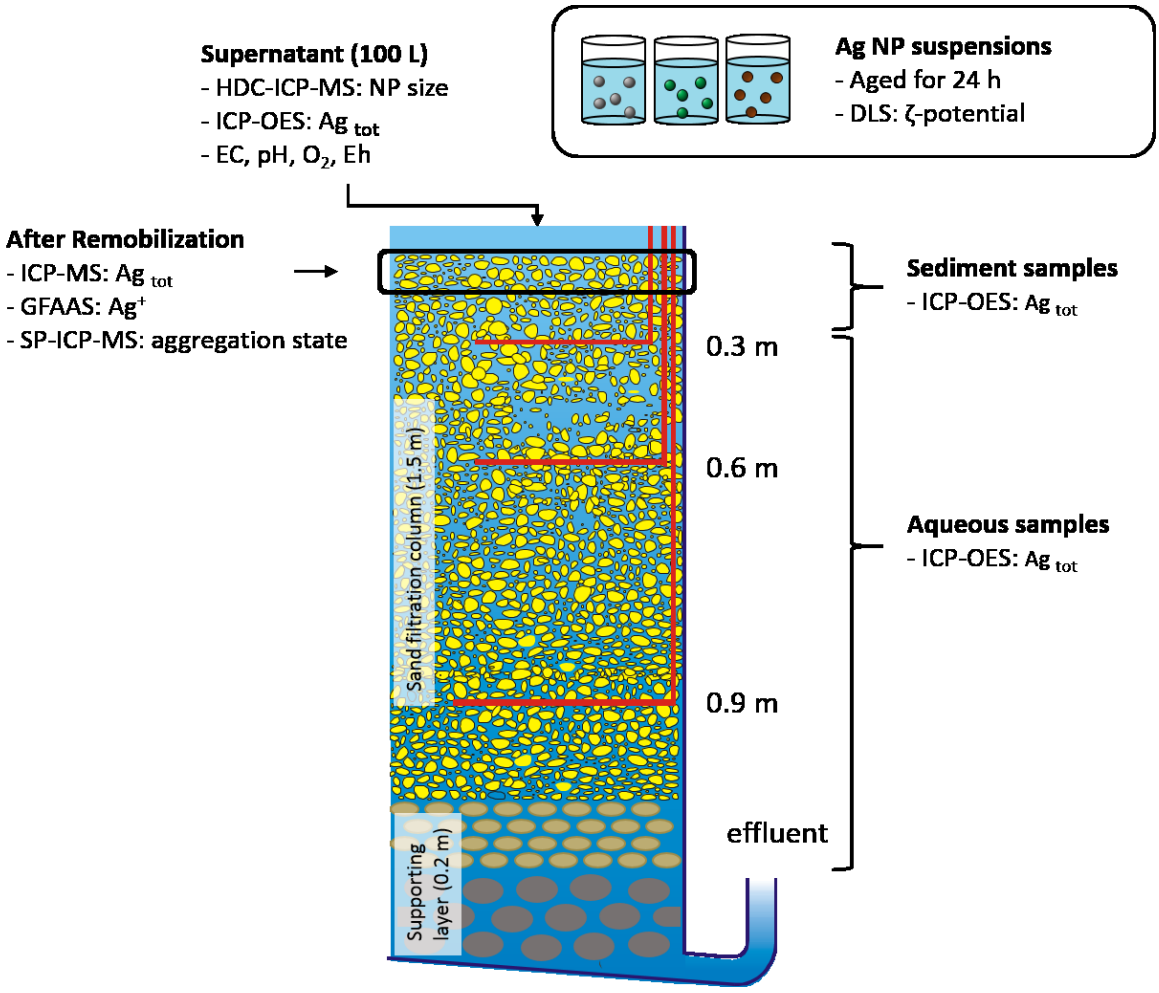


**Fig. 4. 1:** Cross section of water-saturated sediment columns. The horizontal tube of the sampling ports in 0.3, 0.5 and 0.9 m depth is composed of PVC, the vertical tube of stainless steel. At the top end of the stainless steel tubes, PTFE tubes lead to a vacuum pump. Explanations surrounding the graph describe the main analytical techniques used and parameters measured during this study, including total silver (Ag tot ), dynamic light scattering (DLS), electrical conductivity (EC) and redox potential (Eh).

### 4.3.4 Design of near-natural column experiments

A filter velocity of 0.2 m $d^{-1}$ (pore velocity 0.5 m $d^{-1}$) was adjusted and kept constant throughout the entire experiment. This filter velocity was selected to allow for diffusive transport and to minimize any potential shear forces in the flow system. Tracer experiments were conducted prior to NP application. As tracer 400 mL of a NaCl solution (25 weight-%), diluted up to 5 L with infiltrating water, was added to the supernatant as pulsed application. For the detection of the tracer the EC was recorded in the water head above the column, in the 3 sampling depths, and at the outflow. The tracer experiments were conducted 15 days prior to the start of NP

application to ensure that added NaCl had completely left the system to avoid any interference with the NP due to increasing ionic strength.

Prior to the start of NP injection, blank samples of the water head, as well as from the individual depths and the outflow were taken. In each of the three columns, a suspension of one kind of the differently aged NP was added to the supernatant as pulsed application to reach a final concentration of 1 mg $L^{-1}$ Ag in the supernatant. This is higher than environmentally relevant concentrations but high enough to still analytically quantify the particles. The infiltrating volume of the spiked supernatant amounted to 100 L (i.e. 0.2 pore volumes of the entire column volume). After gentle stirring of the supernatant of the column, water samples were taken to determine initial Ag NP concentrations (5 replicates) in the water head and to characterize Ag NP size using Hydrodynamic Chromatography coupled with an Inductively Coupled Plasma- Mass Spectrometer (HDC-ICP-MS, XSeries 2, Thermo Scientific; for detailed information see SI). Water samples at the outflow and in the various depths were taken over the course of 19 weeks (29$^{th}$ of April 2014 until 13$^{th}$ of September 2014). For analysis, a sample volume of 10 mL was transferred into a crucible and dried at 40 °C until complete evaporation of the water. To digest Ag NP, concentrated nitric acid was added. The acid was evaporated to a remainder of approximately 0.5 mL and subsequently diluted with UPW to a volume of 25 mL. The recovery of this method was determined to be 95 ± 10 % (Table S 4. 4 in SI)

To quantify concentrations of Ag NP retained in the column, sediment samples in 0-10, 10-20, and 20-30 cm depth were taken at three different ”zones” to account for any heterogeneity in the system at the end of the experiment. At each zone, four to six samples were taken. The samples of each depth were homogenized to one sample and stored at 4 °C. Sediment samples were dried for 24 h at 105 °C, prior to

digestion. Concentrations of Ag were determined following nitric acid ($HNO_3$, 69 %) digestion in closed vessels at 185 °C for 8 h.

The total Ag content in aqueous and sediment samples was analyzed using ICP-OES (iCAP 6000, Thermo Scientific, λ = 328.0 nm).

Recoveries (R) of Ag in the sand were calculated according to equation 1:

$$R = \frac{(c_{sand1} + c_{sand2} + c_{sand3}) * d_{bulk} * V_{sand}}{c_{water} * V_{water}} \quad (1)$$

with $c_{sand1}$ being Ag concentration in the sand (depth 0-10 cm), $c_{sand2}$ being Ag concentration in the sand (depth 10-20 cm), $c_{sand3}$ being Ag concentration in the sand (depth 20-30 cm) all in mg $kg^{-1}$; $d_{bulk}$ being the bulk density of the sand [kg $L^{-1}$]; $V_{sand}$ being the volume of the sand in the respective depth [L]; $c_{water}$ being the initial Ag concentration in the supernatant [mg $L^{-1}$]; $V_{water}$ being the water volume of the supernatant [L].

4.3.5 Zeta potential and size of nanoparticles

Nanoparticles used for the column experiments were characterized prior to and after the aging procedure regarding their size and ζ- potential.

The ζ- potential of aged NP stock suspensions ($c_{Ag}$ = 20 mg $L^{-1}$) was analysed using a Zetasizer 2000 photon correlation spectrometer (Malvern instruments) and calculated based on the electrophoretic mobility of the NP (using the Helmholtz-Smoluchowsky equation).

Particle sizes in the column supernatant were determined by HDC-ICP-MS (SI, section 2.2) as the presence of natural colloids would interfere with measurements of Ag NP by dynamic light scattering (DLS).

### 4.3.6 Remobilization experiments

Batch experiments with the sediment samples of the first 10 cm of the three columns, each containing NP with a different aging history, were conducted to understand the reversibility of NP attachment. We investigated the amount of potentially remobilizable Ag as well as the characteristics of remobilized Ag to gain information on remobilization mechanisms. Silver concentrations in these sediments accumulated during column experiments were 0.48, 0.70 and 0.31 mg $kg^{-1}$ for UPW-, river water- and soil-aged Ag NP. The sediment samples were subjected to a remobilization procedure with varying mechanical forces as well as hydrochemical conditions (Table 4. 1). Batch experiments were conducted in triplicates.

**Table 4. 1:** Remobilization procedure which includes applying mechanical forces and changing hydrochemical conditions.

| **Mechanical forces** | | **Hydrochemical conditions** | |
|---|---|---|---|
| **Force** | **Concept** | **Remobilization medium** | **Concept** |
| Manual shaking, 5 s | Weak forces | UPW | Ionic strength reduction |
| Horizontal shaking, 24 h, 130 rpm | Medium forces | Soil extract (DOC 5.5 mg/l) | Presence of NOM and $Ca^{2+}$ |
| Ultrasonic bath[1] (USB), 5 min, 35 kHz | Strongest forces (operationally defined) | SR-NOM (30 mg/l) | Presence of Model-NOM |
| | | $NH_4NO_3$ (0.1 M) | Potential of $Ag^+$ release |

[1] USB: 2x240 W, Bandelin Sonorex RK 255H

The soil extract was obtained from the floodplain soil of the River Rhine using the same procedure as for aging experiments (see section 2.2). The Suwannee River-NOM (SR-NOM) powder was obtained from the International Humic Substances Society (IHSS). The preparation of the stock solution is described in the SI.

$NH_4NO_3$ solution can be used for the determination of the cation exchange capacity of soils (DIN ISO 13536) due to the strong sorption of $NH_4^+$ to soil surfaces, thereby exchanging cations originally bound to surfaces. $NH_3$ also forms stable complexes with $Ag^+$ ions which promotes the dissolution of Ag. Therefore, $NH_4NO_3$ solution was

used as remobilizing medium before GFAAS measurements to investigate the potential of $Ag^+$ ion release of retained Ag NP.

The chemical composition of soil extract and SR-NOM solution are summarized in Table S 4. 5.

Sediments were mixed with each of the four types of remobilizing media (Table 1) in a ratio of 1:5 (10 g sediment + 50 mL of remobilizing medium). The pH of the solutions was measured and adjusted with dilute NaOH to 8 ± 1 if necessary (pH-Meter 761 Calimatic, Knick, Th. Karow GmbH). In this pH range Ag NP have a negative ζ-potential. After the remobilization procedure the pH was checked again.

At the end of the remobilization procedure sediments were down-centrifuged using a cut-off diameter of 3 µm (corresponding to 1.25 µm for Ag NP) which was smaller than the mean size of the sand particles in the columns (7.3 x *g* calculated for spherical $SiO_2$ particles, 5 min). The supernatant containing remobilized Ag was stored in amber bottles at 4 °C until analyses. The samples were analyzed for total Ag and Al by ICP-MS following acid microwave digestion (section 2.7.1).

Particle size and morphology as well as elemental composition were determined by Scanning Electron Microscopy (SEM) coupled with an Energy Dispersive X-Ray (EDX) analysis (section 2.7.4).

A combined approach of filtration and SP-ICP-MS was used in order to investigate the aggregation state of remobilized Ag NP (section 2.7.3). Differentiation of particulate and dissolved Ag was done using GFAAS (section 2.7.2).

### 4.3.7 Analyses of remobilization samples

<u>Determination of total Ag and Al in remobilization experiments</u>

In order to determine the concentration of total Ag remobilized from sediment samples, the supernatants obtained after centrifugation were digested by acid microwave digestion (MARS Xpress, CEM, Matthews, USA). For the digestion, a mixture of nitric acid ($HNO_3$, ≥65%, p.a., ISO, ROTIPURAN, Carl Roth, Karlsruhe, Germany) and hydrochloric acid (HCl, 35%, ROTIPURAN Supra, Carl Roth, Karlsruhe, Germany) was prepared at a volume ratio of 1:1. In Teflon digestion vessels 10 mL sample were mixed with 4 mL acid mixture. In order to check the background concentration of analyzed elements, 10 mL UPW were also mixed with 4 mL acid mixture. The digestion was performed using a two-step temperature program (temperature ramp of 30 min from room temperature to 95 °C and subsequent 30 min irradiation at a constant temperature of 95 °C at 800 W). After cooling, the digested samples were diluted with 28 mL UPW and analyzed by ICP-MS (XSeries 2, Thermo Scientific). The detector signal drift was corrected by an internal standard Rh (Rhodium internal ICP-MS standard Fluka, Sigma-Aldrich, St. Louis, USA). In order to observe a trend in the remobilization of natural inorganic colloids, the concentration of Al was also measured in the digested samples.

For quality control of the ICP-MS analysis we also measured the reference materials TMDA-51.5 and TMDA-54.5 (both from LGC Standards, Wesel, Germany) containing Ag and Al. The determined concentrations of Ag and Al in both reference materials were in the range of the nominal values given by the provider showing high accuracy of the ICP-MS measurements (Fig. S 4. 2). The limit of detection (LOD) and limit of quantification (LOQ) were 0.05-0.2 µg/L and 0.14-0.5 µg/L for Ag and 1-5 µg/L and 3-11 µg/L for Al, respectively.

Graphite Furnace Atomic Absorption Spectroscopy

Graphite furnace AAS measurements were conducted from selected samples of the remobilization experiment treated with ultrasonic bath (USB) in UPW, soil extract, and $NH_4NO_3$ for the three types of differently aged Ag NP. Measurements were performed using a high-resolution continuum source atomic absorption spectrometer contraAA 600 (Analytik Jena AG, Germany).

For data interpretation, the atomization delay ($t_{ad}$) was determined as first described by Feichtmeier and Leopold (2014). Briefly, $t_{ad}$ is the time from the starting point of the atomization process until the maximum of the absorbance signal. The maximum was determined by fitting a polynomial or Gaussian function on the absorbance signal, depending on the signal shape. Obtained $t_{ad}$ values indicate the presence of $Ag^+$ and/or can be used to determine Ag NP size after calibration of the method (for details see SI, section 1.1, Theoretical considerations). To prove the applicability of this method to the samples of the remobilization experiment, the matrices of those samples were spiked with $Ag^+$ and Ag NP and GFAAS measurements were conducted. Statistically significant differences of $t_{ad}$ values were obtained when comparing $t_{ad}$ of $Ag^+$ ions with 5 nm Ag NP ($t_{ad}(Ag^+)$=1.338 ± 0.009 s; $t_{ad}$(5-nm-AgNP)=2.201 ± 0.016 s; n=4). Hence, an indication for $Ag^+$ ions was given by an early peak or shoulder at $t_{ad}$= 1.34 ± 0.01 s, which was clearly detectable in a concentration range from 5 to 30 µg $L^{-1}$. Precision of $t_{ad}$ determination calculated as standard deviation (SD) with n≥4 was found to range between 0.01 and 0.08 s for replicate measurements. Day to day variation of $t_{ad}$ - including usage of different graphite platforms - was in a range of 0.15 s. Moreover, no matrix effects on $t_{ad}$ were observed in the media studied here, independent on whether $Ag^+$, Ag NP or a mixture were present (see Fig. S 4. 4). The detection limit of Ag with this method was 1.23 µg $L^{-1}$.

Size calibration was performed using commercially available Ag NP suspensions with defined particle sizes as standard solutions in a size range from 5 to 200 nm, diluted to the desired concentration. With the found $t_{ad}$-size-correlation, NP size given as modal diameter (most commonly found size distribution) was calculated. The resulting calibration function ($t_{ad}$ = 0.144 ln (NP size [nm]) + 1.963; $R^2$= 0.9902; N= 32) is shown in Fig. S 4. 3 and revealed high precision. The lower size limit as derived from this calibration was found to be as small as 1.1 nm. Hence, the minimum Ag NP size that can be distinguished from $Ag^+$ ions using this size calibration is 1.1 nm. Furthermore, no effect on $t_{ad}$ was observed when silver concentration varied in a range between 2.5 and 40 µg $L^{-1}$.

Further experimental details on sample preparation, calibration and instrumental parameters of GFAAS measurements can be found in the SI (section 2.2).

Single Particle- Inductively Coupled Plasma- Mass Spectrometry

Analyses by SP-ICP-MS (XSeries 2, Thermo Scientific) were performed in order to investigate the size range of Ag-containing aggregates (smaller or larger than 1 µm) as well as the number of Ag NP per aggregate. Hereby, the presence or absence of heteroaggregates of Ag with natural colloids was detected. Therefore, samples were measured by SP-ICP-MS before as well as after filtration (PTFE, 1 µm, Puradisc 25 TF, Whatman, GE Healthcare Life Science).

The samples were diluted 1:10 with UPW prior to filtration and the measurements to minimize particle coincidence. A dwell time of 5 ms was used for monitoring $^{107}$Ag. The particle size detection limit of the instrument was approximately 30 nm for Ag NP. Citrate and tannic acid capped Ag NP standards (Nanocomposix) of a size of 40, 80, and 100 nm were measured prior to and after sample measurement for size calibration as well as for monitoring the sensitivity drift which was found to be

negligable. Detailed characterization of these standards can be found elsewhere (Philippe et al., 2014).

The data of SP-ICP-MS were analyzed using a self-programmed R-Script which is described in detail in the SI. In short, the background signal was determined and spike signal intensities were corrected for the background value. Subsequently, the average number of Ag NP per aggregate ($\overline{N}$) and the portion of linear homoaggregates >1 µm ($W_{linear>1}$) of total Ag-containing aggregates were calculated for each sample (equation 2 - 4). For all calculations, we assumed that the size of the primary particles was not significantly changed in the samples e.g. through dissolution processes.

$$\overline{N} = \frac{\bar{\mathrm{I}}}{\mathrm{I_{prim}}} \quad (2)$$

where $\bar{\mathrm{I}}$ is the average spike signal intensity in the sample and $I_{prim}$ is the average signal intensity of primary Ag NP measured separately.

$$d_{linear} = \frac{\mathrm{I}_x}{\mathrm{I_{prim}}} * d_{prim} \quad (3)$$

$$W_{linear} = \frac{N_{linear>1\mu m}}{\mathrm{N_{tot}}} \quad (4)$$

with $d_{linear}$ being the length of a homoaggregate assumed to be linear calculated for each spike, $I_x$ each spike signal intensity and $d_{prim}$ the average size of primary Ag NP, $N_{linear>1}$ the number of linear homoaggregates >1 µm and $N_{tot}$ the total number of peaks per sample. With this calculation, the portion of homoaggregates will most probably be overestimated as the linear shape is unlikely. Therefore, the portion of homoaggregates >1 µm might be smaller than calculated.

The maximal portion of homoaggregate larger than 1 µm was compared to the portion of peaks actually removed by filtration ($W_{removed}$: obtained by stubstraction of spike numbers in filtered samples from numbers in unfiltered samples). The

difference between both portions was assumed to be caused by the presence of heteroaggregates of Ag NP and natural colloids (for more detailed information see section 1.2 in the SI). Therefore, the portion of Ag-containing heteroaggregates >1 µm ($W_{hetero}$) was calculated using equation 5.

$$W_{hetero} = \mathrm{W}_{\mathrm{removed}} - W_{linear} \quad (5)$$

As filtration is often biased due to the possibility for filter clogging (Zirkler et al., 2012), we calculated the recovery of the filtration step by filtering a sample of primary Ag NP (34 nm) with a concentration comparable to remobilization samples, subsequently measuring the Ag concentration by ICP-MS. This recovery of 66 % was taken into account in the calculation of particle numbers by multiplying the calculated values with 1.5.

Scanning Electron Microscopy

Three samples of the remobilization experiment were selected for SEM/EDX analysis (24 h shaking, 130 rpm, aged in UPW, river water and soil extract, and remobilized in UPW). The samples were air-dried on a silicon waver. Analyses were conducted at the Center for Electron Microscopy (ZELMI) of the TU Berlin with an SEM (Zeiss DSM 982 Gemini) coupled with an EDX detector (EDX; EDAX, software 'TEAM', detector 'Apollo' — acquisition parameters of the beam: accelerating voltage: 15 and 20 kV). Due to low Ag concentrations, no quantitative information was gained, but shape and size of the Ag NP as well as the elemental composition in the area of the particle were investigated.

Additionally, a sample of the surficial sediment of two of the columns was studied by SEM to demonstrate the presence of biofilm-forming organisms in the system using measurement conditions as described above. The sediments were taken three years after the transport experiment, but columns had been fed with pond water before and

after the experiment, continuously. Although the ecological community might have changed during this time, evidence for the presence or absence of organisms can be provided.

## 4.4 Results

### 4.4.1 Nanoparticle properties in the column supernatant

The ζ- potentials of Ag NP aged in both soil extract (-26.8 ± 1.4 mV; pH 8.3, EC 347 µS/cm) and river water (-24.8 ± 0.7 mV; pH 8.2, EC 462 µS/cm) were similar but less negative than the value of the Ag NP aged in UPW (-42.0 ± 1.2 mV; pH 9.0, EC 324 µS/cm).

In HDC-ICP-MS measurements, samples collected from the supernatant showed that Ag NP aggregated after addition to the supernatant of the column. Largest aggregate sizes were measured for Ag NP aged in river water (406 ± 31 nm) and smallest aggregate sizes for Ag NP aged in UPW (244 ± 15 nm), whereas soil-aged Ag NP aggregates had an intermediate size (317 ± 10 nm). In all cases the aggregate size in the supernatant was an order of magnitude larger than the primary particle size of original, unaged Ag NP (34 ± 1 nm).

### 4.4.2 Characteristics of the columns

Values of pH and EC in the column supernatant did not differ significantly before and after NP addition (Table S 4. 2). The tracer broke through after one pore volume which means on average after 46.5 h (Fig. S 4. 5). Hydrochemical parameters (Fig. S 4. 6 – Fig. S 4. 9) measured at the column outflow showed pH values of 7.9 ± 0.3, mostly oxic conditions and EC between 200 and 400 µS $cm^{-1}$ that was reduced to values below 150 µS $cm^{-1}$ by several rain events during the experiment.

The SEM picture of surficial sediments of two columns shows a high number of diatoms distributed over the entire range of the analyzed sediment sample (Fig. S 4. 15). This highlights the presence of biofilm forming organisms in the near-natural sediment system.

### 4.4.3 Silver breakthrough and retention

In general, we observed low and irregular Ag breakthrough in all depths of the column that appeared only in erratic events leading to single peaks in the graphs instead of the expected breakthrough curve (Fig. S 4. 10 - Fig. S 4. 12). The most frequent breakthrough events were detected in 30 cm depth (Fig. 4. 2). A complete mass balance was not obtained from our results as the sampling frequency during breakthrough was not high enough due to logistic and time constraints. A correlation between NP breakthrough and the intensity of precipitation events, i.e. mobilization of particles due to dilution of the feeding water, was not detected.

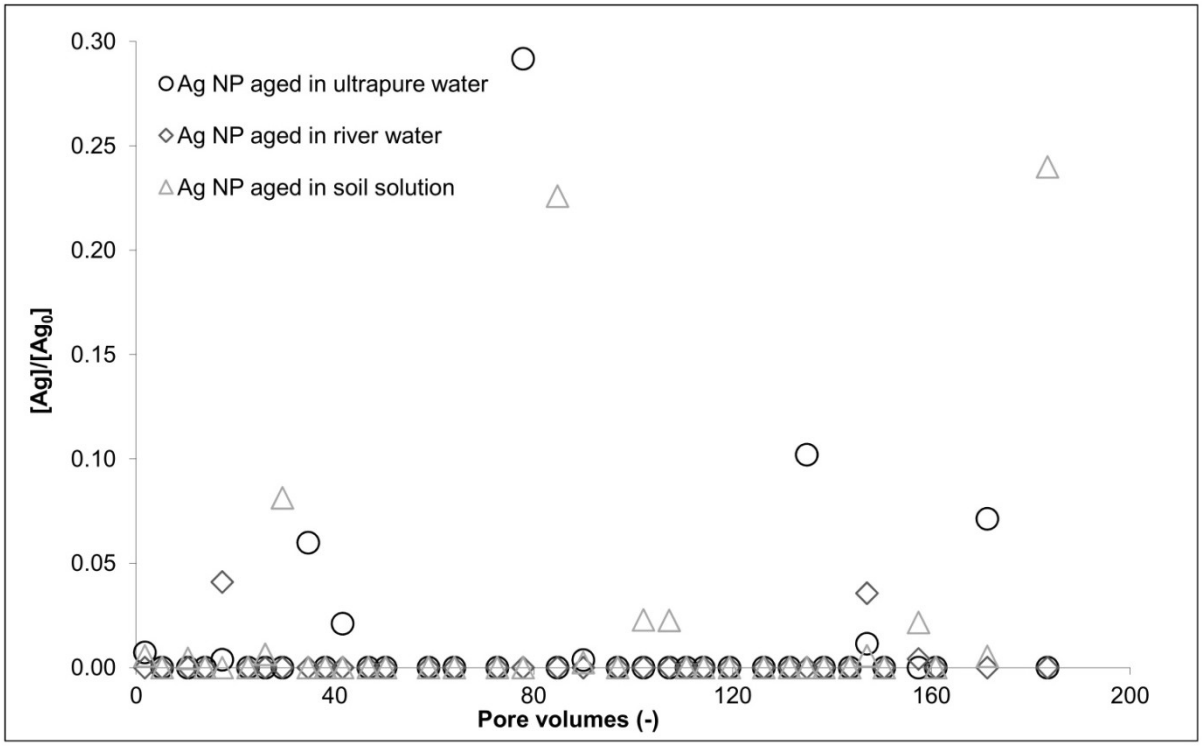


**Fig. 4. 2:** Breakthrough of the differently aged Ag NP in 30 cm depth as a function of pore volumes. Initial Ag concentration: c 0 = 0.96 mg $L^{-1}$ (ultrapure water); c 0 = 1.02 mg $L^{-1}$ (river water); c 0 = 1.02 mg $L^{-1}$ (soil extract).

Silver contents in the sand were largest in a depth of 0-10 cm, and significant amounts were also measured between 10 and 20 cm. However, no Ag was detected below 20 cm (Fig. 4. 3). The data showed a high variability between different sample locations of the same depth. Measured Ag contents in the sediments indicated lowest retention for soil-aged Ag NP (recovery of 54 ± 24 % in sand) and strongest retention for river water- and UPW- aged Ag NP (recoveries of 132 ± 25 % and 116 ± 20 % in sand, respectively). A retention of only 54 % of soil-aged Ag NP indicates that those NP were transported below a depth of 30 cm even though a breakthrough was not proven by Ag concentrations in the aqueous samples. Silver NP aged in river water and UPW, instead, were almost completely retained in the upper 20 cm of the sediments.

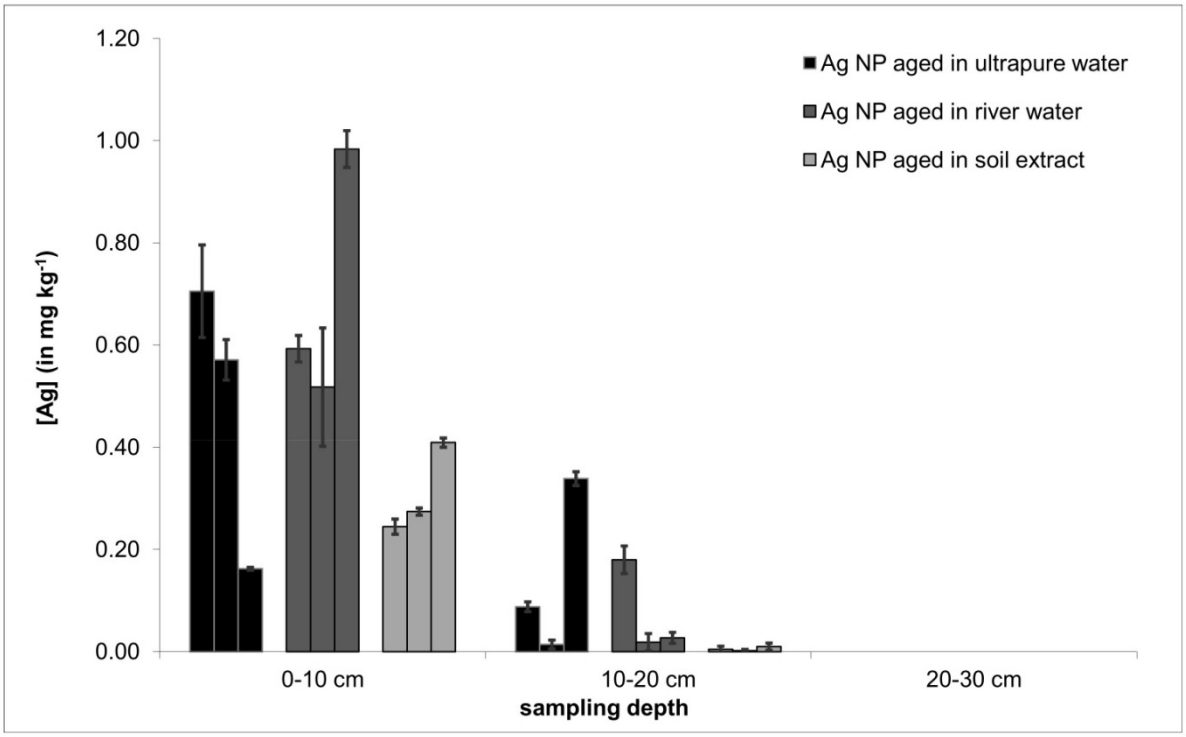


**Fig. 4. 3:** Ag concentration in sand at various depths (0–10, 10–20, 20–30 cm) and for differently aged Ag NP. The same colors for each depth depict the values for different sampling locations in the column. Error bars depict the standard deviations from three replicates.

### 4.4.4 Remobilization of Ag NP from sediments

Amount of remobilized Ag

Between 8 and 50 % of Ag was potentially remobilizable by mechanical forces and hydrochemical changes (Fig. 4. 4). Increasing mechanical forces led to an enhanced release of Ag from the sediments. A difference between treatments was assumed when the standard deviation of replications was smaller than the difference between treatments (i.e. when the standard deviations of treatments were not overlapping). Due to the low number of replicates further statistical evaluation was not undertaken.

A short manual shaking procedure in the different remobilizing media introducing only weak and short pulse shear forces, remobilized 8-15 % of Ag from sediments, most likely mainly by changing hydrochemical conditions, i.e. the reduction of ionic strength and the input of NOM. An effect of the aging history was not visible in the case of soil extract and SR-NOM as remobilizing medium. In both cases, 8-12 % of Ag was remobilized. A reduction in ionic strength (i.e. the remobilization in UPW) led to a slightly higher remobilization of up to 15 % of retained Ag for NP that had been aged in solutions with higher ionic strength and NOM content (i.e. Ag NP aged in river water and soil extract) compared to particles aged in UPW.

When medium mechanical forces acted on the sediments in the form of horizontal shaking for an extended time period (i.e. 24 h), more Ag was remobilized (18-30 %), irrespective of the hydrochemical conditions of the remobilizing medium. However, the degree of remobilization differed depending on the aging history of Ag NP: soil-aged Ag NP showed the highest remobilization while Ag from UPW-aged Ag NP was remobilized in lowest amounts.

Remobilization in UPW and soil extract at strongest mechanical forces (i.e. USB treatment) detached on average one third of retained Ag irrespective of NP aging

history. While the release of Ag slightly, but not significantly increased in the case of UPW- and river water-aged Ag NP compared to 24 h shaking, soil-aged Ag NP did not show stronger remobilization after ultrasonic treatment despite of the increased mechanical forces.

The presence of SR-NOM during USB treatment led to a remobilization of up to 50% of retained Ag NP and a significantly increased Ag remobilization at strongest mechanical forces compared to horizontal shaking. Compared to remobilization in UPW and soil extract an increased Ag release of around 25 % for UPW-aged, 33 % for river water-aged and even 74 % for soil-aged Ag NP was observed.

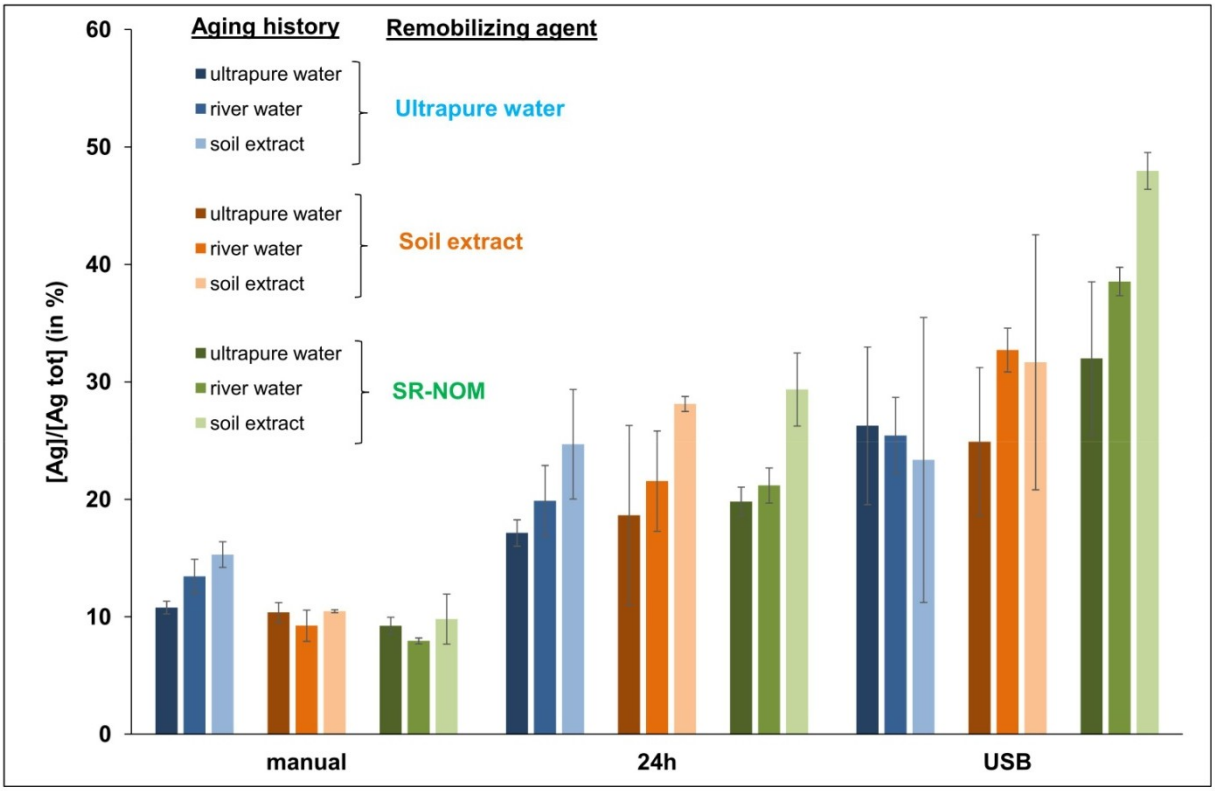


**Fig. 4. 4:** Portion of Ag remobilized by UPW (blue bars), soil extract (orange bars), and SR-NOM (green bars) from sediments applied in the riverbank filtration experiments with differently aged Ag NP. The portion of remobilized Ag is normalized to Ag concentrations of the respective sediments (different color scales show different aging history, bars reflect the median, arrow bars depict the standard deviation from 3 replicates).

## Characteristics of remobilized Ag

**Discrimination between Ag NP and $Ag^+$ ions**

Graphite furnace- AAS was applied to selected samples of the remobilization experiment to gain information about the size of Ag NP as well as the appearance of $Ag^+$ ions. For the latter goal, $NH_4NO_3$ was used as remobilizing medium to measure the potential for $Ag^+$ release from retained Ag NP or sediment surfaces.

Largest particle sizes were measured for Ag NP aged in river water compared to UPW- and soil-aged Ag NP in all remobilizing media (Table 2). This is in accordance with HDC-ICP-MS measurements of Ag NP after addition to the column supernatant (3.1). Nevertheless, particle sizes of remobilization cannot be compared directly with the ones in the column experiment as mechanical forces of the remobilization procedure are expected to have an influence.

Additionally, the remobilizing medium had a strong influence on the size of remobilized Ag NP. While remobilization in $NH_4NO_3$ solution and UPW preserved the primary particle size range of Ag NP (12-40 nm), Ag NP remobilized in soil extract formed larger aggregates (188-220 nm). The aging of Ag NP and their residence in the sediment column enhanced NP stability as spiking of $NH_4NO_3$ solution and soil extract with primary ('unaged') Ag NP (Table 2, sample 1 and 3) led to a larger size of Ag NP compared to differently aged Ag NP remobilized in $NH_4NO_3$ and soil extract (Table 2, sample 7-12). This illustrates that unaged Ag NP were less stable against ionic strength induced aggregation than aged Ag NP.

The GFAAS is a promising method for distinguishing NP from ions in samples containing larger particles and organic molecules where filtration would be biased by removal of adsorbed or complexed $Ag^+$ that would not pass the filter. Preliminary experiments of GFAAS suggested that this method cannot distinguish between free and complexed or adsorbed $Ag^+$ (see Theoretical background in the SI).

Samples from remobilization experiments using $NH_4NO_3$ solution as remobilizing medium exhibited peaks at $t_{ad}$ = 1.6 - 1.8 s which corresponds to $Ag^+$ ions (Fig. 4. 5, sample 8) whereas samples with soil extract or UPW did not show a clear indication for the presence of $Ag^+$ (Fig. 4. 5, sample 6 and 12). This suggests that the main Ag species after remobilization experiments was particulate Ag. Only in the presence of $NH_4NO_3$ the complexation of $Ag^+$ with $NH_3$ most likely enhanced Ag dissolution.

Dissolved Ag was also found in soil extract that was spiked with primary Ag NP but not in samples where soil extract was used as remobilizing medium (compare sample 12 and 3 in Fig. 4. 5 and Fig. S 4. 13, respectively). This suggests that soil extract increased the dissolution of Ag NP. But when Ag NP had been aged and exposed to natural surface water in the column experiments they seemed to be stabilized against dissolution during remobilization experiments.

**Table 4. 2:** Atomization delay ($t_{ad}$) and average size of Ag NP in selected samples of remobilization experiment with USB treatment measured by GFAAS and calculated from calibration curve (Fig. S 4. 3), 'Unaged' samples contain the respective remobilizing medium and primary Ag NP (30 nm) added shortly before analysis. Grey lines mark the samples depicted in Fig.4. 5.

| | Aging History* | Remobilizing medium | $t_{ad}$ [s] | NP size [nm] |
|---|---|---|---|---|
| **1** | unaged | $NH_4NO_3$ | 2.66 ± 0.01 | **123 ± 9** |
| **2** | unaged | UPW | 2.43 ± 0.02 | **26 ± 4** |
| **3** | unaged | Soil Extract | 2.71 ± 0.02 | **172 ± 25** |
| **4** | UPW | UPW | 2.34 ± 0.08 | **15 ± 7** |
| **5** | RW | UPW | 2.42 ± 0.02 | **25 ± 4** |
| **6** | SE | UPW | 2.31 ± 0.01 | **12 ± 1** |
| **7** | UPW | $NH_4NO_3$ | 2.44 ± 0.03 | **29 ± 5** |
| **8** | RW | $NH_4NO_3$ | 2.49 ± 0.04 | **40 ± 11** |
| **9** | SE | $NH_4NO_3$ | 2.39 ± 0.03 | **20 ± 5** |
| **10** | UPW | Soil Extract | 2.72 ± 0.02 | **188 ± 21** |
| **11** | RW | Soil Extract | 2.75 ± 0.02 | **220 ± 37** |
| **12** | SE | Soil Extract | 2.72 ± 0.06 | **194 ± 74** |

*RW: River Water; SE: Soil Extract

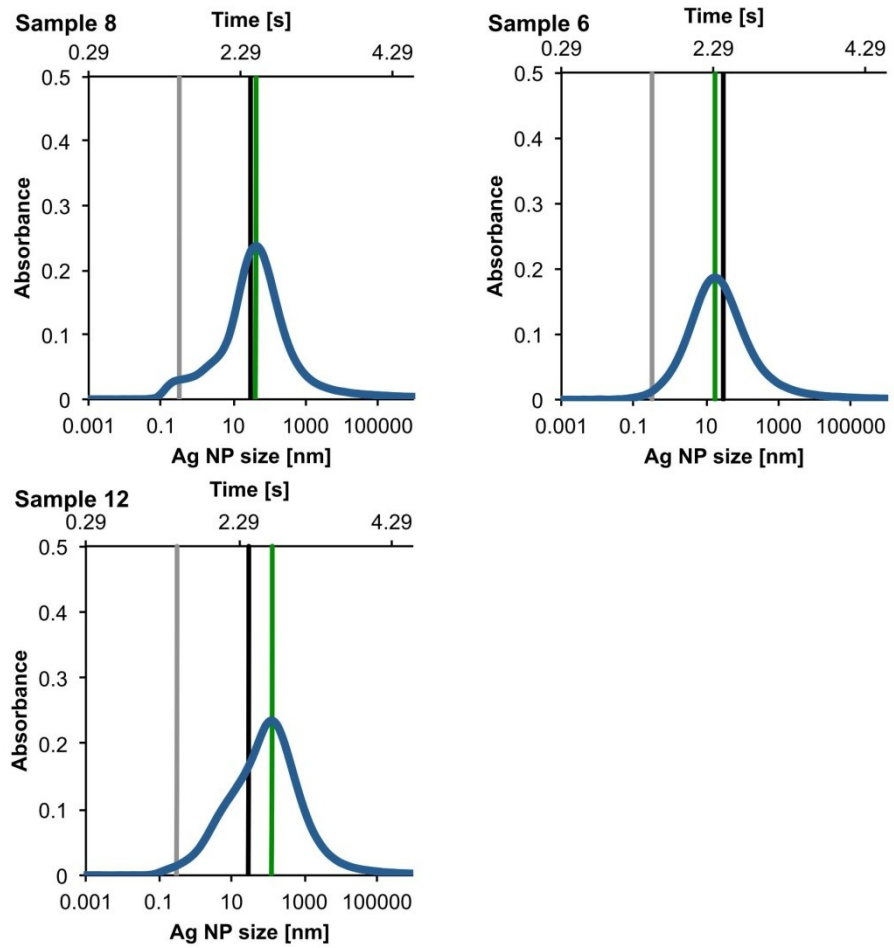


**Fig. 4. 5:** GFAAS absorbance signal (blue) of the samples 8 (remobilization in NH 4 NO 3 ), 6 (remobilization in UPW) and 12 (remobilization in soil extract). The grey line corresponds to free silver ions, the black line shows the size of initial unaged Ag NP (30 nm), and the green line represents the mode of particle size distribution of the respective sample.

## Aggregation and transformation state of remobilized Ag NP

In order to investigate the potential correlation between remobilized Ag and inorganic colloids released from sediments in the samples of remobilization experiments the concentration of Al was measured as a tracer for natural inorganic colloids such as clay particles. With increasing Ag concentration, the Al concentration also increased (Fig. 4. 6) indicating a co-mobilization of Ag NP with Al-containing natural colloids. The remobilization of Al-containing colloids increased also with increasing mechanical forces as shown by a grouping of the data points treated with similar mechanical forces.

As a second approach to characterize Ag NP aggregation state, SP-ICP-MS combined with 1 µm-filtration of selected samples containing remobilized Ag was used. Thereby, the size range of the remobilized aggregates or particles and the amount of Ag-containing heteroaggregates were investigated. The average spike signal intensities of unfiltered samples indicate that particles contained between one and two primary Ag NP on average (Table 3). Most Ag- containing particles should therefore be smaller than the cut-off of the used filter (1 µm) if they were primary particles or homoaggregates. The recovery rate of the filtration step proved that 66 % of primary Ag NP passed the filter (section 2.7.3); hence we corrected our calculations by this factor. From signal intensities, we calculated the maximal possible size of homoaggregates for a given number of primary particles by assuming their shape to be linear. The linear geometry is highly unlikely as most homoaggregates should be more compact with fractal dimensions of 1.7-2.5 (Meakin, 1988). Therefore, the maximal possible length for a homoaggregate proposed here was a quite rigid criterion for distinguishing hetero- from homoaggregates. Still, those calculations suggest that most Ag-containing aggregates (99.7 ± 0.3 %) should pass the filter. In contrast, filtration of the samples led to a low count rate (average number of spikes) of only 7-26 % of unfiltered samples in SP-ICP-MS measurements (exemplary graphs are shown in section 3 of SI). Hence, only a small amount of Ag-containing particles or aggregates smaller than 1 µm was present in the samples (Table 3). This indicates that the majority (at least 74-93 %) of the detected particles were heteroaggregates larger than 1 µm. As the recovery of the filtration step was included in this calculation, filter clogging cannot be the process responsible for particle exclusion. Although we cannot exclude that some smaller homoaggregates of Ag NP might have co-precipitated during the filtration step, the high recovery of single

Ag NP during filtration showed that the interaction between NP and the filter material was low.

During SEM measurements only few Ag NP were found due to the low Ag concentrations in the range of µg $L^{-1}$. Those had a size of 120 nm and EDX spectra showed the coexistence of Ag with S and Fe (data not shown). Sulfur was not present at other Ag-free spots of the sample which suggests a correlation with Ag. The measurements were not interpreted quantitatively due to the low sample concentration but showed that at least a part of Ag NP was sulfidized.

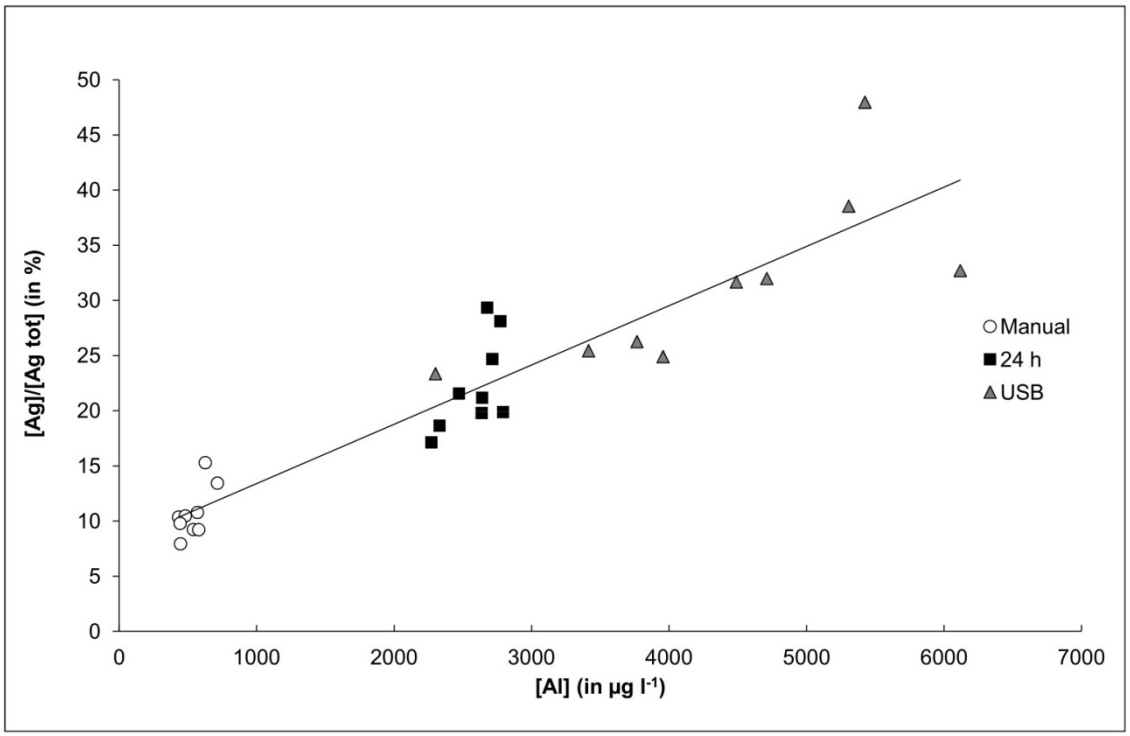


**Fig. 4. 6:** Correlation of remobilized Al and Ag concentrations measured in the corresponding samples from remobilization experiments. The concentration of remobilized Ag is normalized to the total Ag concentration of the respective sediment. Circles represent data from manually shaken samples, squares exhibit data from 24 h shaken samples and triangles represent data from samples treated with USB. The line corresponds to a linear regression with $R^2$ = 0.8614.

**Table 4. 3:** Results of SP-ICP-MS measurements of selected samples. The number of particles per aggregate was calculated from sample spike intensity divided by the average spike intensity of primary Ag NP. The minimal portion of heteroaggregates was determined based on the amount of spikes removed by filtration minus the number of homoaggregates being large enough to be filtered out. The latter value is estimated based on the spike intensities assuming a linear geometry for the aggregates (see SI, chapter 4.2.2 for more details).

| **Sample (Aging / Remobilization medium / Mech. force)[2]** | **Average number of primary NP per particle ($\bar{N}$)** | **Portion of spike counts after filtration ($W_{removed}$) [%] [1]** | **Portion of linear homoaggregates > 1 µm ($W_{linear}$) [%] [1]** | **Minimal portion of heteroaggregates ($W_{hetero}$) [%] [1]** |
|---|---|---|---|---|
| SE / UPW / man. | 1.47 | 9.56 | 1.20 | 89.24 |
| SE / UPW / man. | 1.43 | 13.49 | 0.30 | 86.21 |
| SE / UPW / man. | 1.41 | 21.23 | 0.32 | 78.45 |
| SE / UPW / 24h | 1.49 | 16.23 | 0.30 | 83.47 |
| SE / UPW / 24h | 1.87 | 9.91 | 0.50 | 89.59 |
| SE / UPW / 24h | 1.44 | 25.24 | 0.35 | 74.41 |
| UPW / $NH_4NO_3$ / USB | 2.05 | 15.40 | 0.18 | 84.42 |
| RW / $NH_4NO_3$ / USB | 1.99 | 16.73 | 0.36 | 82.91 |
| SE / $NH_4NO_3$ / USB | 1.80 | 15.53 | 0.26 | 84.21 |
| UPW / UPW / 24h | 2.00 | 13.34 | 0.12 | 86.54 |
| SE / UPW / 24h | 2.19 | 13.58 | 0.30 | 86.12 |
| SE / SE / man. | 1.32 | 18.75 | 0.24 | 81.01 |
| SE / SE / man. | 1.40 | 16.28 | 0.32 | 83.40 |
| SE / SE / man. | 1.37 | 25.74 | 0.06 | 74.20 |
| SE / SE / USB | 1.93 | 8.94 | 0.24 | 90.82 |
| SE / SE /USB | 2.05 | 7.04 | 0.26 | 92.70 |

[1] corrected by recovery of filtration (66 %)

[2] SE: Soil extract; UPW: Ultrapure Water; RW: River water

## 4.5 Discussion

### 4.5.1 Transformation reactions of Ag NP in aging media and column water

The aging of citrate-stabilized Ag NP in three different media (i.e. UPW, river water, and soil extract) led to varying surface properties of the NP. Compared to Ag NP aged in UPW, less negative ζ- potentials were observed for river water- and soil-aged Ag NP which may be attributed to charge neutralization caused by cations such as Ca in the respective media since Ca was a major element present in soil extract and river water (Table S 4. 1). This is in line with previous studies showing the predominant role of Ca ions for charge neutralization of citrate-stabilized Ag NP in soil extract (Klitzke et al., 2015) and river water (Metreveli et al., 2015).

In the column supernatant, the differently aged Ag NP were subjected to diluted, natural pond water which induced particle aggregation, most likely due to the presence of Ca (1.2 mM). Despite their similar ζ- potentials, soil-aged and river water-aged Ag NP differed significantly in aggregate size once in the column supernatant. The smaller aggregate size of soil-aged Ag NP may be attributed to the larger DOC concentration in the soil extract, forming a stabilizing coating layer on the surface of Ag NP (Klitzke et al., 2015). The larger aggregate size of the Ag NP aged in river water can be explained by the elevated Ca concentration and the relatively low DOC concentration in the aging medium facilitating the destabilization of Ag NP. UPW- aged Ag NP had smallest aggregate sizes as no Ca was present during aging and therefore the ζ- potential was strongly negative.

### 4.5.2 Retention mechanisms in riverbank filtration systems

Our study showed that the breakthrough of Ag NP in the sediments of an artificial riverbank filtration system was irregular and very erratic. This was similar for all differently aged Ag NP. Large Ag contents were found in the sediments of the upper 10 cm of the columns which was in line with the finding that Ag NP aged in river water and UPW were almost completely retained in the column. Nevertheless, only 54 ± 24 % recovery of soil-aged NP in the upper 30 cm of the sediments was calculated. Thus, the aging of Ag NP in soil extract seems to have led to a higher mobility of the soil-aged NP in the columns. Still, those Ag NP were also accumulated in the upper 10 cm of the column. The different retention behavior cannot be correlated with the size of differently aged Ag NP as UPW-aged NP had smallest sizes but were still strongly retained. Instead, the organic coating of soil-aged NP was the determining factor for the higher mobility due to steric repulsion forces.

The retention of Ag NP aged in UPW (Fig. S 4. 10) differed significantly from the retention curves obtained in a laboratory study with water-saturated sand columns by Zhang and Zhang (2014), showing almost complete breakthrough for citrate-stabilized Ag NP (particle size: 15 nm, ζ- potential: -38 mV in deionized water). This pronounced difference may be explained by the application of a completely artificial mobile phase containing only $MgSO_4$ and larger initial concentration of Ag NP (10 mg $L^{-1}$) in the work of Zhang and Zhang. Magnesium ions are known to have a less strongly destabilizing effect on citrate-coated Ag NP due to a lower stability of Mg-citrate complexes compared to Ca-citrate complexes (Baalousha et al., 2013; Field et al., 1975; Metreveli et al., 2015). Additionally, in our sediments the presence of a well-established biofilm can be expected in contrast to the experiments of Zhang and Zhang, as our columns are located outside and fed with natural pond water throughout the whole year. Microscopy images underline the presence of biofilm-forming organisms (i.e. diatoms) in the top sediment layer of the columns (Fig. S 4.

15). Biofilms are known to accumulate NP in natural systems (Ikuma et al., 2015). The erratically occurring peaks in our experiments may be the result of a sudden release of Ag NP aggregates from the biofilm when the biofilms got disturbed or the flow conditions changed due to natural processes (i.e. siltation) in the columns. Retention of NP in sand filters due to the presence of biofilms was already shown by Li et al., 2013. The authors compared the transport of nanoparticles through unused, biofilm-free drinking water sand filters with used sand filters having an established biofilm. They observed high breakthrough of citrate-coated Ag NP in unused sand, whereas sand which contained a biofilm reduced Ag NP breakthrough by at least 40 %. Even though the authors used higher filter velocities (47 m $d^{-1}$ as opposed to 0.2 m $d^{-1}$ in our experiments) and much larger initial concentrations of NP (45 mg $L^{-1}$ as opposed to 1 mg $L^{-1}$ in our experiments) their explanation i.e. the presence of biofilms would contribute to increased retention of NP in sand filters may still be valid for our experiments. The attachment to and entrapment in biofilms in the sand column might have been one relevant retention mechanisms in our experiment. Further studies should therefore focus on this process in more detail.

Additionally, attachment to sediment surfaces and straining processes are expected to play a role for Ag NP retention in the riverbank filtration columns as shown by previous studies (such as Adrian et al., 2018; Emerson et al., 2014).

The retention mechanisms are dependent on the aging history of the Ag NP, most likely due to the change of NP surface properties. Aging in soil extract that had a larger DOC- and a lower Ca concentration than river water enhanced the colloidal stability of the Ag NP which led to a lower retention in the upper 30 cm of the sediment column. This shows that a coating layer of soil organic matter can partially inhibit the attachment of Ag NP onto grain surfaces of sand in the columns. It might also affect the interaction of the Ag NP with the biofilm as observed by Nevius et al.,

2012 and Morrow et al., 2010. In contrast, the presence of high Ca concentrations during aging, such as in the river water of our study supported the NP retention. This is most likely caused by the compression of the electrical double layer of Ag NP by Ca ions leading to decreased repulsion forces in the sediment column. As Ca was also present in the pond water flushing the column, the formation of Ca-bridges between NOM-coated Ag NP and riverbank sediments might contribute to the retention.

### 4.5.3 Remobilization mechanisms from sediments

The results of our study suggest that a co-mobilization of Ag NP with Al-containing colloids was the prevailing remobilization mechanism. The majority of remobilized Ag seemed to be associated with natural colloids >1 µm. This has been reported for transport of NP in soils by previous studies (such as Hoppe et al., 2015; Makselon et al., 2017; Zhang and Zhang, 2014). As sediments of the riverbank filtration system were flushed with natural water of the surrounding pond, it is expected that organic and inorganic colloids were constantly introduced in the columns. The colloids seem to aggregate with Ag NP and were then remobilized together during batch experiments. A second possibility is that heteroaggregates were formed after remobilization. Remobilization of single Ag NP played a minor role highlighting the importance of co-mobilization of NP with natural colloids also in riverbank filtration systems and river bed sediments.

The results of the GFAAS analysis underlined that the release of $Ag^+$ ions was of minor importance during remobilization. As $Ag^+$ ions were not detected for samples remobilized in UPW and soil extract, the main part of remobilized Ag was present as particulate Ag NP, most likely attached to natural colloids > 1 µm. Nevertheless, in

the presence of $NH_4NO_3$ Ag dissolution was observed. Due to the ecotoxicological relevance of $Ag^+$ ions (Beer et al., 2012), it is important to consider that retained Ag NP in sediment systems can act as a source for $Ag^+$ release when complexing agents such as $NH_3$ enter the riverbank system. However, EDX analysis of remobilized Ag NP suggest that at least partial sulfidation of Ag NP took place. This would reduce the toxicity of Ag NP to aquatic and terrestrial organisms (Lee et al., 2016; Levard et al., 2013). As sulfidation was only observed for the few NP found under the microscope it should be confirmed by further studies.

Our experiments showed that increasing mechanical forces as well as longer exposure times to these forces led to enhanced Ag remobilization, possibly through enhanced remobilization of natural, Al-containing colloids. The comparison of Ag NP remobilized in SR-NOM during 24 h of shaking and USB treatment shows that about 40 % of the remobilizable Ag was only remobilized by very strong mechanical forces (Fig. S 4. 16). This was independent of the aging history of Ag NP which suggests a strong binding mechanism of this part of Ag NP to sediments that could only be disrupted by very strong mechanical forces. Of course, USB treatment results in mechanical forces much stronger than what can be found in natural systems caused by water turbulence and high flow rates. However, the application of USB treatment allowed us to determine the maximal remobilizable amount of Ag in our experiments in order to distinguish between weakly and strongly bound Ag NP.

In river systems, increasing turbulences during high-flow conditions might remobilize sediment particles and consequently also engineered NP accumulated in surficial sediment layers. Flooding events can also change hydrochemical conditions in the water phase. Those were identified as a second important factor for the remobilization of Ag NP from sediments. In the following paragraph, the determining parameters are summarized:

*The presence of Ca reduced the amount of remobilizable Ag.* On the one hand, Ca ions probably favored destabilization of Ag NP remobilized by strong mechanical forces and hence led to reattachment of remobilized particles. On the other hand, it most likely reduced the remobilization potential by the formation of Ca-bridges between organic matter coated NP and sediment surfaces. Liang et al., 2013 hypothesized that cation bridges enhance the interaction of Ag NP with sediment surfaces hindering the remobilization process. Moreover, at high cation concentration the energy barrier around the particle surfaces can completely disappear and the NP and their homo- and heteroaggregates can attach to the sediments irreversibly in a primary energy minimum. These mechanisms can explain the low remobilization potential observed for Ag NP aged in media with larger Ca concentrations (such as river water) as well as for Ag NP remobilized in media containing high Ca concentrations (such as soil extract).

*The presence of organic matter enhanced the remobilization potential.* The formation of an organic coating on the NP surface during aging in soil extract most likely led to reduced attraction forces between Ag NP and sediment grains by steric hindrance and electrostatic repulsion (Delay et al., 2011) facilitating detachment in remobilization experiments. Therefore, Ag NP aged in soil extract were remobilized to largest extents already with medium mechanical forces (i.e. 24 h of horizontal shaking). The same amount of river water- and UPW-aged Ag NP (aged in solutions with lower DOC content) was only remobilized by the strongest mechanical forces of USB treatment. However, the presence of NOM in the remobilizing medium enhanced the remobilization only when strong mechanical forces (i.e. USB treatment) were applied. While SR-NOM did not show any stronger remobilization effect during manual or horizontal shaking, it led to clearly higher remobilization during USB treatment compared to remobilization in soil extract and UPW. This suggests that

NOM had an indirect remobilizing effect by stabilizing remobilized, colloidally instable Ag NP or Ag-containing natural colloids against aggregation and reattachment to sediments. Our results are in good agreement with findings of Metreveli et al., 2015 who demonstrated the important role of NOM and shear forces on the disaggregation of Ag NP homoaggregates. In their study, only strong mechanical forces (i.e. USB treatment) in combination with SR-Humic Acid caused disaggregation.

*A reduction in ionic strength* (i.e. remobilization in UPW) *enhanced the remobilization potential of Ag NP aged in media with higher ionic strength and DOC concentration* (i.e. river water and soil extract). Silver NP with an organic coating were most likely loosely attached in a secondary energy minimum. Those NP were remobilized by the reduction in ionic strength under soft mechanical forces since the kinetic energy of diffusion was sufficient to detach particles attached in a secondary minimum (Liang et al., 2013). Instead, more of Ag NP aged in UPW were attached to sediment surfaces in a stable primary minimum where a reduction in ionic strength is not sufficient for remobilization. This effect was only small as clay minerals and the sand as well as the NP are negatively charged at neutral pH, so that soft shear forces might have been sufficient to remobilize loosely bound Ag NP as well as Ag-containing colloids. Increasing remobilization forces (i.e. horizontal shaking and USB) then disrupted stronger bonds such as Ca bridges between NOM-coated sediment surfaces and particles leading to enhanced remobilization and overruling the effect of ionic strength reduction.

To summarize, Ag NP in sediment columns of an artificial riverbank filtration system were strongly retained and retention occurred predominantly in the top sediment layers. Sedimentation in the column head, entrapment in biofilms, aggregation and straining processes as well as adsorption to mineral surfaces are proposed to be the

main retention mechanisms. Those mechanisms have a lower effect on Ag NP that experienced aging processes in soils. Instead, the retention is supported by the presence of divalent cations, such as Ca. The higher remobilization potential of soil-aged Ag NP illustrates that an aging in soil also leads to weaker bonds between NP and sediment surfaces. A combination of mechanical forces and hydrochemical changes can remobilize up to 50 % of retained Ag NP. The presence of divalent cations, such as Ca reduces the remobilization potential by destabilizing Ag NP and increasing interactions between NP and sediment surfaces. According to our results, the remobilization of Ag NP predominantly takes place in the form of heteroaggregates with natural colloids larger than 1 µm while $Ag^+$ ions are only remobilized in the presence of strong complexing agents.

## 4.6 Conclusions

Due to a strong retention in surficial sediments, Ag NP accumulate in riverbank filtration systems where they form a potential source for the release of Ag NP and $Ag^+$ ions. Although the mobility of Ag NP is low, the aging of NP in soil extract can promote their breakthrough and remobilization potential. Hence, Ag NP once entering soils can form a potential source for more mobile Ag NP when they are further transported into riverbank filtration systems. There, Ag NP are retained but a remobilization is possible under changing environmental conditions. However, hydrochemical conditions alone are not enough to control the remobilization of Ag NP. The presence of moderate or strong mechanical forces which can be induced, for example, by turbulence in river systems or increasing flow velocities during flooding events, are necessary to remobilize Ag NP. The co-mobilization of Ag NP with natural clay colloids seems to be the main mechanism for remobilizing Ag from sediments of the riverbank filtration system, induced by increasing mechanical forces and the colloidal stabilization of Ag NP by NOM and ionic strength reduction.

As a potential scenario, strong precipitation events can lead to higher flow velocities, thus increasing mechanical forces and reducing the ionic strength of the surrounding solution. Additionally, flooding events might transport large amounts of NOM from floodplain soils into river systems which can then act as a stabilizing agent for the Ag NP remobilized through increasing mechanical forces. These facts suggest that even though our column experiment showed a strong retention of Ag NP in riverbank filtration systems, the potential risk of remobilization should not be neglected, although Ag concentrations are expected to be low. Nevertheless, the relevance of the identified mechanisms should be checked under more complex environmental

conditions. Future studies should also focus on the effect of biofilms in sediment systems on breakthrough and remobilization, as they seem to control NP retention.

# 5 The fate of silver nanoparticles in riverbank filtration systems- The role of biological components and flow velocity

Authors: Laura Degenkolb, Frederic Leuther, Simon Lüderwald, Allan Philippe, George Metreveli, Sayed Amininejad, Hans-Jörg Vogel, Martin Kaupenjohann, Sondra Klitzke

Pre-print, published in “Science of the Total Environment”, original publication (open-access) can be found under: https://doi.org/10.1016/j.scitotenv.2019.134387

## 5.1 Abstract

Riverbank filtration is a natural process that may ensure the cleaning of surface water for producing drinking water. For silver nanoparticles (AgNP), physico-chemical interaction with sediment surfaces is one major retention mechanism. However, the effect of flow velocity and the importance of biological retention, such as AgNP attachment to biomass, are not well understood, yet.

We investigated AgNP (c = 0.6 mg $L^{-1}$) transport at different spatial and temporal scales in pristine and previously pond water-aged sediment columns. Transport of AgNP under near-natural conditions was studied in a long-term riverbank filtration experiment over the course of one month with changing flow scenarios (i.e. transport at 0.7 m $d^{-1}$, stagnation, and remobilization at 1.7 m $d^{-1}$). To elucidate retention processes, we conducted small-scale lab column experiments at low (0.2 m $d^{-1}$) and high (0.7 m $d^{-1}$) flow rate using pristine and aged sediments.

Overall, AgNP accumulated in the upper centimeters of the sediment both in lab and outdoor experiments. In the lab study, retention of AgNP by attachment to biological components was very effective under high and low flow rate with nearly complete NP accumulation in the upper 2 mm. When organic material was absent, abiotic filtration

mechanisms led to NP retention in the upper 5 to 7 cm of the column. In the long-term study, AgNP were transported up to a depth of 25 cm. For the pristine sediment in the lab study and the outdoor experiments only erratic particle breakthrough was detected in a depth of 15 cm.

We conclude that physico-chemical interactions of AgNP with sediment surfaces are efficient in retaining AgNP. The presence of organic material provides additional retention sites which increase the filtration capacity of the system. Nevertheless, erratic breakthrough events might transport NP into deeper sediment layers.

Keywords: Nanomaterial, long-term experiment, water-saturated transport, near-natural condition, biological retention, mechanical filtration

## 5.2 Introduction

Riverbank filtration is an important process for drinking water production with the advantage of cleaning surface water by natural filtration mechanisms such as adsorption and degradation of anthropogenic pollutants. In Germany, about 16 % of the drinking water is produced by managed aquifer recharge using bank filtration (Sprenger et al., 2017). Substances that can pass riverbank filtration systems may thus pose a risk for drinking water resources. The increasing use of silver nanoparticles (Ag NP) in industrial processes, medical products, textiles, and household appliances leads to an increasing release of Ag NP into the environment (Li et al., 2008; Tolaymat et al., 2010). For drinking water risk assessment, it is therefore important to investigate the transport of Ag NP in saturated sediments that act as natural filters for drinking water resources.

Since the early 2000s, NP fate and effects have been increasingly studied by many researchers (Fabrega et al., 2011; Sani-Kast et al., 2017). The risk for adverse effects of Ag NP to aquatic organisms was suggested by various studies (Andreï et al., 2016; Rajala et al., 2018; Ribeiro et al., 2017). Nanoparticle transport was mainly investigated in small-scale column experiments, using glass beads (Ben-Moshe et al., 2010 for metal oxide NP; Lecoanet and Wiesner, 2004 for fullerenes and metal oxide NP), quartz sand (Petosa et al., 2013 for $CeO_2$ NP), and soil columns (Cornelis et al., 2013; Sagee et al., 2012 for Ag NP). These experiments identified that the following physico-chemical filtration mechanisms dominate the transport and retention of NP:

(I) The extent of NP transport strongly depends on the hydrochemical *properties of the mobile phase*, such as pH, ionic strength, and natural organic matter (NOM) concentration. Increasing ionic strength leads to the compression of the electrical double

layer of NP as well as of sediment grains of porous media. According to DLVO theory, this decreases repulsion forces between particles and collector surfaces and causes NP attachment and retention (Derjaguin and Landau, 1941). On the one hand, adsorption of NOM to NP surfaces leads to steric and electrostatic stabilization and may enhance NP mobility (i.e. Chen et al., 2012). On the other hand, the presence of multivalent cations may also reduce NP mobility by promoting NOM-NP flocculation (Kumahor et al., 2016; Philippe and Schaumann, 2014). As NOM is ubiquitous in the environment those organic molecules play an important role for NP fate in natural systems (Philippe and Schaumann, 2014).

(II) The physical *properties of the sediment system*, such as pore size distribution and flow velocity, have a strong impact on NP transport (e.g. Braun et al., 2015; Sagee et al., 2012). Due to the small size of NP, their mobility is strongly influenced by Brownian motion and, thus, diffusion. At low flow rates, NP mass transfer is dominated by diffusion to attachment sites (Adrian et al., 2018; Braun et al., 2015). Furthermore, low hydrodynamic shear forces reduce the probability of detachment (Metreveli et al., 2015). Therefore, NP retention increases with decreasing flow rate. However, most studies have been conducted at relatively high flow rates (ranging from 2.4 up to 55 m $d^{-1}$ Darcy flux; Cornelis et al., 2013; El Badawy et al., 2013; Li et al., 2013; Lin et al., 2011; Petosa et al., 2013; Sagee et al., 2012; Sun et al., 2015; Taghavy et al., 2013) that might be unrealistic for saturated porous media (Kunkel and Wendland, 1997; Schubert, 2002). In these cases, high NP breakthrough was found. In contrast, flow rates below 1 m $d^{-1}$ caused a very low Ag NP breakthrough in loamy sand in a study by Braun et al. (2015), but the effect of changing flow rates in the low flow range has not been studied so far.

(III) The *properties of the NP* themselves affect their interaction with the stationary phase and thus, their mobility. Although intrinsic properties of particles of different material lead to a wide range of NP surface charge and reactivity, organic capping agents prevent NP from aggregating. In pure quartz sand with a negative surface charge, the transport of citrate coated Ag NP follows the behavior of a conservative tracer while positively charged iron oxides or clay particles restrain citrate coated Ag NP (El Badawy et al., 2013). Thus, intrinsic NP properties might be masked by capping agents. Furthermore, increasing initial NP concentrations were found to enhance NP breakthrough as the limited number of attachment or straining sites becomes saturated at high NP concentrations (Bradford et al., 2006).

These retention mechanisms all focus on interactions of NP with the inorganic matrix of a saturated sediment system. However, biological surfaces such as biofilms, microorganisms, and detritus offer a high variety of potential attachment sites and can change the properties of the pore system (Hoffmann and Gunkel, 2011). In aquatic mesocosm experiments and transport studies a strong attachment of NP to biofilms and plants has been observed (Avellan et al., 2018; Nevius et al., 2012; Tripathi et al., 2012). Furthermore, aquatic sediments have been identified as important sinks for NP possibly due to biological surfaces (Geitner et al., 2018). Nevertheless, the role of biological structures in sediment systems is not taken into account in most column experiments and limits the transferability of lab results to natural systems.

In a previous study, we investigated the transport of citrate-coated Ag NP in the near-natural riverbank filtration system (Degenkolb et al., 2018) which is also used for the present experiments. Strong retention of Ag NP in the upper 10 cm of the column was

observed which was explained by the low flow velocity (0.2 m $d^{-1}$) and the presence of biofilms and organic material without further exploration on these factors.

The present study aims at investigating the effect of different flow velocities and the presence of organic material on the retention and transport of Ag NP in saturated sediment systems based on the previous study. Therefore, the large-scale, long-term experiment was conducted with a higher flow velocity (0.7 m $d^{-1}$) than used in the previous study and changing flow scenarios (i.e. transport at 0.7 m $d^{-1}$, stagnation, and remobilization at 1.7 m $d^{-1}$). Subsequently, we studied the importance of biological material (i.e. dead and living organic matter from biofilms, algae, and plants) on NP retention in lab column experiments by comparing the transport in pond water-aged and pristine sediments at low and high flow rate. The ecotoxicological relevance of NP transport behavior in near-natural sediment systems was verified by toxicity tests with the applied Ag NP as well as the effluents in different column depths. Hereby, the following two main hypotheses were tested:

I) The retention of Ag NP is strongly enhanced by NP attachment to biomass.

II) Increasing flow velocities increases transport and decreases retention of Ag NP in riverbank filtration systems.

## 5.3 Material and Methods

### 5.3.1 Experimental design

To test the impact of organic retention mechanisms and flow velocity on Ag NP transport and retention in riverbank filtration systems, two kinds of experiments were performed: i) large-scale outdoor experiments with different flow velocities, i.e. 0.2 m $d^{-1}$ (Degenkolb et al., 2018) and 0.7 m $d^{-1}$, and ii) laboratory column experiments with pristine and pond water-aged sediment for both flow rates. Fig. 1 provides an overview of the experimental design:

Transport of citrate-coated Ag NP was investigated in outdoor, near-natural riverbank filtration columns (length 1.5 m, surface area 1 $m^2$) imbedded in a slow sand filtration pond (a) over the course of one month. Within this time, a stagnation period (stopped flow) and a remobilization scenario (flow rate increased to 1.7 m $d^{-1}$) were included (b). The role of dead and living organic material on NP transport and retention was studied in lab-scale columns (c) using pristine (d) and pond water-aged sediments (e).

Both lab and outdoor columns were filled with coarse-grained medium sand ($d_{50}$: 0.38 mm, bulk density in the top 10 cm: 1.78 g $cm^{-3}$, size distribution see Figure S 1, provided by Sand + Kies Union GmbH, Hartmannsdorf), mainly containing quartz and trace amounts of several elements such as Fe ($Fe_{tot}$: 1.143 ± 0.094 g $kg^{-1}$), Al ($Al_{tot}$: 0.869 ± 0.135 g $kg^{-1}$), and Ti (observed by the EDX detector of the electron microscope, not quantified). As mobile phase, natural pond water diluted with reverse osmosis water to an electrical conductivity (EC) of 250-300 µS $cm^{-1}$ was applied (Table 1).

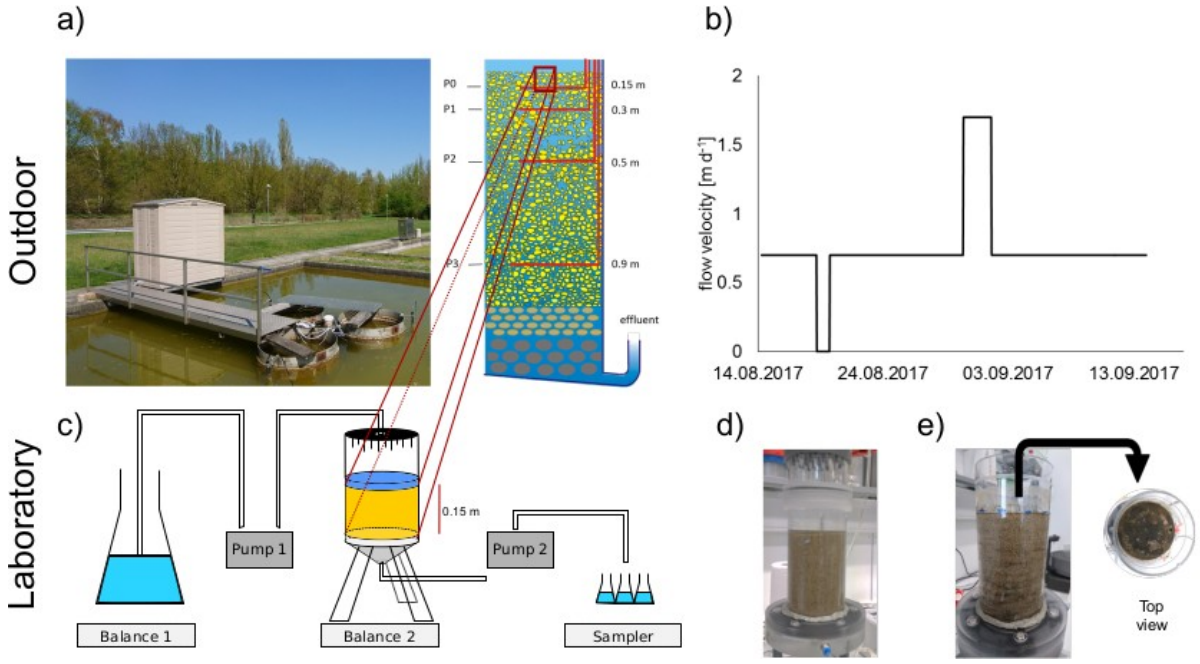


**Fig. 5. 1:** Experimental design of the study where a) is the near-natural riverbank filtration system, surrounded of a slow sand filtration pond, b) the flow schedule of the outdoor experiment, c) the laboratory setup for the column experiments with pristine (d) and pond-aged sediment (e).

**Table 5. 1:** Background ion and NP concentration of the mobile phase of lab and outdoor column experiments, mean and standard deviation (SD) of measurements of 3 replicates.

| **Elements / Parameters** | **Lab Experiment High Flow** | | **Lab experiment Low Flow** | | **Outdoor Column** | |
|---|---|---|---|---|---|---|
| | *Mean* | *SD* | *Mean* | *SD* | *Mean* | *SD* |
| **Ag NP [mg $L^{-1}$]** | 0.56 | 0.13 | 0.69 | 0.33 | 0.53 | 0.18 |
| **Al [mM]** | b.d.l[1] | | b.d.l[1] | | b.d.l[1] | |
| **Ca [mM]** | 0.781 | 0.011 | 0.678 | 0.004 | 0.563 | 0.012 |
| **Fe [mM]** | b.d.l[1] | | b.d.l[1] | | 0.111 | 0.012 |
| **K [mM]** | 0.001 | 0.001 | 0.023 | 0.000 | 0.030 | 0.002 |
| **Mg [mM]** | 0.171 | 0.002 | 0.157 | 0.001 | 0.140 | 0.001 |
| **Mn [mM]** | b.d.l[1] | | b.d.l[1] | | 0.039 | 0.011 |
| **Na [mM]** | 0.402 | 0.108 | 0.571 | 0.002 | 0.701 | 0.006 |
| **$F^-$ [mM]** | 0.011 | 0.010 | 0.016 | - | 0.012 | - |
| **$Cl^-$ [mM]** | 0.520 | 0.003 | 0.506 | - | 0.490 | - |
| **$NO_3^-$ [mM]** | 0.016 | 0.014 | 0.012 | - | 0.003 | - |
| **$SO_4^{2-}$ [mM]** | 0.507 | 0.002 | 0.503 | - | 0.453 | - |
| **TOC [mg $L^{-1}$]** | 4.1 | 0.5 | 5.1 | 2.3 | 5.3 | 0.2 |
| **EC [µS $cm^{-1}$]** | 262 | 14 | 297 | 0 | 257 | 8 |
| **pH** | 8.2 | 0.0 | 7.9 | 0.1 | 8.1 | 0.1 |

[1] below detection limit

### 5.3.2 Nanoparticle material

Citrate-coated, isotopically enriched $^{109}$Ag NP with a hydrodynamic diameter of 48 ± 3 nm and a ζ-potential of -41 ± 3 mV were applied in all experiments. A detailed description of the preparation of $^{109}$Ag NP can be found in Metreveli et al. (in prep.). Briefly, metallic granulate of $^{109}$Ag (99.67 ± 0.09% $^{109}$Ag, STB Isotope Germany GmbH, Hamburg) was dissolved in concentrated nitric acid ($HNO_3$, 65%, Suprapur, Merck, Darmstadt) and heated in a water bath. After complete dissolution of the granulate, the solution was further heated until complete evaporation. The crystallized $AgNO_3$ was dissolved in deionized water, ultrafiltered (cut-off of 50 kDa), and adjusted to pH 4. To prepare $^{109}$Ag NP, the method of Turkevich et al. (1951) modified for Ag was applied using $^{109}AgNO_3$ as described elsewhere (i.e. Klitzke et al., 2015).

The citrate coating was used to stabilize Ag NP suspensions against aggregation. For transport experiments, the $^{109}$Ag NP were dispersed in diluted pond water to a final $^{109}$Ag concentration of 0.61 ± 0.22 mg $L^{-1}$ and a background concentration of Suwannee River (SR) NOM of 0.8 mg $L^{-1}$ was adjusted. Stock solution of SR-NOM was prepared as described by Degenkolb et al. (2018). The mixtures were prepared 1 h prior to each column experiment to allow NP equilibration with SR-NOM.

The reader should note that NP suspensions of the outdoor and low flow lab experiment contained a second kind of NP, namely Ag@Au NP (i.e. Ag NP with a gold core, further information given in the Supporting Information and Figure S 2) with $c_{NP}$ = 0.56 ± 0.26 mg $L^{-1}$ which were used to study the different transport of NOM-coated and uncoated Ag NP. However, due to poor recovery results it was not possible to analyze the data in a sufficient way. We assumed that interaction of both NP with each

other was subsidiary as particle concentrations are very low resulting in a low collision frequency. In this manuscript, we show only the data of $^{109}$Ag NP.

### 5.3.3 Near-natural riverbank filtration experiment

To complement the low-flow experiment (0.2 m $d^{-1}$) conducted by Degenkolb et al. (2018), the transport and retention of Ag NP in a near-natural riverbank filtration system was investigated at a higher flow rate (0.7 m $d^{-1}$). For a detailed description of the column system, we refer readers to the previous publication (Degenkolb et al. 2018). In brief, two columns filled with pond water-aged sediments were included in a slow sand filtration pond. At a depth of 15, 30, 50, and 90 cm, sampling ports made of perforated stainless steel tubes were connected with PVC tubes to automatic sampling units; at the outflow water was sampled manually. The experiments were performed in duplicates for the duration of 1 month (14$^{th}$ August – 13$^{th}$ September 2017).

The columns were fed by diluted natural pond water from the surrounding slow sand filtration pond which was mixed with reverse osmosis water to an EC of 250 µS $cm^{-1}$ in a barrel before addition to sediment column. On top of the columns, a supernatant of 70 L was adjusted and hydrochemical parameters and ion concentrations (ICP-OES, iCAP 6000, Thermo Scientific and ion chromatography, DX-120, Dionex for cations and anions, respectively) were measured (Table 1). A tracer experiment in the columns was conducted 6 days before the start of the NP application (Figure S 3): NaCl solution was mixed in 70 L of column supernatant (EC = 1.37 mS $cm^{-1}$) and EC was measured in all 4 depths as well as in the outflow for detection of the tracer.

For the NP experiment, NP suspensions were added to 70 L of column supernatant. After infiltration of the NP-containing supernatant the columns were flushed with diluted pond water during the complete experimental period. A flow velocity of 0.7 m $d^{-1}$ was applied for two weeks with a 24 h stagnation period after 4 d. After two weeks, the flow velocity was increased to 1.7 m $d^{-1}$ for 2 d to test the potential remobilizing effect of enhanced flow velocity on NP transport (Fig. 1b). To detect potential changes in environmental conditions, we continuously monitored EC (EC probe, TetraCon, WTW, Germany) in the column inflow (supernatant) and outflow as well as pH (SenTix 41, WTW) and redox potential (SenTix ORP, WTW, values were corrected for the standard potential of the redox probe relative to the hydrogen normal electrode at 20 °C, i.e.+211mV) in the column outflow (Figure S 4).

Effluent samples of the different depths for quantification of Ag were taken over the whole course of the experiment. Effluent samples for toxicity tests (1.5 L in 15, 30, and 90 cm depth) were taken during the expected breakthrough of highest NP concentrations (i.e. breakthrough of the tracer in the respective depth). . At the end of the experiment, columns were drained and subsequently, sediment samples were taken up to a depth of 75 cm using a soil auger (Pürckhauer, outer diameter 28 mm, inner diameter: 18 mm). Four sample cores were taken and separated into 2 cm intervals for the upper 30 cm, and into 5 cm intervals below. Additional samples of the topmost 10 cm, segmented into 1 cm intervals, were taken to measure organic carbon (C) and nitrogen (N) concentration in addition to Ag.

### 5.3.4 Laboratory column experiments

Clean sediment (termed as “pristine sediment”) directly obtained from the manufacturer, and sediment aged in natural pond water (termed as “aged sediment”) was used for the lab-scale column experiments. The optical difference between the columns was clearly visible: while the pristine sediment was a clean sediment, the aged sediments had layers of greenish-gray material on top as well as in different depths which were formed during column packing of the homogenized substrate under water-saturated conditions (Fig. 1d).

Like in outdoor experiments, the lab sediment columns were flushed with diluted pond water from the slow sand filtration pond. However, water was taken at a sampling point beneath the pond after passing a layer of filter sand. Therefore, natural colloids of the pond were mostly absent (i.e. remained in the sand layer) in the mobile phase of lab column experiments which led to low Fe concentrations, in contrast to the outdoor experiment (Table 1).

The column cylinders were made of polycarbonate with an inner diameter of 9.7 cm and 20 cm in height. The pristine columns were filled up to 15 cm with 1793 g sediment, resulting in a bulk density of 1.78 g $cm^{-1}$. The pond water-aged sediment was continuously saturated to preserve the physico-chemical and biological conditions of the system. The alteration of the natural, pond water-aged sediment (probably caused by accumulation of low density organic material and leaching of fines) led to a reduced bulk density of 1.4 g $cm^{-3}$ (high flow) and 1.7 g $cm^{-3}$ (low flow). Comparable to the outdoor experiment, a supernatant (4 mm) was adjusted, which ensured a continuous saturation of the column during the experiment. Both columns were enwrapped with aluminum foil to reduce the influence of light.

The columns were placed on a sintered glass plate embedded in a tripod, which sealed the column at the lower boundary. An irrigation device with 21 evenly distributed needles was installed on top of the columns to homogenously spread the suspension on the entire surface. A constant inflow of the different suspensions was provided by a peristaltic pump. A flow rate of j = 0.2 and 0.7 m $d^{-1}$, respectively, was applied by a second peristaltic pump connected to the lower boundary (Fig. 1c). By using the same flow rate for both pumps, a stable flow field was adjusted (inflow = outflow). The effluent was continuously sampled by a fraction collector in 7.5 mL test tubes. To control the flow rates, both the suspension reservoir and the column setup were mounted on a balance and the masses were automatically recorded every 60 s.

All transport experiments were conducted in the same order: At first, a stable flow field was established by applying 3 pore volumes (PV) background solution (DI water for pristine columns, and diluted pond water for aged columns); followed by a tracer experiment with KBr (3 PV, EC = 820 µS $cm^{-1}$) and flushing of the column with 7 PV diluted pond water. The following NP-transport experiment was separated into 5 PV of Ag NP suspension application and flushing with 8 PV of diluted pond water.

Samples of the inflow NP suspension were taken to analyze NP concentrations and characterize physico-chemical parameters of the suspension (Table 1). At the end of the experiments, the entire sediment of each column was taken in 1 or 2 cm intervals except for the uppermost layer which was split into 2 samples: 0 to 0.2 cm and 0.2 to 1.0 cm.

### 5.3.5 Analyses

Particle size and ζ-potential

The colloidal stability of Ag NP used in lab column experiments was tested by time-resolved dynamic light scattering (DLS) measurements with a Zetasizer Nano ZS (Malvern Instruments). Silver NP were freshly mixed with diluted pond water including NOM and Ag@Au NP concentrations according to the experimental setup. The size of NP was measured for 24 h every 30 s. The highest peak of the size distribution (i.e. intensity-weighted Peak 1) was used for discussion of the data. The ζ-potential was measured before and after size measurement (Zetasizer Nano ZS, Malvern Instruments) and was calculated from electrophoretic mobility based on the Smoluchowsky approximation.

Particle properties in the supernatant of the outdoor experiment were analyzed by hydrodynamic chromatography (HDC) coupled to ICP-MS as the presence of natural colloids would interfere with DLS measurements. By HDC-ICP-MS, particles were separated by size via a HDC column and the isotopes $^{107}$Ag, $^{109}$Ag, $^{197}$Au, and $^{27}$Al were measured using ICP-MS. The retention time was used to estimate the NP size using citrate-stabilized gold NP (characterized by Rakcheev et al., 2013) as calibration standards, while the isotope composition allows NP identification. The size distributions were determined after signal deconvolution (see supporting information for more details).

The measurement procedure is described in detail by Degenkolb et al. (2018). Briefly, size separation was achieved at room temperature using PL-PSDA type 2 HDC column (separation range: 20–1200 nm. Agilent. Germany) connected to an HPLC system (Agilent 1220. Germany). The flow rate of the eluent (MQ water containing 1.8 mM sodium dodecyl sulphate, 3.2 mM Brij L23, 3.2 mM Triton X-100 and 7.46 mg $L^{-1}$ D-

penicillamine, adjusted to pH 10) was 2.1 mL $min^{-1}$ and injection volume was 60 µL for samples and 5 µL for the internal standard. As internal standard for intensity drift correction and time marking, citrate-stabilized gold nanoparticles with a diameter of 5 nm (Sigma Aldrich) were used.

Quantification of silver in effluent and sediment samples

At the column outflow samples were taken for quantification of Ag concentrations as well as dissolved Ag breakthrough. Samples for NP quantification were stored in glass vessels at 4°C in the dark until digestion and analysis. For quantification of dissolved Ag, samples were separated by centrifugal ultrafiltration (cut-off 50 kDa, Amicon Ultra-15 centrifugal filter device, Merck Millipore) directly after sampling and afterwards stored in plastic vessels at 4°C in the dark until measurement by ICP-MS.

Aqueous samples were digested in HCl/$HNO_3$ (1:1 v/v) for Ag analysis using a two-step temperature program in the microwave (temperature ramp of 30 min from room temperature to 95 °C and subsequent 30 min irradiation at a constant temperature of 95 °C at 800 W). A volume of 10 mL sample was mixed with 4 mL of the acid mixture (final acid concentration of 4.5 and 9 % for HCl and $HNO_3$, respectively) and digested in the microwave in Teflon tubes. Afterwards, samples were diluted to an acid concentration of 1.5 % HCl and 3 % $HNO_3$ with DI water.

All sediment samples were dried at 105°C and homogenized in a disc vibrating mill (Retsch PM 40). For analysis of C and N a subsample of 20 g of the sediment was further ground to finer grain sizes (Narva Vibrator, GDR) and analyzed for total C and N (vario EL III, Elementar Analysensysteme). To calculate the amount of organic C,

sediment samples were additionally dried at 600°C and subsequently measured by CNS analyzer.

Sediment samples were digested in aqua regia as previous tests showed a good recovery for this method (data not shown). Here, 0.5 g sediment was weighed into microwave tubes and 5 mL of acid were added. A similar temperature program as for aqueous samples was applied. A centrifugation step (4.500 rpm, 30 min, Sorvall Lynx 6000, Thermo Scientific) followed the microwave digestion to remove undissolved solids. Silver concentrations were measured by ICP-MS (iCAP Q, Thermo Scientific).

Both methods as well as recovery rates are described by Metreveli et al. (in prep.) in more detail.

Ecotoxicological tests

Test organism

*Daphnia magna* (Eurofins-GAB, Germany) were cultured in a climate-controlled chamber (Weiss Environmental Technology Inc., Germany) at 20±1 °C applying a 16:8 h (light:dark) photoperiod (visible light intensity: 3.14 $W/m^2$; UVA: 0.01 $W/m^2$; UVB: 0.01 $W/m^2$; as detailed in Dabrunz et al., 2011). In groups of 25 individuals (age >14 d), adult organisms were kept in 1.5 L of reconstituted hard freshwater recommended by ASTM International Standard Guide E729 (ASTM 2007). Additionally, the medium was enriched with selenium, vitamins (thiamine hydrochloride, cyanocobalamin, and biotin; ASTM-Medium), and seaweed extract (8.00 mg TOC $L^{-1}$; Marinure®, Glenside, Scotland). The culture medium was renewed three times a week and the animals were daily fed on *Desmodesmus* sp. (200 µg C per organism).

Toxicity studies

For each effluent of the different sampling depths (15, 30, and 90 cm) individual acute toxicity studies were carried out using *D. magna* as test organism. Moreover, the acute toxicity of the applied NP suspensions ($^{109}$Ag NP, and Ag@Au NP) was assessed individually and in mixture similar to the supernatant of the large-scale experiment (diluted pond water, 0.5 mg $L^{-1}$ $^{109}$Ag NP, 0.8 mg $L^{-1}$ SR-NOM, and 0.6 mg $L^{-1}$ Ag@Au NP). The conducted experiments were generally based on the OECD guideline 202 (OECD 2004), with a prolonged test duration to 96 h, as recommended for testing nanoparticulate substances (Dabrunz et al., 2011).

Five juvenile daphnids (age <24 h) were exposed to increasing concentrations of the respective NP suspension ($^{109}$Ag NP: 0, 30, 40, 50, 60, 70, 80, and 100 %; Ag@Au NP: 0, 33, 44, 56, 67, 78, 89, and 100 %; Mix: 0, 0.25, 5, 10, 20, and 30% of the input concentration) and different column effluents (2.5, 5, 10, 20, 30, 50, and 100 % of effluent from 15, 30, and 90 cm depth) using ASTM-Medium as test medium. Each applied concentration was replicated four times. Every 24 h, daphnids were visually checked for their mobility. Animals were considered as immobile when the test beaker was gently agitated and no movement was recognizable within 10 s. Mobility data were used for the calculation of half maximal effect concentrations ($EC_{50}$), illustrating the concentration of NP suspension/column effluent causing immobility in 50% of the exposed daphnids.

Scanning electron microscopy

Scanning electron microscopy was used to visualize retained NP and the presence of organisms in the upper 1 cm of outdoor column sediments. Approximately 1 mg of

sediment sample of each outdoor sediment column was air-dried on a silicon waver. Analyses were conducted at the Center for Electron Microscopy (ZELMI) of the TU Berlin with an low vacuum-SEM (GeminiSEM500 NanoVP, Zeiss) coupled with an EDX detector (Bruker Quantax XFlash 6I60; EDAX, software 'TEAM', detector 'Apollo' — acquisition parameters of the beam: accelerating voltage: 15 kV, chamber pressure: 84 Pa). Per sample, at least 20 different points were investigated under the microscope to get an impression of the distribution of Ag NP on the sediment.

## 5.4 Results

### 5.4.1 Nanoparticle properties

The absolute value of the ζ-potential of citrate stabilized Ag NP (originally -41.3 mV) was only slightly changed by SR-NOM coating (-38.6 mV) but was reduced in diluted pond water to -12 ± 1 mV. However, only slight aggregation was observed during 24 h of time-resolved DLS measurement: From an original size of 48 nm Ag NP size increased to a final diameter of 62 ± 12 nm (Polydispersity index (PdI) 0.3±0.2) in the high flow experiment. During low flow experiment NP size changed from 66 ± 6 nm up to a size of 111 ± 12 nm (PdI 0.4±0.0). In the high flow experiment, only $^{109}$Ag NP with a background SR-NOM concentration of 0.8 ppm were applied. In the low flow experiment, Ag@Au NP were additionally present in the mixture, so that the size measured by DLS is an average of both kinds of NP. This explains the different results of DLS measurements for the low and high flow experiment.

A slight aggregation of NP was also observed in outdoor experiments by HDC-ICP-MS measurements (Figure S 5): $^{109}$Ag NP with an initial particle size of 52.8 ± 2.3 nm aggregated to diameters of 101.8 ± 8.9 nm. Despite of the presence of natural colloids in the outdoor columns, the observed aggregates seemed to be Ag NP homoaggregates as their size was exactly twice as large as primary particles. Sizes measured by HDC-ICP-MS suggest that heteroaggregation with Ag@Au NP was not predominant but may have occurred sporadically.

### 5.4.2 Comparison of pristine and aged sediment column properties

Sediments of all column experiments were analyzed for total C and N concentration. Due to seasonal changes in the ecological community in pond water and on sediments, values differed between the aged sediments of the three different column experiments (Fig. 2a, Figure S 6). Additionally, columns of the outdoor experiment represent an undisturbed sediment profile, whereas lab columns were filled with homogenized sediment material.

Generally, aged sediments had higher N concentrations than pristine sediments (0.02 ± 0.01 % in aged sediments compared to 0.003 ± 0.000 % in pristine sediments, Fig. 2a). Outdoor columns and low flow lab columns showed higher N concentrations in the upper sediment layers. High flow lab columns had highest N concentrations of all sediments without a gradient in depth.

Organic carbon concentrations fluctuated strongly and were generally very low, but except for the high flow experiment did not differ between aged and pristine sediments (0.27 ± 0.21 % in aged sediments compared to 0.13 ± 0.05 in pristine sediments, Figure S 6). The C/N ratio tended to be lower in aged sediments, but trends were not clear (20.5 ± 9.0 % in aged sediments compared to 39.5 ± 15.6 % in pristine sediments, Figure S 6).

Electron microscopy showed the presence of diatoms in the first centimeter of the outdoor columns (Fig. 2b). Additionally, cyanobacteria, green algae, and nematodes were identified under the light microscope in the first centimeter of sediments from lab as well as outdoor experiments (Figure S 7).

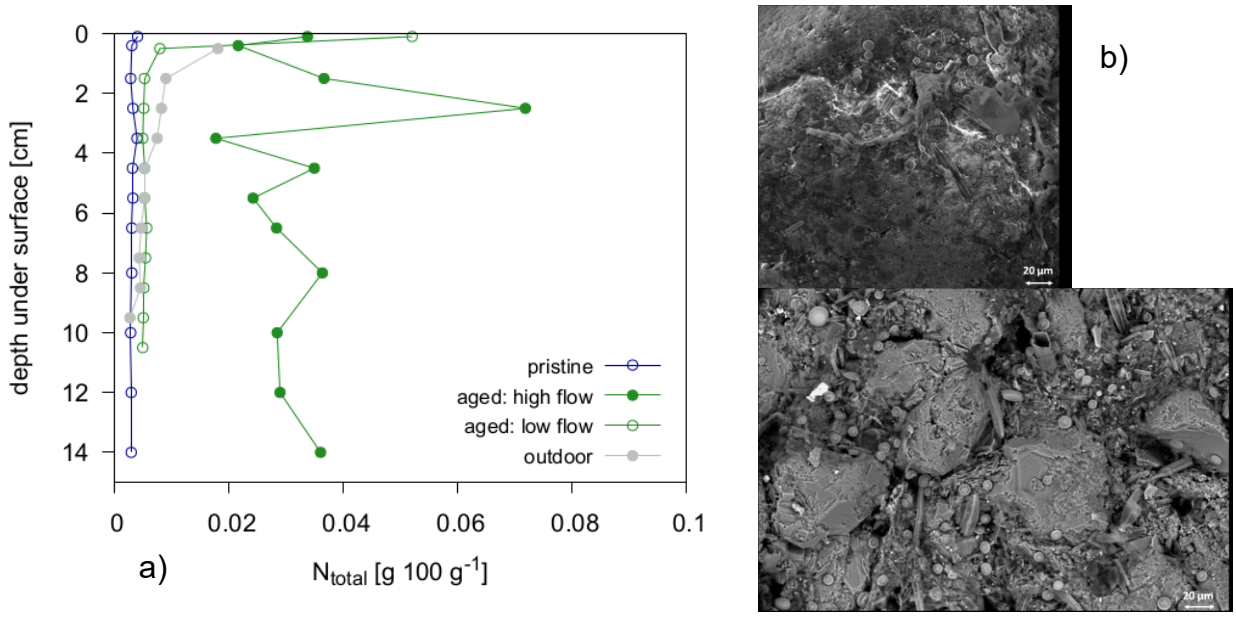


**Fig. 5. 2:** a) N concentration in pond water-aged sediments of outdoor (grey) and lab (green) column experiments at high (filled circles) and low (open circles) flow conditions in comparison to pristine (blue) sediments; b) Diatoms in the upper centimeter of the sediment of outdoor experiments, visualized by SEM (lower image: back-scattered electron detector, upper image: variable pressure secondary electron detector, both: voltage 15 kV, pressure 84 Pa).

### 5.4.3 Outdoor column experiment

In the column supernatant, total $^{109}Ag$ concentrations of 533 ± 180 µg $L^{-1}$ were detected; less than 0.5 % was dissolved $Ag^{+}$ (0.05-1.6 µg L). Silver NP breakthrough was observed as single and rare events in the uppermost depth of 15 cm (Fig. 3); below, no NP breakthrough occurred. Silver concentrations during the single breakthrough events were very low (between 0.1 µg $L^{-1}$ and 1.6 µg $L^{-1}$) and mainly occurred during the first 5 PV, i.e. during NP application (phase I), or directly after changing to diluted pond water application (phase II). The stagnation period (phase III) and the high flow scenario (phase V) did not show any effect on NP breakthrough.

High $^{109}Ag$ contents in the sediments of both columns were observed after one month of flushing with diluted pond water for the top 25 cm of the columns. The Ag NP content was decreasing with depth illustrating high accumulation in the upper 10 cm of the

columns (Fig. 4 for 0 - 30 cm and Figure S 8 for 0 - 75 cm). The indicated error bars from different sampling locations display the high local variability of Ag contents in the column sediment. However, the shape of the profile was detected for both columns, and is in line with the findings of the outdoor low flow experiment of Degenkolb et al. (2018) as illustrated in Fig. 4.

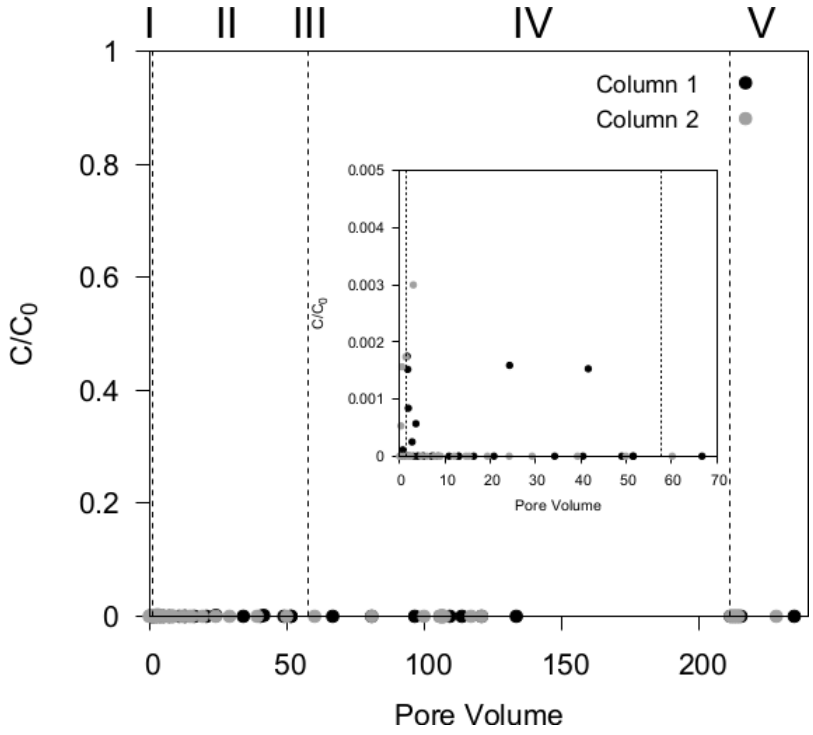


**Fig. 5. 3:** Erratic breakthrough events in a sampling depth of 15 cm in outdoor experiments for the two replicate columns (grey and black circles). Roman numerals mark the phases of the experiment: I) NP application, II) diluted pond water application at flow rate of 0.7 m $d^{-1}$, III) stagnation, IV) diluted pond water application at flow rate of 0.7 m $d^{-1}$, and V) diluted pond water application at flow rate of 1.7 m $d^{-1}$.

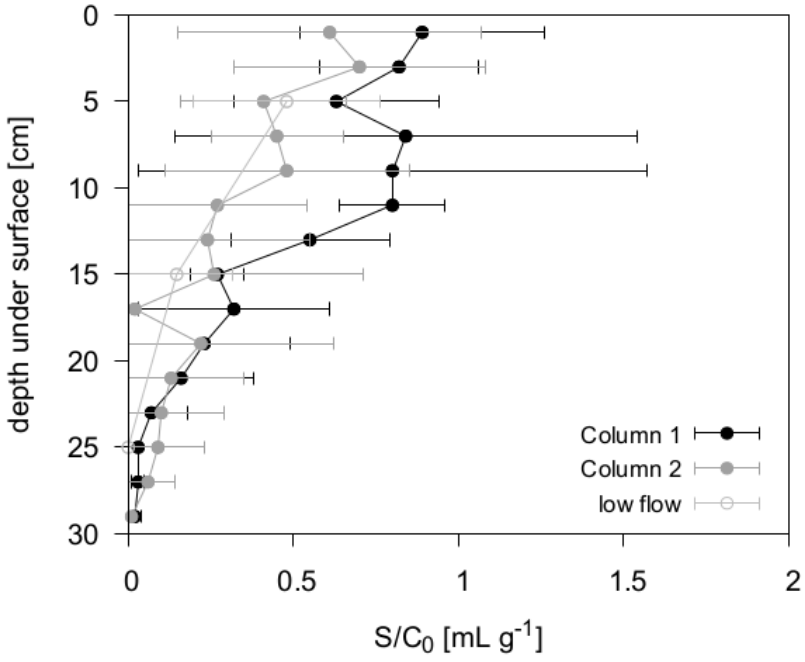


**Fig. 5. 4:** $^{109}$Ag retention profile for the upper 30 cm of sediments for both columns. The error bars margin the 95% confidence interval by two times standard error of 3-4 replicates. For comparison, values gained by Degenkolb et al. (2018) are included as low flow scenario.

Ecotoxicity tests

The 96- h $EC_{50}$ values were evaluated to test the ecotoxicity of Ag NP-containing suspensions entering the riverbank filtration system. In addition, the toxicity of the single particle suspensions (i.e. $^{109}$Ag NP and Ag@Au NP) was investigated. The lowest $EC_{50}$ was observed for the mixture (~0.09 mg $L^{-1}$), followed by $^{109}$Ag NP (~0.14 mg $L^{-1}$), and Ag@Au NP (~0.19 mg $L^{-1}$; Figure S 9 and Table S 1). In contrast, none of the applied effluent suspensions caused any immobility in the test organisms due to the extremely low or absent Ag NP breakthrough in all depths.

### 5.4.4 Lab column experiments

The analysis of the tracer experiments is in good agreement with the gained pore water velocities of the outdoor and laboratory experiments for both flow rates (Figure S 10). Only diffusion was higher in the aged sediment column at high flow rate compared to the outdoor experiment and the pristine sediment column.

The input Ag NP suspensions of low and high flow lab experiments had a $^{109}Ag$ concentration of 559±133 and 691±327 µg $L^{-1}$, respectively, with a dissolved $Ag^{+}$ concentration between 0.5 and 6.9 µg $L^{-1}$.

In pristine sediment columns, almost no NP were measured in outflow samples, but some erratic peaks occurred (Fig. 5). For the low flow scenario, low concentrations of less than 0.5 % of initial NP concentration were measured after 1 PV. For the high flow experiment, no Ag NP breakthrough was observed. Both during high flow and low flow experiments, a single point of Ag breakthrough occurred after changing the inflow from NP suspension to flushing solution (i.e. diluted pond water without Ag NP) which seemed to mobilize a part of retained Ag NP.

In accordance with the breakthrough results, we found large Ag NP contents in the upper part (0 - 7 cm) of both columns after the end of the experiments (Fig. 6). When sediments were aged in pond water with accumulation of organic materials, no Ag NP breakthrough was observed for neither low nor high flow rates (Fig. 5). In contrast to the retention in pristine sediments, Ag NP were accumulated at the very top of the columns and transported not further than 2 cm, irrespective of flow velocity (Fig. 6).

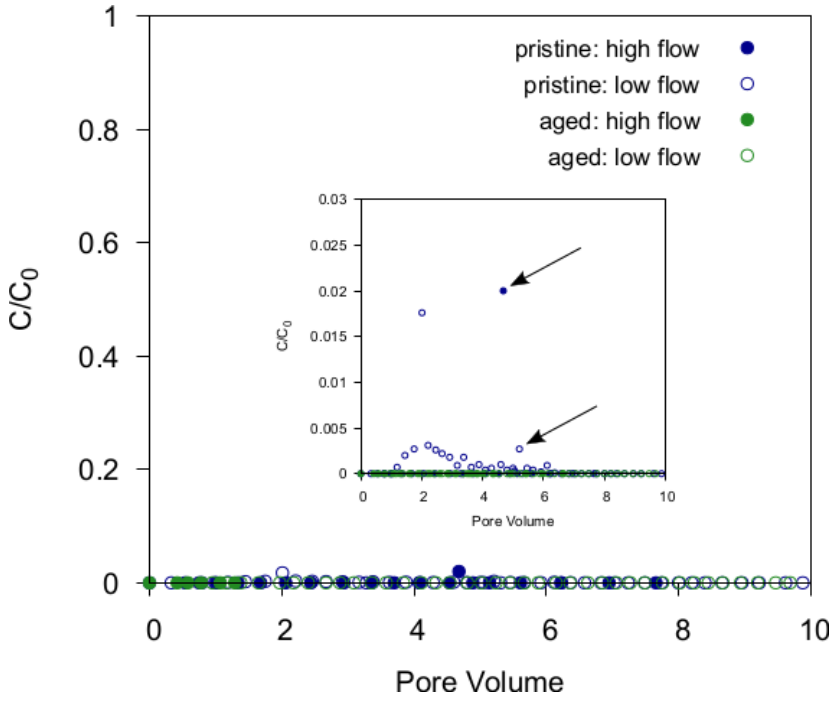


**Fig. 5. 5:** Breakthrough of Ag NP in lab column experiments for both pristine (blue) and aged (green) sediment at high (filled circles) and low (open circles) flow rates: single release events of Ag NP took place in pristine columns. Arrows mark the samples taken after changing from NP suspension to diluted pond water.

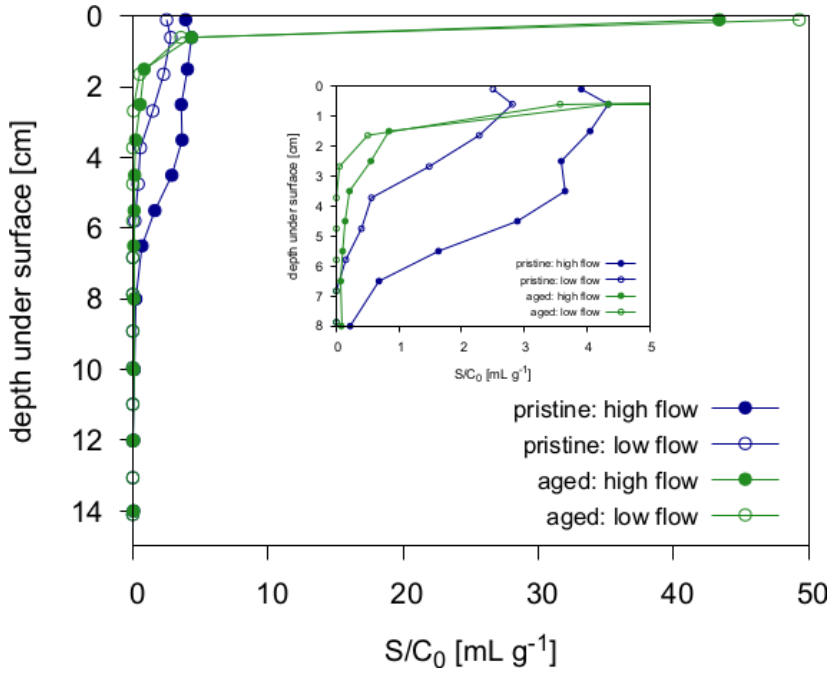


**Fig. 5. 6:** $^{109}$Ag NP retention profiles in pristine (blue) and aged (green) sediments under high flow (filled circles) and low flow (open circles) rate.

### 5.4.5 Mass balance of column experiments

Almost all Ag NP applied in our column experiments were retained in the column sediments with a recovery of 102 ± 32%. However, this retention had a high spatial variability (Table 2), especially in the outdoor experiments. In lab experiments, the complete sediment was dried and homogenized by milling, but only 0.5 g of sediment of each depth was analyzed. Furthermore, highest Ag concentrations at the top of the columns made the mass balance very sensitive to the estimated thickness and bulk density of the upper layers. For the pristine lab experiments, the Ag recovery was significantly lower for the low flow experiment (58.8 %) compared to the high flow experiment (140.8 %).

**Table 5. 2:** Recovery of Ag in sediments of column experiments.

| **Lab experiments** | | | | **Outdoor experiments** | |
|---|---|---|---|---|---|
| Pristine, low | Pristine, high | Aged, low | Aged, high | Column 1 | Column 2 |
| 58.7% | 140.8% | 98.2% | 77.4% | 178±63% | 95±16% |

## 5.5 Discussion

### 5.5.1 The presence of biological components in aged sediments

Both outdoor and aged lab column sediments contained high concentrations of N, especially in the upper centimeters (Fig. 2a). We presume that this is caused by the activity of N-fixing cyanobacteria that are dependent on light available on the surface of the columns. Highest N concentrations distributed over the complete column (high flow scenario) were measured in sediments taken in late autumn (November 2018), when cyanobacteria were not active anymore (Caron et al., 1985). Dead organic material settled on the sediments of the column in large amounts and decomposers' activity was already reduced so that biological substances accumulated on top of the columns (Buscail et al., 1995). This is also supported by the high organic C concentrations in the sediments of the high flow lab experiment as C was distributed over the entire sediment profile during sediment sampling and homogenization for the lab experiments. The high amount of organic material in the high flow experiment can be one explanation of the lower bulk density (1.4 g $cm^3$ compared to 1.7 g $cm^3$) of the sediments as well as the stronger effect of diffusion on tracer breakthrough displayed in Figure S 10.

The presence of living organisms in the upper centimeter of aged lab and outdoor columns was proven by electron and light microscopy. A high number of diatoms (Fig. 2b) as well as cyanobacteria, green algae, and nematodes (Figure S 7) confirm that aged sediments exhibited a high biological activity.

### 5.5.2 Nanoparticle reactions in the column system

Before addition to the columns, citrate-stabilized Ag NP were coated by SR-NOM to enhance the comparability with NP possibly present in natural systems. While the surface charge of citrate stabilized Ag NP is negative both in the presence and absence of SR-NOM, NOM enhances steric repulsion between NP and sediment surfaces which enhances NP stability. Still, Ag NP surface charge was reduced in diluted pond water with $Ca^{2+}$ concentrations of 0.7 mM and Ag NP aggregated slightly. Divalent cations and especially $Ca^{2+}$ are well-known to cause NP aggregation by bridging between organically coated NP and charge neutralization by compression of the electrical double layer of NP (Philippe and Schaumann, 2014). However, the measured particle sizes in high and low flow experiments of 62 and 111 nm, respectively, are much smaller than the pores of the sediment columns where approximately 75 % of the water is stored in pores with a radius larger than 1 µm (according to water content and grain size distribution). Therefore, the slight aggregation will not cause significant mechanical filtration and NP-to grain size- ratio is too small to expect any straining effects or surface filtration (Bradford et al., 2006; McDowell-Boyer et al., 1986).

As observed by the use of ultracentrifugation, only samples of the column supernatant contained dissolved $Ag^{+}$ ions. In the effluent, no $Ag^{+}$ was observed. This suggests that Ag NP dissolution was no relevant process during the column experiment. However, potentially existing $Ag^{+}$ ions might also have sorbed to the solid phase of the porous system.

### 5.5.3 Effect of flow velocity on NP transport and retention

The transport experiments in lab columns with pristine sediments seem to support our expectation that increasing flow rates would enhance NP transport as retention profiles showed Ag NP transport into greater depths when flow velocities were higher. However, due to the significant differences in mass recovery (Table 2) and the resulting uncertainties of the absolute measured concentrations this hypothesis can neither be confirmed nor denied definitely. By analyzing the shape of the profiles, the respective maximum retention of Ag NP was measured in a depth of 2 cm for the low flow scenario and 4 cm for the high flow scenario. Below, Ag concentrations in the sediment sharply decrease in both experiments.

In lab experiments with aged sediments as well as in outdoor experiments no differences were observed in transport and retention under different flow rates. In the lab columns, no NP breakthrough was determined under aged conditions and NP were accumulated in the uppermost 2 mm of the column with no transport below 2 cm depth, irrespective of flow velocity. This suggests that diffusion to attachment sites does not limit NP retention in aged sediments as increasing flow rate does not lead to enhanced NP transport in case of the presence of biological components. Also in near-natural outdoor columns results at 0.7 m $d^{-1}$ flow velocity are comparable to findings at lower flow rate (0.2 m $d^{-1}$, published by Degenkolb et al., 2018). Hence, even 3.5-fold higher flow rates do not lead to NP transport in aged, biomass-containing saturated sediments, such as riverbank filtration systems.

In general, NP mobility was low under all tested conditions in our study. Both flow conditions used in our column experiments (i.e. 0.2 and 0.7 m $d^{-1}$) are in the range of natural flow velocities in sandy aquifers (Kunkel and Wendland, 1997) and smaller than most flow velocities applied in previous studies. Therefore, NP mass transfer in our

study is strongly affected by diffusion to and sorption on the solid phase instead of advection which leads to high NP deposition (Braun et al., 2015). In combination with the low NP concentration (0.6 mg $L^{-1}$ in our study compared to 3-45 mg $L^{-1}$ in other studies), this explains the lack of NP breakthrough which is in contrast to a variety of other studies using citrate coated Ag NP in comparable porous media (El Badawy et al., 2013; Li et al., 2013; Taghavy et al., 2013). These authors used flow rates between 15 and 55 m $d^{-1}$ which is 20-80 times larger than the high flow rate used in our study. A decreased residence time of NP in the pore space due to higher flow rates can reduce the possibility for NP to interact with potential attachment sites. Additionally, a reduced flow rate has been shown to enhance the possibility for NP diffusion in small pore spaces and to increase attachment efficiency in diffusion-determined colloid systems as soon as hydrodynamic drag forces of the water flow overcome interaction forces of colloids with sediment surfaces (Chang and Chan, 2008).

Moreover, a stronger Ag NP stabilization by organic coatings and very high NP concentrations (i.e. 60 mg $L^{-1}$) can cause Ag NP breakthrough even at flow velocities as low as 0.05 m $d^{-1}$ (Braun et al., 2015). This illustrates that although flow velocity is of high importance for NP mobility, factors such as colloidal stability and NP concentration also affect NP transport. Nevertheless, environmental concentrations of engineered NP are currently in the ng-µg $L^{-1}$ range (Gottschalk et al., 2009) and industrial coatings may be replaced or covered by less stabilizing natural coating agents (Louie et al., 2016), which highlights the environmental relevance of the results of our experiments.

### 5.5.4 The role of biomass for NP retention

The presence of biomass in lab column experiments prevented any breakthrough of Ag NP. While a small breakthrough curve (<0.5 % of initially injected NP) at low flow velocity, and single, erratic breakthrough events with higher Ag concentrations at high and low flow velocity were observed for pristine sediments, no Ag was detected in the outflow of aged sediment columns. Furthermore, NP deposition on biological surfaces was unaffected by increasing flow velocity.

Under abiotic conditions, attachment is expected to mainly occur on oppositely charged metal oxides and clay minerals as well as by $Ca^{2+}$-NOM bridging between coated NP and sediment surfaces. As sediment material contained trace amounts of several elements such as Fe, Al, and Ti, physico-chemical filtration on these surfaces seems to occur in pristine sediment columns. The determined maximum retention of Ag NP in the lab experiments with pristine sediment was between 1.3 to 1.6 µg/g for the low flow scenario and 2.4 to 3.0 µg/g for the high flow scenario in the first centimeters. Hence, the abiotic sediment provides geogenic attachment sites for negatively charged Ag NP. However, the progress of the retention front down to a depth of 2 - 4 cm and the erratic breakthrough of NP shows that these geogenic attachment sites are limited.

In contrast, the occurrence of biological components highly increased the maximum retention capacity of the material up to 27.6 µg/g in the low flow and 30.0 µg/g in the high flow column experiment. Enhanced deposition of Ag NP in aged sediments can be related to mechanical filtration and straining as organic matter reduces the pore space of the sediment (Bradford et al., 2011). Additionally, aged sediment surfaces may offer a higher surface roughness than pristine sediments which might have increased NP-sediment interactions (Hoek et al., 2003). However, mechanical retention is not likely in our sediment system due to the large NP-grain size ratio. More importantly, biological

surfaces offer a large number of versatile attachment sites for Ag NP so that NP are retained in the sediment system by chemical interactions. The presence of biocolloids such as proteins, bacteria, and polysaccharides offer various possibilities for interaction with NP. Covalent bonds to functional groups of organic matter are expected to lead to high interaction forces between biological components and Ag NP (Avellan et al., 2018; Nevius et al., 2012). Therefore, NP retention in aged sediments is high and NP are retained in the uppermost layers of the sediment.

In spite of the presence of biomass in outdoor columns, single, erratic breakthrough events were detected in the near-natural system, both at low and high flow velocity. This transport behavior is more comparable to the breakthrough in pristine lab columns, although sediment properties resemble the aged lab columns. Furthermore, Ag NP are transported in depths up to 25 cm in the outdoor column, but were retained on the column surface of aged sediments in the lab. These differences might be the result of the longer duration of the outdoor experiments, leading to slow NP transport through the outdoor sediment system. Potentially, degradation of organic matter in the sediment columns may be one reason for NP detachment and transport at longer experiment duration. Additionally, it has to be noted that sampling by the soil auger may have led to NP carryover in deeper sediment layers so that the transport depth might be overestimated in outdoor experiments.

The erratic breakthrough events, both observed in pristine lab experiments and outdoor columns illustrate that retained NP may be remobilizable under certain circumstances. However, the responsible processes are not well-understood, yet. As the remobilization was also observed in pristine sediment columns it might be an abiotic mechanism. For example, NP interactions with the solid-water interface may not be strong enough so

that small changes in environmental conditions remobilize a part of NP which breaks through at the column outflow. This assumption is supported by the observation in lab columns that breakthrough of Ag NP occurred when changing the input suspension from NP-containing pond water to NP-free pond water.

### 5.5.5 Nanoparticles in surface waters- a risk for potential drinking water reservoirs?

Both lab and outdoor experiments clearly showed a very low Ag NP mobility in riverbank filtration systems at flow velocities between 0.2 and 0.7 m $d^{-1}$ and NP concentrations of 0.6 mg $L^{-1}$. Sediment surfaces and biomass offer a variety of attachment sites for NP and low flow rates enable the diffusion to and interaction with these sites. An aged sediment system with a well established flora and fauna has a higher retention capacity for Ag NP than pristine sediments. Even the enhancement of flow velocity to 1.7 m $d^{-1}$, did not cause significant remobilization of retained Ag NP. However, previous batch experiments suggest a remobilization potential for Ag NP retained in aged sediments of the riverbank filtration system (Degenkolb et al., 2018). Probably, the 2.4-fold higher flow velocity during the high flow scenario in the outdoor experiment caused much lower shear forces than tested in the batch experiments of Degenkolb et al. (2018). Moreover, hydrochemical conditions remained constant during the high flow rate. During increasing flow rates in natural systems which may be caused by heavy rain events, water chemistry is expected to change which was shown to be effective in remobilizing NP when combined with mechanical forces (Degenkolb et al., 2018; Metreveli et al., 2015).

The almost complete retention of NP on the solid phase of the porous system led to an efficient detoxification of NP-containing suspensions. The high toxicity of NP input

suspension to *Daphnia magna* was completely eliminated after passage through 15 cm of a near-natural riverbank filtration system. This suggests a high potential of riverbank filtration for cleaning NP-containing surface water.

## 5.6 Conclusions

Overall, our experiments point out, that retention mechanisms of NP in saturated sediments are highly affected by the presence of biomass. Naturally occurring aging processes on riverbank filtration sediments enhance the efficiency of the system to retain potential NP contaminations in surface water. When biological material is present, NP immediately undergo attachment and deposition and accumulate in the uppermost sediment layers. This may explain the consistent observation of NP fate studies finding NP accumulation mainly in surficial sediment layers of aquatic ecosystems (Espinasse et al., 2018; Geitner et al., 2018; Lowry et al., 2012). Our results suggest that even at increasing flow rates NP attachment on biological material is efficient. However, NP breakthrough can occur in erratic, single peaks, a process that is not well-understood, yet, and needs future research. At larger time scales and in more complex systems, NP transport in deeper sediment layers may therefore take place.

Abiotic retention mechanisms (i.e. interaction with iron oxides, clay minerals or bridging processes in the presence of multivalent cations) also offer great potential for NP retention. Still, these mechanisms allow NP transport in deeper sediment layers. Although our results suggest that the risk for NP transport in riverbank filtrates is low, a constant NP input may lead to ecotoxicological relevant NP concentrations in upper sediments. Especially in areas of waste water discharge, constant NP introduction in surface water and deposition on sediments can be expected. Grazing organisms will feed on those contaminated sediments which might even lead to Ag NP accumulation in the food chain.

# 6 Synthesis and Conclusions

In the preceding chapters, questions about NP mobility in soils and water-saturated sediments were answered by experiments at different temporal and spatial scales with three different kinds of engineered NP. Nanoparticles reach soils and sediments for example through the application of fertilizer in agricultural fields or by flooding of floodplain areas from rivers containing industrial waste water. This raised questions about colloidal NP stability and the possibility for NP transport in these systems. The experiments of my thesis help to understand the effect of natural organic matter on NP stability and the processes that lead to their transport, retention, and remobilization. This will support the risk assessment of the use of NP in industrial and agricultural processes.

## 6.1 Sorption of soil organic matter to nanoparticles

As surface properties of NP are determining for their stability and mobility in the environment, it is crucial to understand sorption of soil organic matter to NP surfaces. The results summarized in chapter 2 of this thesis point out, that differences in soil properties may lead to variable NP fate, and different kinds of NP, i.e. NP of different chemical composition, undergo very different reactions in similar soils. This illustrates the complexity when trying to make predictions on NP fate and therefore ecological exposure in soils. My thesis showed that the quality of soil organic matter and the ionic strength and $Ca^{2+}$ concentration of the soil solution seem to be predominant factors determining the evolution of NP surface coatings.

### 6.1.1 Characteristics of natural organic matter

As shown in chapter 2 of this work, sorption of organic matter greatly varies between different soil solutions as well as for different kinds of NP. Important characteristics responsible for NOM adsorption to NP surfaces are the available amount of NOM and its hydrophobicity. Aromaticity and molecular weight of NOM can be determining for sorption of NOM, but in case of low OC sorption these properties seem to play a minor role. In case of the hydrophilic surface of Ag NP, sorption is most pronounced for hydrophilic organic matter which seems to result in multilayers of OC on NP surfaces. Therefore, strong OC sorption can be expected in water-influenced environments, such as floodplain soils. In contrast, hydrophobic interactions seem to be relevant in case of oxic $TiO_2$ NP. Those interactions are weaker and therefore, the formation of thin NOM monolayers was observed.

My observations challenge the common expectation that NP get coated by NOM as soon as they enter the environment. Instead, NOM sorption depends both on the chemical composition of NP and on the properties of organic molecules. This has important implications for NP risk evaluation as organic coatings have been shown to mitigate NP ecotoxicological risk (Lüderwald et al., 2019). However, NOM of farmland soil solution and floodplain soil solution did not sorb measurably to Ag and $TiO_2$ NP, respectively (chapter 2). This raises the assumption that stable NP without natural organic coatings might exist in natural environments over longer time periods as commonly expected.

### 6.1.2 Ionic composition

With increasing ionic strength in solution, NP stability is decreased due to the compression of NP EDL. This has already been discovered several decades ago

(Evans and Wennerström, 2000). However, the presence of inorganic ions also determines NOM sorption to NP (Seijo et al., 2009) which is supported by the results of this thesis (chapter 2). While low ionic strength seems to reduce the sorption of NOM to NP, high ion concentrations support NOM sorption by reducing the electrostatic repulsion between coating molecules and in the case of $Ca^{2+}$, by the formation of cation bridges between organic macromolecules (Philippe and Schaumann, 2014; Seijo et al., 2009). This leads to sorption of high amounts of NOM to NP surfaces which may be interpreted as multiple NOM layers. Additionally, the presence of cations affects the kind of NOM preferentially sorbing to NP surfaces. This was highlighted by the surprising results summarized in chapter 2 that at high ion concentration low molecular weight OM was preferentially adsorbed compared to high molecular weight OM contradicting the picture commonly drawn for NP sorption processes (e.g. in a current review by Louie et al., 2016). These findings underline the difficulty of transferring knowledge derived from simplified model systems to more complex situations and highlight the value of using environmentally relevant substances.

### 6.1.3 The variable fate of nanoparticles in natural soil solutions

Overall, the fate of NP in soils is highly complex and predictions are difficult. Different kinds of NP are differently affected by similar soil solutions. Soil solution properties, in return, cause different NP behavior depending on organic matter quality and quantity as well as ionic composition. The present work helps understanding the fate of $TiO_2$ and Ag NP in two kinds of soils (i.e. farmland and floodplain soil), but results might not easily be transferred to other soils and nanoparticles.

Schaumann et al., 2015 proposed that NP once entering the environment might undergo aging processes that, with time, align NP properties until they are equally coated by NOM. My thesis contradicts this hypothesis pointing out that aging processes strongly differ depending on the chemical nature of NP. Therefore, I propose that different NP will possess a coating of different organic molecules when entering similar soils. Additionally, dominating mechanisms for NP surface aging as well as stabilization and destabilization were identified to be related to NOM hydrophobicity, available amounts of NOM for sorption to NP, and inorganic ion content of the surrounding medium.

## 6.2 Nanoparticle fate in riverbank filtration systems

### 6.2.1 Transport and retention

The results of my thesis show that nanoparticles entering water-saturated sediment systems are strongly retained in the porous medium. Three main processes are known to cause colloid retention in porous systems: (i) attachment to solid surfaces, (ii) mechanical filtration, and (iii) straining (Bradford et al., 2006). For particles with a size in the range below 100 nm, mechanical filtration is not relevant in a porous system with a pore size distribution in the micrometer range. Straining occurs in dead pore spaces and due to surface roughness, but has been shown to be significant only at colloid-to-grain size ratios above 0.003 (Bradford et al., 2006). Due to the high reactivity of NP, physico-chemical attachment is of highest importance for NP retention in sediments, such as riverbank filtration systems.

The attachment process can be described in three steps (Bradford et al., 2011): *mass transfer* of colloids to the solid phase takes place by diffusion, interception, and

sedimentation leading to *collision* of NP with the solid surface. Subsequently, *retention* at the solid-water-interface (SWI) occurs when NP overcome the energy barrier between themselves and sediment particles. The retention process under unfavorable attachment conditions is governed by the attachment efficiency, i.e. the ratio of particles retained at the SWI compared to the total amount of colliding NP. Depending on the attachment energy, NP can attach in a stable primary minimum or a reversible secondary energy minimum. During my thesis, I elucidated the importance of NOM coating, presence of dead and living organic matter, and flow velocity on NP attachment. These factors influence different steps of the attachment process, thereby reducing or enhancing NP transport.

NOM coating:

As already known from various findings in the literature, surface coating of NP with organic molecules can enhance NP stability due to steric and electrostatic stabilization forces (Chen et al. 2012), but might also increase NP surface interactions when bridging phenomena occur (Akaighe et al., 2012; Philippe and Schaumann, 2014). This can enhance or reduce NP attachment efficiency. Both of these effects have been observed in this work:

(1) Reduction of attachment efficiency was observed for $CeO_2$ NP coated by PAA in saturated sediment systems as PAA stabilized NP electrosterically and led to a high NP mobility (chapter 3). Furthermore, Ag NP aged in NOM-containing soil solution were less stably attached to sediments compared to Ag NP aged in NOM-free DI water (chapter 4) showing the stabilizing effect of NOM-coating. In these cases attachment efficiency was reduced due to electrosteric repulsion, so that NP retention decreased.

(2) Enhancement of attachment efficiency took place when NOM- and HA-coated $CeO_2$ NP entered a sediment system with a mobile phase rich in $Ca^{2+}$ which caused strong NP retention (chapter 3). In a second example, Ag NP aged in river water containing both $Ca^{2+}$ and NOM were less mobile in saturated sediments than Ag NP aged in soil solution with less $Ca^{2+}$. Due to the high attachment energy, river water-aged Ag NP had a lower remobilization potential than soil-aged Ag NP (chapter 4).

Thus, knowing whether organic coatings are present or absent is not sufficient to predict NP mobility. Instead, the complex interplay between NOM and hydrochemical properties of the mobile phase results in different NP mobility.

However, also coating properties themselves (i.e. number and kind of functional groups, binding strength to NP surfaces) determine NP mobility which was shown by a comparison between synthetically and naturally coated $CeO_2$ NP. As synthetic, industrial coatings are designed to induce NP stability, synthetically coated NP were more mobile than naturally coated NP (chapter 3). In this case, the susceptibility of NP to enhanced $Ca^{2+}$ concentrations was larger in case of naturally coated NP. When synthetically coated NP enter the environment, the industrial coating might be covered or replaced by natural organic matter. This is expected to reduce NP mobility and lead to enhanced retention in upper sediment layers. However, my results also illustrate that different natural coatings (i.e. HA and NOM in $CeO_2$ NP in chapter 3) have different effects on NP mobility.

The results of my thesis help to predict the mobility of different kinds of NP (i.e., Ag, $TiO_2$, and $CeO_2$ NP) with a variety of surface coatings (i.e., natural vs. synthetic, and coatings of different environmental origin) in saturated sediment systems under varying environmental conditions (i.e. varying ionic strength, presence and absence of biological components and NOM). However, future studies are still needed to

complete the picture of the complex fate of NP with industrial and natural coatings under different hydrochemical conditions.

Biological surfaces in natural sediments:

The presence of biofilms and other organic material from dead and living organisms in riverbank filtration systems alters NP attachment efficiency in a most prominent way. The results of my thesis highlight that biological attachment is the overwhelming process in naturally aged sediments as it seems to change unfavorable attachment conditions into favorable ones. By this, NP are caught in surficial sediments and are completely retained in the very first centimeters of the sediment (chapter 5). This means that retention on organic material is an instantaneous process that is neither limited by diffusion of particles to the collector surface nor by attachment efficiency.

These results help to understand the outcome of different fate studies of NP that all observed strong accumulation of NP in surficial sediments (Espinasse et al., 2018; Geitner et al., 2018; Lowry et al., 2012). Acknowledging the high affinity of NP to biological surfaces, the particles attach most likely to biofilms and other organisms grown on the sediments by covalent bonds with organic N- and S-containing functional groups.

In spite of the transport-determining effect of biological compounds for engineered NP, retention of NP is also high in the absence of organic components illustrating strong interactions of NP also with abiotic natural surfaces. Nevertheless, the strong NP retention was accompanied by single, erratic breakthrough events. This was observed (i) in the absence of biological surfaces in short-term lab experiments, suggesting the reversibility of abiotic retention mechanisms (chapter 5), and (ii) in the presence of organic material during long-term, near-natural riverbank filtration experiments (chapter 4). Over longer periods of time, organic material might be

decomposed so that NP are remobilized. Still, I was unable to further explore the mechanisms for this phenomenon during my thesis, thus, this point needs future research.

Flow velocity:

Flow velocity mainly affects the first step of the attachment process, i.e. the mass transfer to the solid phase. The lower the flow velocity, the more diffusion-determined is the transport to sediment surfaces and the higher the possibility for NP sorption to the solid phase. With increasing flow rate, the transport of NP through sediments by advection gets more important. Additionally, flow velocity affects attachment efficiency for diffusion-determined systems.

I studied the effect of flow rate on NP transport at the lower range of flow velocities (0.2 and 0.7 m $d^{-1}$) comparable to groundwater flow in sandy sediments (Kunkel and Wendland, 1997). The lower the flow rate the more relevant gets the diffusion of NP from the mobile to the stationary phase which enhances the interaction of NP with the SWI due to long residence times of NP in the pore space. Previous studies have mainly been undertaken at higher flow rates (i.e. 2.4 - 55 m $d^{-1}$, Table 1. 1) and suggest decreasing NP retention with increasing flow rates. In chapter 5, my thesis points out that flow rate might affect NP transport when abiotic retention mechanisms (i.e. interaction with oppositely charged sediment surfaces of Fe-oxides and clay minerals) dominate. However, NP have a high affinity to biological surfaces and their attachment in those systems is not susceptible to increasing flow rate (chapter 5). Both under near-natural and laboratory conditions, flow rate had no effect on NP transport and retention in the presence of organic material. Therefore, increasing flow rate does not enhance NP transport in complex, near-natural riverbank filtration systems. However, induced bank filtration systems may exhibit far larger flow rates.

This case was not studied in my thesis and it needs to be investigated whether biological retention is still dominating at flow rates above 1 m $d^{-1}$.

### 6.2.2 Remobilization potential

Experiments with different NP in chapter 3, 4, and 5 illustrate that NP entering the environment are expected to be retained in the upper centimeters of a sediment system. In return, this might cause the possibility for a NP remobilization by changing physico-chemical forces as surficial sediments are exposed to varying environmental conditions. My results from batch studies point out, that mechanical forces acting on surficial sediment layers can remobilize large amounts of retained NP in case NOM sterically stabilizes those remobilized particles. Additionally, ionic strength reduction causes the remobilization of loosely bound NP. In contrast, enhanced ionic strength and the presence of $Ca^{2+}$ lead to strong NP attachment on sediments and to destabilization of NP once remobilized, thus preventing NP remobilization. The partial remobilization of NP under batch conditions is evidence for different retention mechanisms: When the energy barrier between particles and sediment surfaces is overcome and NP adsorb in a primary energy minimum, remobilization is hardly possible. Stable interactions are promoted by high ionic strength and the presence of $Ca^{2+}$. However, the part of NP which is attached in a less stable secondary energy minimum is susceptible to changing physico-chemical conditions. As shown in chapter 4, an essential part of remobilizable NP seems to be associated to natural (clay) colloids. This illustrates that remobilization is strongly dependent on co-mobilization with natural colloids. Under heavy rain events increasing flow velocities in the sediment system and introducing organic substances from surrounding compartments, the remobilization of initially retained NP is possible.

This means that single transport experiments to observe NP mobility do not cover the whole fate of NP. As a first conclusion, my results show that NP are mainly immobile in natural systems. However, natural conditions offer a variety of situations that might change NP stability and attachment. My data show that the potential for NP remobilization exists, but future studies should investigate whether this plays a relevant role under ambient environmental conditions.

### 6.2.3 Retention and remobilization mechanisms

In summary, my work offers insights in physico-chemical retention and remobilization mechanisms of NP in saturated sediments (Fig. 6. 1 and Table 6. 1). The prominent role of $Ca^{2+}$ and NOM was already described by lab studies before, but prove for its relevance in near-natural sediment systems has been given in this thesis. Moreover, the importance of natural colloids on NP transport, retention, and remobilization was pointed out and there is urgent need to explore NP-colloid interaction mechanisms as well as their consequences for NP fate, in more detail. Flow rate as a hydrodynamic parameter was shown to enhance NP mobility under abiotic conditions (chapter 5). However, the results of my thesis show that it might have minor effects on NP transport in natural sediment systems where biotic retention dominates. In future studies, this should be tested for higher flow rates. My results point out, that NP have a high affinity to biological surfaces as they offer numerous and heterogeneous attachment sites. In the presence of dead and living organic matter, other retention factors might be of subordinate relevance.

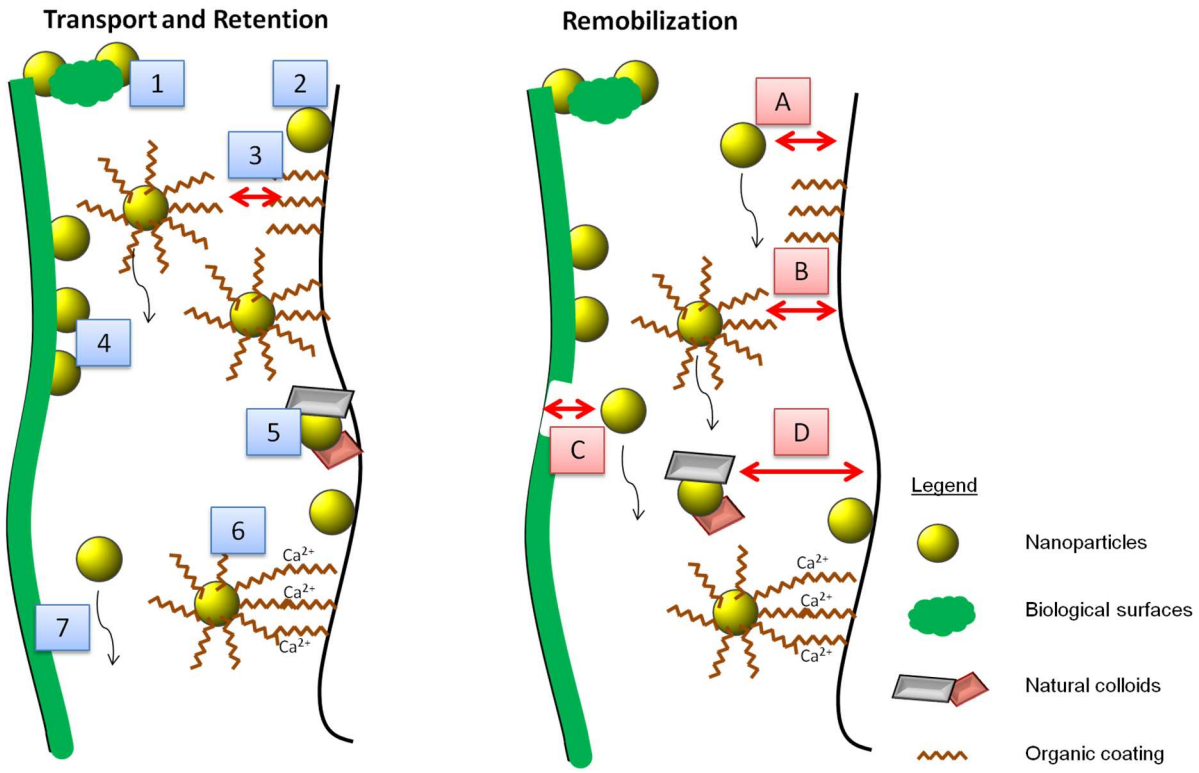


**Fig. 6. 1:** Schematic summary of transport, retention, and remobilization mechanisms of NP in near-natural saturated sediment systems.

**Table 6. 1:** Transport, retention, and remobilization mechanisms occurring in near-natural, saturated sediment systems (see Fig. 6. 1).

| Transport and retention mechanisms | Remobilization mechanisms |
|---|---|
| 1- Mechanical filtration and straining due to pore space narrowing by dead and living organic matter<br><br>2- Attachment of bare NP to the SWI<br><br>3- Steric repulsion of organically coated NP<br><br>4- Stable attachment of NP to dead and living organic matter<br><br>5- Retention of NP on favorable attachment sites (i.e. iron oxide and clay minerals)<br><br>6- $Ca^{2+}$ bridging between coated NP and sediment surfaces<br><br>7- Advection of NP with the mobile phase | A- Remobilization of bare Ag NP<br><br>B- Remobilization and steric repulsion of loosely bound, organically coated NP<br><br>C- Release from biological surfaces (e.g., after decomposition of organic material)<br><br>D- Co-mobilization of NP with natural colloids (i.e. clay minerals, iron oxides) |

### 6.3 From lab scale to near-natural riverbank filtration systems

Studies on NP have so far been mainly undertaken under laboratory conditions. Data about NP stability originates from batch experiments; NP transport is mostly investigated by well-defined column experiments. The reason for these simplifications is the difficulty to analyze NP in complex matrices on the one hand and the challenge of identifying processes in less well-defined systems with numerous variables on the other hand. However, large-scale, more complex experiments are necessary to value results gained by simplified systems. To fill this gap, I investigated different scenarios of NP release in a near-natural riverbank filtration system. Although different nanoparticles (i.e. $CeO_2$ NP, unaged and aged Ag NP) and different conditions (i.e. various flow velocities and background ionic strength) were applied, NP were generally retained in the upper 5-15 cm of the sediment. Adjusting similar conditions in lab-scale experiments, I observed that the general trend of high NP retention is reflected in simplified studies. However, retention mechanisms differ noteworthy between lab and technical-scale experiments: Biological retention is the main driver under near-natural conditions while being absent in pristine lab columns. This is of high importance for the effectiveness of riverbank filtration on NP retention as NP are transported into deeper sediment layers in the absence of biological retention sites. Under lab conditions, the importance of natural colloids for NP retention and remobilization potential is also underestimated even though NP co-transport with clay colloids seems to be one driver for NP remobilization in natural systems. To enhance the understanding of NP fate in saturated sediment systems, more complex studies are highly valuable and should be extended in future research.

## 6.4 Future Research

Nanoparticles are one of the emerging industrial chemicals whose unique properties lead to increasing use and therefore increasing potential for the release into the environment. However, their definition by size and not chemical nature leads to a high variety in NP properties and expected reactions in different environmental compartments. By experiments of my thesis, enhanced understanding of the sorption of NOM to $TiO_2$ and Ag NP and its effect on NP mobility in natural soil solutions was gained. Still, predictions of the fate of different kinds of NP in soils are highly challenging. Therefore, more studies on NP in environmentally relevant concentrations and natural soil environments are needed to allow a NP risk assessment and reasonable regulations. Especially the effect of numerous, connected factors (e.g., ionic strength, NOM, and natural colloids) on NP fate is far from being thoroughly understood, so that a deeper mechanistic understanding of processes determining NP stability is still missing.

Transport of NP in saturated porous media is a highly investigated field and the low mobility of NP can be sufficiently confirmed by numerous research studies. My own results support this conclusion. However, this implies that NP are accumulated on top of soils and sediments. Continuous NP input may then lead to high NP concentrations in these compartments which might affect microorganisms, plants, and soil biota. This problem should get into focus of future ecotoxicity and fate studies.

In addition, most transport studies are undertaken in pristine, simplified lab systems while field experiments are rare as NP analysis in more complex matrices remains challenging. Therefore, I applied medium-scaled field studies which illustrated that

relevant retention mechanisms differ between lab and near-natural systems. This shows a need for further medium-scale studies with a higher variety of NP and influencing variables to be tested. As an example, the investigation of $TiO_2$ NP fate in soils and sediments is still hindered by the high background $TiO_2$ concentration in naturally occurring minerals which needs advanced analytical solutions. Moreover, research should focus on possibilities to increase the scale and complexity to even more environmentally relevant scenarios. To the best of my knowledge, studies on NP in the field have not been undertaken so far, and are therefore replaced by modeling or mesocosm approaches. The realization of experiments with NP in the environment needs development of more sophisticated analytical tools, but is needed to understand the relevance of findings from smaller scales.

A parameter that is not sufficiently covered by current research is the effect of natural colloids on NP fate. My thesis showed that natural colloids might be determining for transport and remobilization processes in sediment systems. But also in soils where natural colloids are ubiquitous the effects are not well understood, yet. Furthermore, they might offer important surfaces for biogeochemical reaction of NP that lead to their transformation, i.e. by dissolution, sulfidation, or oxidation. Those topics should be included in future research studies.

# 7 References


Abraham, P. M., Barnikol, S., Baumann, T., Kuehn, M., Ivleva, N. P., & Schaumann, G. E. (2013). Sorption of Silver Nanoparticles to Environmental and Model Surfaces. *Environmental Science & Technology*, *47*(10), 5083–5091. doi:10.1021/es303941e

Adrian, Y.F., Schneidewind, U., Bradford, S.A., Simunek, J., Fernandez-Steeger, T.M., Azzam, R., 2018. Transport and retention of surfactant- and polymer-stabilized engineered silver nanoparticles in silicate-dominated aquifer material. Environmental Pollution 236, 195–207. https://doi.org/10.1016/j.envpol.2018.01.011

Akaighe, N., Depner, S.W., Banerjee, S., Sharma, V.K., Sohn, M., 2012. The effects of monovalent and divalent cations on the stability of silver nanoparticles formed from direct reduction of silver ions by Suwannee River humic acid/natural organic matter. Science of The Total Environment 441, 277–289. https://doi.org/10.1016/j.scitotenv.2012.09.055

Ali, M. A., & Dzombak, D. A. (1996). Competitive Sorption of Simple Organic Acids and Sulfate on Goethite. *Environmental Science & Technology*, *30*(4), 1061–1071. doi:10.1021/es940723g

Andersen, D. O., & Gjessing, E. T. (2002). Natural organic matter (NOM) in a limed lake and its tributaries. *Water Research*, *36*(9), 2372–2382. doi:10.1016/S0043-1354(01)00432-8

Andreï, J., Pain-Devin, S., Felten, V., Devin, S., Giambérini, L., Mehennaoui, K., Cambier, S., Gutleb, A.C., Guérold, F., 2016. Silver nanoparticles impact the functional role of Gammarus roeseli (Crustacea Amphipoda). Environmental Pollution 208, 608–618. https://doi.org/10.1016/j.envpol.2015.10.036

Auffan, M., Rose, J., Bottero, J.-Y., Lowry, G. V., Jolivet, J.-P., & Wiesner, M. R. (2009). Towards a definition of inorganic nanoparticles from an environmental, health and safety perspective. *Nature Nanotechnology*, *4*(10), 634–641. doi:10.1038/nnano.2009.242

Avellan, A., Simonin, M., McGivney, E., Bossa, N., Spielman-Sun, E., Rocca, J.D., Bernhardt, E.S., Geitner, N.K., Unrine, J.M., Wiesner, M.R., Lowry, G.V., 2018. Gold nanoparticle biodissolution by a freshwater macrophyte and its associated microbiome. Nature Nanotechnology 1. https://doi.org/10.1038/s41565-018-0231-y

Baalousha, M., Nur, Y., Römer, I., Tejamaya, M., & Lead, J. R. (2013). Effect of monovalent and divalent cations, anions and fulvic acid on aggregation of citrate-coated silver nanoparticles. *Science of The Total Environment*, *454–455*, 119–131. doi:10.1016/j.scitotenv.2013.02.093

Beckett, R., Le, N.P., 1990. The role or organic matter and ionic composition in determining the surface charge of suspended particles in natural waters. Colloids and Surfaces 44, 35–49. https://doi.org/10.1016/0166-6622(90)80185-7

Beer, C., Foldbjerg, R., Hayashi, Y., Sutherland, D.S., Autrup, H., 2012. Toxicity of silver nanoparticles—Nanoparticle or silver ion? Toxicology Letters 208, 286–292. https://doi.org/10.1016/j.toxlet.2011.11.002

Ben-Moshe, T., Dror, I., Berkowitz, B., 2010. Transport of metal oxide nanoparticles in saturated porous media. Chemosphere 81, 387–393. https://doi.org/10.1016/j.chemosphere.2010.07.007

Bolster, C. H., Mills, A. L., Hornberger, G. M., & Herman, J. S. (1999). Spatial distribution of deposited bacteria following Miscible Displacement Experiments in intact cores. *Water Resources Research*, *35*(6), 1797–1807. doi:10.1029/1999WR900031

Booth, A., Størseth, T., Altin, D., Fornara, A., Ahniyaz, A., Jungnickel, H., et al. (2015). Freshwater dispersion stability of PAA-stabilised cerium oxide nanoparticles and toxicity towards Pseudokirchneriella subcapitata. *Science of The Total Environment*, *505*(Supplement C), 596–605. doi:10.1016/j.scitotenv.2014.10.010

Bradford, S. A., Simunek, J., Bettahar, M., van Genuchten, M. T., & Yates, S. R. (2006). Significance of straining in colloid deposition: Evidence and implications: SIGNIFICANCE OF STRAINING IN COLLOID DEPOSITION. *Water Resources Research*, *42*(12). doi:10.1029/2005WR004791

Bradford, S. A., Torkzaban, S., & Simunek, J. (2011). Modeling colloid transport and retention in saturated porous media under unfavorable attachment conditions: MODELING COLLOID TRANSPORT AND RETENTION. *Water Resources Research*, *47*(10). doi:10.1029/2011WR010812

Bradford, S. A., Yates, S. R., Bettahar, M., & Simunek, J. (2002). Physical factors affecting the transport and fate of colloids in saturated porous media: FACTORS AFFECTING THE FATE OF COLLOIDS. *Water Resources Research*, *38*(12), 63-1-63–12. doi:10.1029/2002WR001340

Braun, A., Klumpp, E., Azzam, R., & Neukum, C. (2015). Transport and deposition of stabilized engineered silver nanoparticles in water saturated loamy sand and silty loam. *Science of The Total Environment*, *535*, 102–112. doi:10.1016/j.scitotenv.2014.12.023

Buffle, J., Wilkinson, K. J., Stoll, S., Filella, M., & Zhang, J. (1998). A generalized description of aquatic colloidal interactions: the three-colloidal component approach. *Environmental Science & Technology*, *32*(19), 2887–2899.

Buscail, R., Pocklington, R., Germain, C., 1995. Seasonal variability of the organic matter in a sedimentary coastal environment: sources, degradation and accumulation (continental shelf of the Gulf of Lions—northwestern Mediterranean Sea). Continental Shelf Research 15, 843–869. https://doi.org/10.1016/0278-4343(94)E0035-K

Capriel, P., Beck, T., Borchert, H., Gronholz, J., & Zachmann, G. (1995). Hydrophobicity of the organic matter in arable soils. *Soil Biology and Biochemistry*, *27*(11), 1453–1458. doi:10.1016/0038-0717(95)00068-P

Caron, D.A., Pick, F.R., Lean, D.R.S., 1985. CHROOCOCCOID CYANOBACTERIA IN LAKE ONTARIO: VERTICAL AND SEASONAL DISTRIBUTIONS DURING

19821. Journal of Phycology 21, 171–175. https://doi.org/10.1111/j.0022-3646.1985.00171.x

Carson, R., 2002. Silent Spring. Houghton Mifflin Harcourt.

Celi, L., Schnitzer, M., & Nègre, M. (1997). Analysis of carboxyl groups in soil humic acids by a wet chemical method, Fourier-transform infrared spectrophotometry, and solution-state carbon-13 nuclear magnetic resonance. A comparative study. *Soil Science*, *162*(3), 189–197.

Chang, Y.-I., Chan, H.-C., 2008. Correlation equation for predicting filter coefficient under unfavorable deposition conditions. AIChE Journal 54, 1235–1253. https://doi.org/10.1002/aic.11466

Chanteau, B., Fresnais, J., & Berret, J.-F. (2009). Electrosteric Enhanced Stability of Functional Sub-10 nm Cerium and Iron Oxide Particles in Cell Culture Medium. *Langmuir*, *25*(16), 9064–9070. doi:10.1021/la900833v

Chen, G., Liu, X., & Su, C. (2012). Distinct effects of humic acid on transport and retention of TiO2 rutile nanoparticles in saturated sand columns. *Environmental Science & Technology*, *46*(13), 7142–7150. doi:10.1021/es204010g

Chen, K.L., Mylon, S.E., Elimelech, M., 2007. Enhanced aggregation of alginate-coated iron oxide (hematite) nanoparticles in the presence of calcium, strontium, and barium cations. Langmuir 23, 5920–5928. https://doi.org/10.1021/la063744k

Chowdhury, I., Cwiertny, D. M., & Walker, S. L. (2012). Combined Factors Influencing the Aggregation and Deposition of nano-$TiO_2$ in the Presence of Humic Acid and Bacteria. *Environmental Science & Technology*, *46*(13), 6968–6976. doi:10.1021/es2034747

Cleveland, D., Long, S.E., Pennington, P.L., Cooper, E., Fulton, M.H., Scott, G.I., Brewer, T., Davis, J., Petersen, E.J., Wood, L., 2012. Pilot estuarine mesocosm study on the environmental fate of Silver nanomaterials leached from consumer products. Science of The Total Environment, Special Section: Reviews of Trace Metal Pollution in China 421–422, 267–272. https://doi.org/10.1016/j.scitotenv.2012.01.025

Coleman J. G., Kennedy A. J., Bednar A. J., Ranville J. F., Laird J. G., Harmon A. R., Hayes C. A., Gray E. P., Higgins C. P., Lotufo G., Steevens J. A., 2013. Comparing the effects of nanosilver size and coating variations on bioavailability, internalization, and elimination, using Lumbriculus variegatus. Environmental Toxicology and Chemistry 32, 2069–2077. https://doi.org/10.1002/etc.2278

Collin, B., Oostveen, E., Tsyusko, O. V., & Unrine, J. M. (2014). Influence of Natural Organic Matter and Surface Charge on the Toxicity and Bioaccumulation of Functionalized Ceria Nanoparticles in Caenorhabditis elegans. *Environmental Science & Technology*, *48*(2), 1280–1289. doi:10.1021/es404503c

Cornelis, G., Pang, L., Doolette, C., Kirby, J. K., & McLaughlin, M. J. (2013). Transport of silver nanoparticles in saturated columns of natural soils. *Science*

*of The Total Environment*, *463–464*(Supplement C), 120–130. doi:10.1016/j.scitotenv.2013.05.089 https://doi.org/10.1016/j.scitotenv.2013.05.089

Cornelis, G., Ryan, B., McLaughlin, M.J., Kirby, J.K., Beak, D., Chittleborough, D., 2011. Solubility and Batch Retention of CeO2 Nanoparticles in Soils. Environ. Sci. Technol. 45, 2777–2782. https://doi.org/10.1021/es103769k

Dabrunz, A., Duester, L., Prasse, C., Seitz, F., Rosenfeldt, R., Schilde, C., Schaumann, G.E., Schulz, R., 2011. Biological surface coating and molting inhibition as mechanisms of TiO2 nanoparticle toxicity in Daphnia magna. PLoS ONE 6, e20112. https://doi.org/10.1371/journal.pone.0020112

Dahle, J.T., Arai, Y., 2015. Environmental Geochemistry of Cerium: Applications and Toxicology of Cerium Oxide Nanoparticles. International Journal of Environmental Research and Public Health 12, 1253–1278. https://doi.org/10.3390/ijerph120201253

Darlington, T.K., Neigh, A.M., Spencer, M.T., Guyen, O.T., Oldenburg, S.J., 2009. Nanoparticle characteristics affecting environmental fate and transport through soil. Environmental Toxicology and Chemistry 28, 1191–1199.

Davis, J. A., & Gloor, R. (1981). Adsorption of dissolved organics in lake water by aluminum oxide. Effect of molecular weight. *Environmental Science & Technology*, *15*(10), 1223–1229. doi:10.1021/es00092a012

de Laat, A. W. M., & van den Heuvel, G. L. T. (1995). Molecular weight fractionation in the adsorption of polyacrylic acid salts onto BaTiO3. *Colloids and Surfaces A: Physicochemical and Engineering Aspects*, *98*(1), 53–59. doi:10.1016/0927-7757(95)03096-V

Degenkolb, L., Metreveli, G., Philippe, A., Brandt, A., Leopold, K., Zehlike, L., et al. (2018). Retention and remobilization mechanisms of environmentally aged silver nanoparticles in an artificial riverbank filtration system. *Science of The Total Environment*. doi:https://doi.org/10.1016/j.scitotenv.2018.07.079 0048-9697

Delay, M., Dolt, T., Woellhaf, A., Sembritzki, R., Frimmel, F.H., 2011. Interactions and stability of silver nanoparticles in the aqueous phase: Influence of natural organic matter (NOM) and ionic strength. Journal of Chromatography A 1218, 4206–4212. https://doi.org/10.1016/j.chroma.2011.02.074

Derjaguin, B., & Landau, L. (1941). Theory of stability of highly charged lyophobic sols and adhesion of highly charged particles in solutions of electrolytes. *Acta Physicochim. USSR*, (14), 633–662.

Dippon, U., Pabst, S., & Klitzke, S. (2018). Colloidal stabilization of CeO 2 nanomaterials with polyacrylic acid, polyvinyl alcohol or natural organic matter. *Science of The Total Environment*, *645*, 1153–1158. doi:10.1016/j.scitotenv.2018.07.189

El Badawy, A.M., Aly Hassan, A., Scheckel, K.G., Suidan, M.T., Tolaymat, T.M., 2013. Key Factors Controlling the Transport of Silver Nanoparticles in Porous Media. Environmental Science & Technology 47, 4039–4045. https://doi.org/10.1021/es304580r

Ellerbrock, R. H., Höhn, A., & Gerke, H. H. (2001). FT-IR studies on soil organic matter from long-term field experiments. *Sustainable Management of Soil Organic Matter (eds R.M. Rees, B.C. Ball, C.D. Campbell & C.A. Watson)*, 34–41.

Emerson, H.P., Hart, A.E., Baldwin, J.A., Waterhouse, T.C., Kitchens, C.L., Mefford, O.T., Powell, B.A., 2014. Physical transformations of iron oxide and silver nanoparticles from an intermediate scale field transport study. J Nanopart Res 16, 2258. https://doi.org/10.1007/s11051-014-2258-9

Erhayem, M., & Sohn, M. (2014). Effect of humic acid source on humic acid adsorption onto titanium dioxide nanoparticles. *Science of The Total Environment*, *470–471*, 92–98. doi:10.1016/j.scitotenv.2013.09.063

Espinasse, B. P., Geitner, N. K., Schierz, A., Therezien, M., Richardson, C. J., Lowry, G. V., et al. (2018). Comparative Persistence of Engineered Nanoparticles in a Complex Aquatic Ecosystem. *Environmental Science & Technology*, *52*(7), 4072–4078. doi:10.1021/acs.est.7b06142

Evans, D.F., Wennerström, H., 2000. The Colloidal Domain: Where Physics, Chemistry, Biology, and Technology Meet, 2nd ed. Wiley-VCH. https://doi.org/10.1016/S0255-2701(00)00102-1

Everett, D.H., 1988a. Chapter 2:Why are Colloidal Dispersions Stable? I Basic Principles, in: Basic Principles of Colloid Science. pp. 16–29. https://doi.org/10.1039/9781847550200-00016

Fabrega, J., Luoma, S.N., Tyler, C.R., Galloway, T.S., Lead, J.R., 2011. Silver nanoparticles: Behaviour and effects in the aquatic environment. Environment International 37, 517–531. https://doi.org/10.1016/j.envint.2010.10.012

Fang, J., Wang, M., Lin, D., & Shen, B. (2016). Enhanced transport of CeO 2 nanoparticles in porous media by macropores. *Science of The Total Environment*, *543*, 223–229. doi:10.1016/j.scitotenv.2015.11.039

Feichtmeier, N.S., Leopold, K., 2014. Detection of silver nanoparticles in parsley by solid sampling high-resolution–continuum source atomic absorption spectrometry. Analytical and Bioanalytical Chemistry 406, 3887–3894. https://doi.org/10.1007/s00216-013-7510-0

Ferry, J.L., Craig, P., Hexel, C., Sisco, P., Frey, R., Pennington, P.L., Fulton, M.H., Scott, I.G., Decho, A.W., Kashiwada, S., Murphy, C.J., Shaw, T.J., 2009. Transfer of gold nanoparticles from the water column to the estuarine food web. Nature Nanotechnology 4, 441–444. https://doi.org/10.1038/nnano.2009.157

Field, T.B., Coburn, J., McCourt, J.L., McBryde, W.A.E., 1975. Composition and stability of some metal citrate and diglycolate complexes in aqueous solution. Analytica Chimica Acta 74, 101–106.

Filgueiras, A. V., Lavilla, I., & Bendicho, C. (2002). Chemical sequential extraction for metal partitioning in environmental solid samples. *Journal of Environmental Monitoring*, *4*(6), 823–857. doi:10.1039/b207574c

Franchi, A., O'Melia, C.R., 2003. Effects of Natural Organic Matter and Solution Chemistry on the Deposition and Reentrainment of Colloids in Porous Media. Environ. Sci. Technol. 37, 1122–1129. https://doi.org/10.1021/es015566h

French, R. A., Jacobson, A. R., Kim, B., Isley, S. L., Penn, R. L., & Baveye, P. C. (2009). Influence of Ionic Strength, pH, and Cation Valence on Aggregation Kinetics of Titanium Dioxide Nanoparticles. *Environmental Science & Technology*, *43*(5), 1354–1359. doi:10.1021/es802628n

Furtado, L.M., Norman, B.C., Xenopoulos, M.A., Frost, P.C., Metcalfe, C.D., Hintelmann, H., 2015. Environmental Fate of Silver Nanoparticles in Boreal Lake Ecosystems. Environ. Sci. Technol. 49, 8441–8450. https://doi.org/10.1021/acs.est.5b01116

Gallego-Urrea, J.A., Perez Holmberg, J., Hassellöv, M., 2014. Influence of different types of natural organic matter on titania nanoparticle stability: effects of counter ion concentration and pH. Environ. Sci.: Nano 1, 181–189. https://doi.org/10.1039/C3EN00106G

García, A., Delgado, L., Torà, J. A., Casals, E., González, E., Puntes, V., et al. (2012). Effect of cerium dioxide, titanium dioxide, silver, and gold nanoparticles on the activity of microbial communities intended in wastewater treatment. *Journal of Hazardous Materials*, *199–200*(Supplement C), 64–72. doi:10.1016/j.jhazmat.2011.10.057

Garcia, T., Solsona, B., & Taylor, S. H. (2005). Nano-crystalline Ceria Catalysts for the Abatement of Polycyclic Aromatic Hydrocarbons. *Catalysis Letters*, *105*(3–4), 183–189. doi:10.1007/s10562-005-8689-2

Geelhoed, J. S., Hiemstra, T., & Van Riemsdijk, W. H. (1998). Competitive Interaction between Phosphate and Citrate on Goethite. *Environmental Science & Technology*, *32*(14), 2119–2123. doi:10.1021/es970908y

Geitner, N. K., O'Brien, N. J., Turner, A. A., Cummins, E. J., & Wiesner, M. R. (2017). Measuring Nanoparticle Attachment Efficiency in Complex Systems. *Environmental Science & Technology*, *51*(22), 13288–13294. doi:10.1021/acs.est.7b04612

Geitner, N.K., Cooper, J.L., Avellan, A., Castellon, B.T., Perrotta, B.G., Bossa, N., Simonin, M., Anderson, S.M., Inoue, S., Hochella, M.F., Richardson, C.J., Bernhardt, E.S., Lowry, G.V., Ferguson, P.L., Matson, C.W., King, R.S., Unrine, J.M., Wiesner, M.R., Hsu-Kim, H., 2018. Size-Based Differential Transport, Uptake, and Mass Distribution of Ceria ($CeO_2$) Nanoparticles in Wetland Mesocosms. Environmental Science & Technology 52, 9768–9776. https://doi.org/10.1021/acs.est.8b02040

Ghosh, S., Jiang, W., McClements, J. D., & Xing, B. (2011). Colloidal stability of magnetic iron oxide nanoparticles: influence of natural organic matter and synthetic polyelectrolytes. *Langmuir*, *27*(13), 8036–8043.

Gmür, T.A., Goel, A., Brown, M.A., 2016. Quantifying Specific Ion Effects on the Surface Potential and Charge Density at Silica Nanoparticle–Aqueous Electrolyte Interfaces. J. Phys. Chem. C 120, 16617–16625. https://doi.org/10.1021/acs.jpcc.6b02476

Gottschalk, F., Sonderer, T., Scholz, R. W., & Nowack, B. (2009). Modeled Environmental Concentrations of Engineered Nanomaterials (TiO2, ZnO, Ag, CNT, Fullerenes) for Different Regions. *Environmental Science & Technology*, *43*(24), 9216–9222. doi:10.1021/es9015553

Gottschalk, F., Sun, T., & Nowack, B. (2013). Environmental concentrations of engineered nanomaterials: Review of modeling and analytical studies. *Environmental Pollution*, *181*, 287–300. doi:10.1016/j.envpol.2013.06.003

Grasso, D., Subramaniam, K., Butkus, M., Strevett, K., Bergendahl, J., 2002. A review of non-DLVO interactions in environmental colloidal systems. Re/Views in Environmental Science and Bio/Technology 1, 17–38. https://doi.org/10.1023/A:1015146710500

Gu, B., Schmitt, J., Chen, Z., Liang, L., & McCarthy, J. F. (1994). Adsorption and desorption of natural organic matter on iron oxide: mechanisms and models. *Environmental Science & Technology*, *28*(1), 38–46. doi:10.1021/es00050a007

Haberhauer, G., & Gerzabek, M. . (1999). Drift and transmission FT-IR spectroscopy of forest soils: an approach to determine decomposition processes of forest litter. *Vibrational Spectroscopy*, *19*(2), 413–417. doi:10.1016/S0924-2031(98)00046-0

Hahn, M.W., O'Melia, C.R., 2004. Deposition and Reentrainment of Brownian Particles in Porous Media under Unfavorable Chemical Conditions: Some Concepts and Applications. Environ. Sci. Technol. 38, 210–220. https://doi.org/10.1021/es030416n

Halsall, C.J., Bailey, R., Stern, G.A., Barrie, L.A., Fellin, P., Muir, D.C.G., Rosenberg, B., Rovinsky, F.Y., Kononov, E.Y., Pastukhov, B., 1998. Multi-year observations of organohalogen pesticides in the Arctic atmosphere. Environmental Pollution 102, 51–62. https://doi.org/10.1016/S0269-7491(98)00074-8

Han, F.X., Kingery, W.L., Selim, and H.M., 2001. Accumulation, Redistribution, Transport, and Bioavailability of Heavy Metals in Waste-Amended Soils [WWW Document]. Trace Elements in Soil. https://doi.org/10.1201/9781420032734-11

Harremoës, P., Gee, D., MacGarvin, M., Stirling, A., Keys, J., Wynne, B., Vaz, S.G., 2001. Late lessons from early warnings: the precautionary principle 1896-2000. Citeseer.

Hoek, E.M.V., Bhattacharjee, S., Elimelech, M., 2003. Effect of Membrane Surface Roughness on Colloid−Membrane DLVO Interactions. Langmuir 19, 4836–4847. https://doi.org/10.1021/la027083c

Hoffmann, A., Gunkel, G., 2011. Bank filtration in the sandy littoral zone of Lake Tegel (Berlin): Structure and dynamics of the biological active filter zone and clogging processes. Limnologica 41, 10–19. https://doi.org/10.1016/j.limno.2009.12.003

Hoppe, M., Mikutta, R., Utermann, J., Duijnisveld, W., Kaufhold, S., Stange, C. F., & Guggenberger, G. (2015). Remobilization of sterically stabilized silver

nanoparticles from farmland soils determined by column leaching: Remobilization of silver nanoparticles from soil. *European Journal of Soil Science*, *66*(5), 898–909. doi:10.1111/ejss.12270

Huang, J., Cheng, J., Yi, J., 2016. Impact of silver nanoparticles on marine diatom Skeletonema costatum. Journal of Applied Toxicology 36, 1343–1354. https://doi.org/10.1002/jat.3325

Hur, J., & Schlautman, M. A. (2003). Molecular weight fractionation of humic substances by adsorption onto minerals. *Journal of Colloid and Interface Science*, *264*(2), 313–321. doi:10.1016/S0021-9797(03)00444-2

Hutchinson, T.C., Whitby, L.M., 1977. The effects of acid rainfall and heavy metal particulates on a boreal Forest ecosystem near the sudbury smelting region of Canada. Water Air Soil Pollut 7, 421–438. https://doi.org/10.1007/BF00285542

Ikuma, K., Decho, A. W., & Lau, B. L. T. (2015). When nanoparticles meet biofilms-interactions guiding the environmental fate and accumulation of nanoparticles. *Frontiers in Microbiology*, *6*. doi:10.3389/fmicb.2015.00591

Kaegi, R., Ulrich, A., Sinnet, B., Vonbank, R., Wichser, A., Zuleeg, S., Simmler, H., Brunner, S., Vonmont, H., Burkhardt, M., Boller, M., 2008. Synthetic TiO2 nanoparticle emission from exterior facades into the aquatic environment. Environmental Pollution 156, 233–239. https://doi.org/10.1016/j.envpol.2008.08.004

Kaegi, R., Voegelin, A., Ort, C., Sinnet, B., Thalmann, B., Krismer, J., Hagendorfer, H., Elumelu, M., Mueller, E., 2013. Fate and transformation of silver nanoparticles in urban wastewater systems. Water Res. 47, 3866–3877. https://doi.org/10.1016/j.watres.2012.11.060

Keller, A.A., Lazareva, A., 2014. Predicted Releases of Engineered Nanomaterials: From Global to Regional to Local. Environ. Sci. Technol. Lett. 1, 65–70. https://doi.org/10.1021/ez400106t

Klitzke, S., Metreveli, G., Peters, A., Schaumann, G. E., & Lang, F. (2015). The fate of silver nanoparticles in soil solution — Sorption of solutes and aggregation. *Science of The Total Environment*, *535*, 54–60. doi:10.1016/j.scitotenv.2014.10.108

Kumahor, S. K., Hron, P., Metreveli, G., Schaumann, G. E., Klitzke, S., Lang, F., & Vogel, H.-J. (2016). Transport of soil-aged silver nanoparticles in unsaturated sand. *Journal of Contaminant Hydrology*, *195*, 31–39. doi:10.1016/j.jconhyd.2016.10.001

Kunkel, R., Wendland, F., 1997. WEKU - a GIS-Supported stochastic model of groundwater residence times in upper aquifers for the supraregional groundwater management. Environmental Geology 30, 1–9. https://doi.org/10.1007/s002540050126

Lau, B. L. T., Hockaday, W. C., Ikuma, K., Furman, O., & Decho, A. W. (2013). A preliminary assessment of the interactions between the capping agents of silver nanoparticles and environmental organics. *Colloids and Surfaces A: Physicochemical and Engineering Aspects*, *435*, 22–27. doi:10.1016/j.colsurfa.2012.11.065

Lecoanet, H. F., Bottero, J.-Y., & Wiesner, M. R. (2004). Laboratory Assessment of the Mobility of Nanomaterials in Porous Media. *Environmental Science & Technology*, *38*(19), 5164–5169. doi:10.1021/es0352303

Lee, S.-W., Park, S.-Y., Kim, Y., Im, H., Choi, J., 2016. Effect of sulfidation and dissolved organic matters on toxicity of silver nanoparticles in sediment dwelling organism, Chironomus riparius. Science of The Total Environment 553, 565–573. https://doi.org/10.1016/j.scitotenv.2016.02.064

Levard, C., Hotze, E.M., Colman, B.P., Dale, A.L., Truong, L., Yang, X.Y., Bone, A.J., Brown, G.E., Tanguay, R.L., Di Giulio, R.T., Bernhardt, E.S., Meyer, J.N., Wiesner, M.R., Lowry, G.V., 2013. Sulfidation of Silver Nanoparticles: Natural Antidote to Their Toxicity. Environmental Science & Technology 47, 13440–13448. https://doi.org/10.1021/es403527n

Li, Q., Mahendra, S., Lyon, D.Y., Brunet, L., Liga, M.V., Li, D., Alvarez, P.J.J., 2008. Antimicrobial nanomaterials for water disinfection and microbial control: Potential applications and implications. Water Research 42, 4591–4602. https://doi.org/10.1016/j.watres.2008.08.015

Li, Y., Yang, C., Guo, X., Dang, Z., Li, X., & Zhang, Q. (2015). Effects of humic acids on the aggregation and sorption of nano-TiO2. *Chemosphere*, *119*, 171–176. doi:10.1016/j.chemosphere.2014.05.002

Li, Z., Aly Hassan, A., Sahle-Demessie, E., & Sorial, G. A. (2013). Transport of nanoparticles with dispersant through biofilm coated drinking water sand filters. *Water Research*, *47*(17), 6457–6466. doi:10.1016/j.watres.2013.08.026

Liang, Y., Bradford, S. A., Simunek, J., Heggen, M., Vereecken, H., & Klumpp, E. (2013). Retention and Remobilization of Stabilized Silver Nanoparticles in an Undisturbed Loamy Sand Soil. *Environmental Science & Technology*, *47*(21), 12229–12237. doi:10.1021/es402046u

Lin, S., Cheng, Y., Bobcombe, Y., L Jones, K., Liu, J., Wiesner, M.R., 2011. Deposition of silver nanoparticles in geochemically heterogeneous porous media: predicting affinity from surface composition analysis. Environ. Sci. Technol. 45, 5209–5215. https://doi.org/10.1021/es2002327

Lin, W., Huang, Y., Zhou, X.-D., & Ma, Y. (2006). Toxicity of Cerium Oxide Nanoparticles in Human Lung Cancer Cells. *International Journal of Toxicology*, *25*(6), 451–457. doi:10.1080/10915810600959543

Liu, J., Legros, S., von der Kammer, F., Hofmann, T., 2013. Natural Organic Matter Concentration and Hydrochemistry Influence Aggregation Kinetics of Functionalized Engineered Nanoparticles. Environmental Science & Technology 47, 4113–4120. https://doi.org/10.1021/es302447g

Louie, S. M., Spielman-Sun, E. R., Small, M. J., Tilton, R. D., & Lowry, G. V. (2015). Correlation of the Physicochemical Properties of Natural Organic Matter Samples from Different Sources to Their Effects on Gold Nanoparticle Aggregation in Monovalent Electrolyte. *Environmental Science & Technology*, *49*(4), 2188–2198. doi:10.1021/es505003d

Louie, S. M., Tilton, R. D., & Lowry, G. V. (2013). Effects of Molecular Weight Distribution and Chemical Properties of Natural Organic Matter on Gold

Nanoparticle Aggregation. *Environmental Science & Technology*, *47*(9), 4245–4254. doi:10.1021/es400137x

Louie, S. M., Tilton, R. D., & Lowry, G. V. (2016). Critical review: impacts of macromolecular coatings on critical physicochemical processes controlling environmental fate of nanomaterials. *Environmental Science: Nano*, *3*(2), 283–310. doi:10.1039/C5EN00104H

Lowry, G.V., Gregory, K.B., Apte, S.C., Lead, J.R., 2012. Transformations of Nanomaterials in the Environment. Environmental Science & Technology 46, 6893–6899. https://doi.org/10.1021/es300839e

Lüderwald, S., Dackermann, V., Seitz, F., Adams, E., Feckler, A., Schilde, C., Schulz, R., Bundschuh, M., 2019. A blessing in disguise? Natural organic matter reduces the UV light-induced toxicity of nanoparticulate titanium dioxide. Science of The Total Environment 663, 518–526. https://doi.org/10.1016/j.scitotenv.2019.01.282

Luo, M., Huang, Y., Zhu, M., Tang, Y., Ren, T., Ren, J., et al. (2016). Properties of different natural organic matter influence the adsorption and aggregation behavior of TiO 2 nanoparticles. *Journal of Saudi Chemical Society*, *22*(2), 146–154. doi:10.1016/j.jscs.2016.01.007

Lv, X., Gao, B., Sun, Y., Dong, S., Wu, J., Jiang, B., & Shi, X. (2016). Effects of grain size and structural heterogeneity on the transport and retention of nano-TiO2 in saturated porous media. *Science of The Total Environment*, *563–564*, 987–995. doi:10.1016/j.scitotenv.2015.12.128

Makselon, J., Siebers, N., Meier, F., Vereecken, H., & Klumpp, E. (2018). Role of rain intensity and soil colloids in the retention of surfactant-stabilized silver nanoparticles in soil. *Environmental Pollution*, *238*, 1027–1034. doi:10.1016/j.envpol.2018.02.025

Makselon, J., Zhou, D., Engelhardt, I., Jacques, D., Klumpp, E., 2017. Experimental and Numerical Investigations of Silver Nanoparticle Transport under Variable Flow and Ionic Strength in Soil. Environmental Science & Technology 51, 2096–2104. https://doi.org/10.1021/acs.est.6b04882

Markus, A. A., Parsons, J. R., Roex, E. W. M., de Voogt, P., & Laane, R. W. P. M. (2015). Modeling aggregation and sedimentation of nanoparticles in the aquatic environment. *Science of The Total Environment*, *506–507*(Supplement C), 323–329. doi:10.1016/j.scitotenv.2014.11.056

McDowell-Boyer, L.M., Hunt, J.R., Sitar, N., 1986. Particle transport through porous media. Water Resources Research 22, 1901–1921. https://doi.org/10.1029/WR022i013p01901

Metreveli, G., David, J., Schneider, R., Kurtz, S., Degenkolb, L., Schaumann, G., in prep. Sulfidized and isotopically enriched silver nanoparticles for long term mesocosm studies: Preparation, characterization, and quantification.

Metreveli, G., Frombold, B., Seitz, F., Grün, A., Philippe, A., Rosenfeldt, R. R., et al. (2016). Impact of chemical composition of ecotoxicological test media on the stability and aggregation status of silver nanoparticles. *Environ. Sci.: Nano*, *3*(2), 418–433. doi:10.1039/C5EN00152H

Metreveli, G., Philippe, A., Schaumann, G.E., 2015. Disaggregation of silver nanoparticle homoaggregates in a river water matrix. Science of The Total Environment 535, 35–44. https://doi.org/10.1016/j.scitotenv.2014.11.058

Morrow, J.B., P., C.A., Holbrook, R.D., 2010. Association of Quantum Dot Nanoparticles with Biofilm. Journal of Environmental Quality 39, 1934–1941. https://doi.org/10.2134/jeq2009.0455

Mueller, N.C., Nowack, B., 2008. Exposure Modeling of Engineered Nanoparticles in the Environment. Environmental Science & Technology 42, 4447–4453. https://doi.org/10.1021/es7029637

Nason, J. A., McDowell, S. A., & Callahan, T. W. (2012). Effects of natural organic matter type and concentration on the aggregation of citrate-stabilized gold nanoparticles. *Journal of Environmental Monitoring*, *14*(7), 1885. doi:10.1039/c2em00005a

National Research Council, 2014. Triennial review of the national nanotechnology initiative. National Academies Press.

Nel, A., Xia, T., Mädler, L., Li, N., 2006. Toxic Potential of Materials at the Nanolevel. Science 311, 622–627. https://doi.org/10.1126/science.1114397

Neukum, C., Braun, A., Azzam, R., 2014. Transport of engineered silver (Ag) nanoparticles through partially fractured sandstones. Journal of Contaminant Hydrology 164, 181–192. https://doi.org/10.1016/j.jconhyd.2014.05.012

Nevius, B.A., Chen, Y.P., Ferry, J.L., Decho, A.W., 2012. Surface-functionalization effects on uptake of fluorescent polystyrene nanoparticles by model biofilms. Ecotoxicology 21, 2205–2213. https://doi.org/10.1007/s10646-012-0975-3

Oriekhova, O., & Stoll, S. (2016). Stability of uncoated and fulvic acids coated manufactured CeO2 nanoparticles in various conditions: From ultrapure to natural Lake Geneva waters. *The Science of the Total Environment*, *562*, 327–334. doi:10.1016/j.scitotenv.2016.03.184

Pacyna, J.M., Oehme, M., 1988. Long-range transport of some organic compounds to the Norwegian Arctic. Atmospheric Environment (1967) 22, 243–257. https://doi.org/10.1016/0004-6981(88)90031-5

Petosa, A. R., Öhl, C., Rajput, F., & Tufenkji, N. (2013). Mobility of nanosized cerium dioxide and polymeric capsules in quartz and loamy sands saturated with model and natural groundwaters. *Water Research*, *47*(15), 5889–5900. doi:10.1016/j.watres.2013.07.006

Philippe, A., Gangloff, M., Rakcheev, D., Schaumann, G.E., 2014. Evaluation of hydrodynamic chromatography coupled with inductively coupled plasma mass spectrometry detector for analysis of colloids in environmental media – effects of colloid composition, coating and shape. Anal. Methods 6, 8722–8728. https://doi.org/10.1039/C4AY01567C

Philippe, A., Schaumann, G.E., 2014. Interactions of Dissolved Organic Matter with Natural and Engineered Inorganic Colloids: A Review. Environmental Science & Technology 48, 8946–8962. https://doi.org/10.1021/es502342r

Praetorius, A., Labille, J., Scheringer, M., Thill, A., Hungerbühler, K., Bottero, J.-Y., 2014. Heteroaggregation of Titanium Dioxide Nanoparticles with Model

Natural Colloids under Environmentally Relevant Conditions. Environmental Science & Technology 48, 10690–10698. https://doi.org/10.1021/es501655v
Rabinowitz, M.B., Wetherill, G.W., 1973. Identifying sources of lead contamination by stable isotope techniques. Reply to comments. Environ. Sci. Technol. 7, 556–557. https://doi.org/10.1021/es60078a013
Rai, M., Yadav, A., Gade, A., 2009. Silver nanoparticles as a new generation of antimicrobials. Biotechnology Advances 27, 76–83. https://doi.org/10.1016/j.biotechadv.2008.09.002
Rajala, J.E., Vehniäinen, E.-R., Väisänen, A., Kukkonen, J.V.K., 2018. Toxicity of silver nanoparticles to Lumbriculus variegatus is a function of dissolved silver and promoted by low sediment pH. Environmental Toxicology and Chemistry 37, 1889–1897. https://doi.org/10.1002/etc.4136
Rakcheev, D., Philippe, A., Schaumann, G.E., 2013. Hydrodynamic chromatography coupled with single particle-inductively coupled plasma mass spectrometry for investigating nanoparticles agglomerates. Anal. Chem. 85, 10643–10647. https://doi.org/10.1021/ac4019395
Reed, K., Cormack, A., Kulkarni, A., Mayton, M., Sayle, D., Klaessig, F., & Stadler, B. (2014). Exploring the properties and applications of nanoceria: is there still plenty of room at the bottom? *Environmental Science: Nano*, *1*(5), 390–405. doi:10.1039/C4EN00079J
Reinfelder, J.R., Chang, S.I., 1999. Speciation and Microalgal Bioavailability of Inorganic Silver. Environmental Science & Technology 33, 1860–1863. https://doi.org/10.1021/es980896w
Ribeiro, F., Van Gestel, C.A.M., Pavlaki, M.D., Azevedo, S., Soares, A.M.V.M., Loureiro, S., 2017. Bioaccumulation of silver in Daphnia magna: Waterborne and dietary exposure to nanoparticles and dissolved silver. Science of The Total Environment 574, 1633–1639. https://doi.org/10.1016/j.scitotenv.2016.08.204
Ritchie, J. D., & Perdue, E. M. (2003). Proton-binding study of standard and reference fulvic acids, humic acids, and natural organic matter. *Geochimica et Cosmochimica Acta*, *67*(1), 85–96. doi:10.1016/S0016-7037(02)01044-X
Sagee, O., Dror, I., Berkowitz, B., 2012. Transport of silver nanoparticles (AgNPs) in soil. Chemosphere 88, 670–675. https://doi.org/10.1016/j.chemosphere.2012.03.055
Sänger, A., Reibe, K., Mumme, J., Kaupenjohann, M., Ellmer, F., Roß, C.-L., & Meyer-Aurich, A. (2017). Biochar application to sandy soil: effects of different biochars and N fertilization on crop yields in a 3-year field experiment. *Archives of Agronomy and Soil Science*, *63*(2), 213–229. doi:10.1080/03650340.2016.1223289
Sani-Kast, N., Labille, J., Ollivier, P., Slomberg, D., Hungerbühler, K., Scheringer, M., 2017. A network perspective reveals decreasing material diversity in studies on nanoparticle interactions with dissolved organic matter. Proceedings of the National Academy of Sciences 114, E1756–E1765. https://doi.org/10.1073/pnas.1608106114

Schaumann, G.E., Philippe, A., Bundschuh, M., Metreveli, G., Klitzke, S., Rakcheev, D., Grün, A., Kumahor, S.K., Kühn, M., Baumann, T., Lang, F., Manz, W., Schulz, R., Vogel, H.-J., 2015. Understanding the fate and biological effects of Ag- and TiO2-nanoparticles in the environment: The quest for advanced analytics and interdisciplinary concepts. Science of The Total Environment 535, 3–19. https://doi.org/10.1016/j.scitotenv.2014.10.035

Schlich, K., Hoppe, M., Kraas, M., Fries, E., Hund-Rinke, K., 2017. Ecotoxicity and fate of a silver nanomaterial in an outdoor lysimeter study. Ecotoxicology 26, 738–751. https://doi.org/10.1007/s10646-017-1805-4

Schmidt, C.K., Lange, F.T., Brauch, H.-J., Kühn, W., 2003. Experiences with riverbank filtration and infiltration in Germany 17.

Schubert, J., 2002. Hydraulic aspects of riverbank filtration—field studies. Journal of Hydrology 266, 145–161. https://doi.org/10.1016/S0022-1694(02)00159-2

Sehgal, A., Lalatonne, Y., Berret, J.-F., & Morvan, M. (2005). Precipitation−Redispersion of Cerium Oxide Nanoparticles with Poly (acrylic acid): Toward Stable Dispersions. *Langmuir*, *21*(20), 9359–9364.

Seijo, M., Ulrich, S., Filella, M., Buffle, J., & Stoll, S. (2009). Modeling the Adsorption and Coagulation of Fulvic Acids on Colloids by Brownian Dynamics Simulations. *Environmental Science & Technology*, *43*(19), 7265–7269. doi:10.1021/es9002394

Selck, H., Handy, R.D., Fernandes, T.F., Klaine, S.J., Petersen, E.J., 2016. Nanomaterials in the aquatic environment: A European Union-United States perspective on the status of ecotoxicity testing, research priorities, and challenges ahead: Nanomaterials in the aquatic environment. Environmental Toxicology and Chemistry 35, 1055–1067. https://doi.org/10.1002/etc.3385

Shen, C., Huang, Y., Li, B., Jin, Y., 2010. Predicting attachment efficiency of colloid deposition under unfavorable attachment conditions. Water Resources Research 46. https://doi.org/10.1029/2010WR009218

Spencer, R. G. M., Bolton, L., & Baker, A. (2007). Freeze/thaw and pH effects on freshwater dissolved organic matter fluorescence and absorbance properties from a number of UK locations. *Water Research*, *41*(13), 2941–2950. doi:10.1016/j.watres.2007.04.012

Sprenger, C., Hartog, N., Hernández, M., Vilanova, E., Grützmacher, G., Scheibler, F., Hannappel, S., 2017. Inventory of managed aquifer recharge sites in Europe: historical development, current situation and perspectives. Hydrogeology Journal 25, 1909–1922. https://doi.org/10.1007/s10040-017-1554-8

Stankus, D. P., Lohse, S. E., Hutchison, J. E., & Nason, J. A. (2011). Interactions between Natural Organic Matter and Gold Nanoparticles Stabilized with Different Organic Capping Agents. *Environmental Science & Technology*, *45*(8), 3238–3244. doi:10.1021/es102603p

Sun, P., Shijirbaatar, A., Fang, J., Owens, G., Lin, D., Zhang, K., 2015. Distinguishable Transport Behavior of Zinc Oxide Nanoparticles in Silica Sand

and Soil Columns. Science of The Total Environment 505, 189–198. https://doi.org/10.1016/j.scitotenv.2014.09.095

Taghavy, A., Mittelman, A., Wang, Y., Pennell, K.D., Abriola, L.M., 2013. Mathematical Modeling of the Transport and Dissolution of Citrate-Stabilized Silver Nanoparticles in Porous Media. Environmental Science & Technology 130719135526002. https://doi.org/10.1021/es400692r

Thio, B. J. R., Montes, M. O., Mahmoud, M. A., Lee, D.-W., Zhou, D., & Keller, A. A. (2012). Mobility of Capped Silver Nanoparticles under Environmentally Relevant Conditions. *Environmental Science & Technology*, *46*(13), 6985–6991. doi:10.1021/es203596w

Thurman, Earl M., & Malcolm, R. L. (1981). Preparative isolation of aquatic humic substances. *Environmental Science & Technology*, *15*(4), 463–466. doi:10.1021/es00086a012

Tipping, E., & Higgins, D. C. (1982). The effect of adsorbed humic substances on the colloid stability of haematite particles. *Colloids and Surfaces*, *5*(2), 85–92. doi:10.1016/0166-6622(82)80064-4

Tiraferri, A., & Borkovec, M. (2015). Probing effects of polymer adsorption in colloidal particle suspensions by light scattering as relevant for the aquatic environment: An overview. *Science of The Total Environment*, *535*(Supplement C), 131–140. doi:10.1016/j.scitotenv.2014.11.063

Tolaymat, T.M., El Badawy, A.M., Genaidy, A., Scheckel, K.G., Luxton, T.P., Suidan, M., 2010. An evidence-based environmental perspective of manufactured silver nanoparticle in syntheses and applications: a systematic review and critical appraisal of peer-reviewed scientific papers. Sci. Total Environ. 408, 999–1006. https://doi.org/10.1016/j.scitotenv.2009.11.003

Tong, M., Li, X., Brow, C. N., & Johnson, W. P. (2005). Detachment-Influenced Transport of an Adhesion-Deficient Bacterial Strain within Water-Reactive Porous Media. *Environmental Science & Technology*, *39*(8), 2500–2508. doi:10.1021/es049013t

Torkzaban, S., Wan, J., Tokunaga, T. K., & Bradford, S. A. (2012). Impacts of bridging complexation on the transport of surface-modified nanoparticles in saturated sand. *Journal of Contaminant Hydrology*, *136–137*, 86–95. doi:10.1016/j.jconhyd.2012.05.004

Tripathi, D. K., Tripathi, A., Shweta, Singh, S., Singh, Y., Vishwakarma, K., et al. (2017). Uptake, Accumulation and Toxicity of Silver Nanoparticle in Autotrophic Plants, and Heterotrophic Microbes: A Concentric Review. *Frontiers in Microbiology*, *08*. doi:10.3389/fmicb.2017.00007

Tripathi, S., Champagne, D., Tufenkji, N., 2012. Transport Behavior of Selected Nanoparticles with different Surface Coatings in Granular Porous Media coated with Pseudomonas aeruginosa Biofilm. Environ. Sci. Technol. 46, 6942–6949. https://doi.org/10.1021/es202833k

Troester, M., Brauch, H.-J., & Hofmann, T. (2016). Vulnerability of drinking water supplies to engineered nanoparticles. *Water Research*, *96*, 255–279. doi:10.1016/j.watres.2016.03.038

Tufenkji, N., Elimelech, M., 2004. Deviation from the Classical Colloid Filtration Theory in the Presence of Repulsive DLVO Interactions. Langmuir 20, 10818–10828. https://doi.org/10.1021/la0486638

Turkevich, J., Stevenson, P.C., Hillier, J., 1951. A study of the nucleation and growth processes in the synthesis of colloidal gold. Discussions of the Faraday Society 11, 55–75. https://doi.org/10.1039/df9511100055

Van Hoecke, K., De Schamphelaere, K., Van Der Meeren, P., Smagghe, G., & Janssen, C. (2011). Aggregation and ecotoxicity of CeO2 nanoparticles in synthetic and natural waters with variable pH, natural organic matter concentration and ionic strength. *ENVIRONMENTAL POLLUTION*, *159*(4), 970–976. doi:http://dx.doi.org/10.1016/j.envpol.2010.12.010

Vance, M.E., Kuiken, T., Vejerano, E.P., McGinnis, S.P., Hochella, M.F., Rejeski, D., Hull, M.S., 2015. Nanotechnology in the real world: Redeveloping the nanomaterial consumer products inventory. Beilstein J Nanotechnol 6, 1769–1780. https://doi.org/10.3762/bjnano.6.181

Vermeer, A. W. P., & Koopal, L. K. (1998). Adsorption of Humic Acids to Mineral Particles. 2. Polydispersity Effects with Polyelectrolyte Adsorption. *Langmuir*, *14*(15), 4210–4216. doi:10.1021/la970836o

Verwey, E. J. W., & Overbeek, J. T. G. (1948). *Theory of the Stability of Lyophobic Colloids: The interaction of Sol Particles Having an Electric Double Layer*. Amsterdam: Elsevier.

Wang, D., Jaisi, D. P., Yan, J., Jin, Y., & Zhou, D. (2015). Transport and Retention of Polyvinylpyrrolidone-Coated Silver Nanoparticles in Natural Soils. *Vadose Zone Journal*, *14*(7). doi:10.2136/vzj2015.01.0007

Weggler-Beaton, K., Graham, R.D., McLaughlin, M.J., 2003. The influence of low rates of air-dried biosolids on yield and phosphorus and zinc nutrition of wheat (Triticum durum) and barley( Hordeum vulgare). Soil Res. 41, 293–308. https://doi.org/10.1071/sr02074

Weishaar, J. L., Aiken, G. R., Bergamaschi, B. A., Fram, M. S., Fujii, R., & Mopper, K. (2003). Evaluation of Specific Ultraviolet Absorbance as an Indicator of the Chemical Composition and Reactivity of Dissolved Organic Carbon. *Environmental Science & Technology*, *37*(20), 4702–4708. doi:10.1021/es030360x

Wigger, H., Hackmann, S., Zimmermann, T., Köser, J., Thöming, J., & von Gleich, A. (2015). Influences of use activities and waste management on environmental releases of engineered nanomaterials. *Science of The Total Environment*, *535*, 160–171. doi:10.1016/j.scitotenv.2015.02.042

Yan, N.D., 1979. Phytoplankton community of an acidified, heavy metal—Contaminated lake near Sudbury, Ontario: 1973–1977. Water Air Soil Pollut 11, 43–55. https://doi.org/10.1007/BF00163517

Yang, K., Lin, D., & Xing, B. (2009). Interactions of Humic Acid with Nanosized Inorganic Oxides. *Langmuir*, *25*(6), 3571–3576. doi:10.1021/la803701b

Yin, Y., Shen, M., Tan, Z., Yu, S., Liu, J., & Jiang, G. (2015). Particle Coating-Dependent Interaction of Molecular Weight Fractionated Natural Organic

Matter: Impacts on the Aggregation of Silver Nanoparticles. *Environmental Science & Technology*, *49*(11), 6581–6589. doi:10.1021/es5061287

Zhang, H., Zhang, C., 2014. Transport of silver nanoparticles capped with different stabilizers in water saturated porous media. Journal of Materials and Environmental Science 5, 231–236.

Zhang, T., Murphy, M., Yu, H., Huh, C., Bryant, S.L., 2016. Mechanistic Model for Nanoparticle Retention in Porous Media. Transport in Porous Media 115, 387–406. https://doi.org/10.1007/s11242-016-0711-1

Zirkler, D., Lang, F., Kaupenjohann, M., 2012. “Lost in filtration”—The separation of soil colloids from larger particles. Colloids and surfaces.

# 8 Danksagung

Eine Doktorarbeit zu schreiben ist ein Projekt, das viel Durchhaltevermögen und Motivation benötigt. Diese positive Energie für alle Experimente, Auswertungen, Entwürfe, Neufassungen, Manuskripte usw. verdanke ich ganz wesentlich meiner unermüdlichen Betreuerin Dr. Sondra Klitzke. Sie war es nie leid, meine kleinen und größeren Fragen zu beantworten, Diskussionen zu führen und damit meine Gedanken und Taten in die richtige Richtung zu lenken. Für diese Geduld und Wertschätzung, die sie mir von Beginn an entgegengebracht hat, möchte ich ihr von Herzen danken. Sie hat diese erste Phase meines Berufslebens ganz wesentlich geprägt und mir das nötige Selbstvertrauen gegeben, mich auch an schwierige Aufgaben heranzuwagen und wissenschaftliche Fragestellungen als lösbare Herausforderungen zu erkennen und zu schätzen.

Während Sondra Klitzke mit ihrer engen Betreuung dafür gesorgt hat, dass ich stets Energie fand, auch schwierige Situationen anzugehen und letztlich zu meistern, war Prof. Martin Kaupenjohann eine Quelle der Inspiration für mich, um aus den Tiefen meines Themas wieder an die Oberfläche zu kommen und den Überblick für das große Ganze zu behalten. Die Gespräche mit ihm haben Türen zu neuen Ideen geöffnet. Sein umfassendes Wissen zu allen denkbaren bodenchemischen Fragestellungen im Laufe meiner Promotion nutzen zu können, war von unschätzbarem Wert für die nun vorliegende Arbeit.

Neben der großartigen fachlichen Betreuung durch Sondra Klitzke und Martin Kaupenjohann bin ich jedoch mindestens ebenso dankbar für die Menschlichkeit, Aufrichtigkeit, Offenheit und persönliche Wertschätzung, mit der mir beide begegnet sind. Erst dies hat die Zeit der Promotion zu einem unvergesslichen Lebensabschnitt gemacht, in dem ich meine Neugier auf die Welt der Kolloide und Bodenchemie, ja die Umweltwissenschaft im Allgemeinen entdecken konnte. Mit der Begeisterung, die beide stets für meine Arbeit zeigten, haben sie mich angesteckt und meinen Forschergeist geweckt.

Zudem wäre meine Forschung kaum von Erfolg gekrönt gewesen, hätte es nicht die Forschergruppe Internano gegeben, in der nicht nur spannende Workshops und Meetings organisiert wurden, die stets ein Quell der Inspiration für mich waren, sondern in der ein beständiger Austausch an Ideen, Methoden und Erkenntnissen

bestand. Insbesondere Dr. George Metreveli und Dr. Allan Philippe bin ich sehr dankbar, dass sie mich mit ihrer Erfahrung und ihren Ideen unterstützt haben und jederzeit ein offenes Ohr für mich hatten. Aber auch die gemeinsamen Projekte mit Sandra Kurtz, Dr. Frederic Leuther und Simon Lüderwald haben mich während meiner Experimente ganz besonders motiviert. Ich bin ihnen sehr dankbar für die großartige und respektvolle Zusammenarbeit, sei es in Experimenten oder während des Organisierens unseres Abschlussworkshops.

Rebekka Meier, Sebastian Knödler, Prof. Friederike Lang und Dr. Helmer Schack-Kirchner von der Universität Freiburg möchte ich für die gemeinsame Arbeit an dem herausfordernden und selten einfachen Projekt zu Silberionenverfügbarkeit in Böden danken. Trotz der vielen Hürden und einer letztlich schwer umsetzbaren Methode haben wir immer spannende Diskussionen geführt und gemeinsam neue Ideen entwickelt. Rebekka und Sebastian bin ich ganz besonders dankbar für die unermüdliche Arbeit an oftmals schwierigen Laborversuchen, die großartige Datenauswertung und den stets herzlichen Empfang in Freiburg.

In den Laboren des Umweltbundesamtes und der TU Berlin hatte ich wertvolle Unterstützung, ohne deren Hilfe und Einsatzbereitschaft kein einziges Experiment hätte stattfinden können. Ich konnte bis zum Ende meiner Arbeit immer wieder nur staunen über die Hilfsbereitschaft, Motivation und den Einsatz, mit dem Silke Pabst meine Probenmengen aufgeschlossen und nebenamtlich ein ganzes Labor geleitet hat und zudem noch wertvolle Ideen für die Umsetzung von Experimenten beigesteuert hat. An Optimismus, Fleiß und Kollegialität von Maike Mai werde ich mir in meinem künftigen Berufsleben versuchen ein Beispiel nehmen. Zudem möchte ich Claudia Kuntz, Iris Pieper, Eduard Sandyk, Sabine Rautenberg und Sabine Dumke für ihre stete Unterstützung im Labor und am Versuchsstand danken.

Meinen WiMi-Kollegen an der TU Berlin und dem Umweltbundesamt gehört nicht nur ein Dank dafür, dass sie jederzeit ein offenes Ohr für meine wissenschaftlichen Fragestellungen hatten, sondern vor allem dafür, dass sie mir während meiner Zeit in Berlin Rückhalt, Optimismus, viele tolle Erlebnisse und Freundschaft gegeben haben. Ich werde meine Jahre in Berlin wegen euch in wunderbarer Erinnerung behalten, denn ich habe von euch viel über Freundschaft, Empathie, Gelassenheit und Toleranz gelernt. Danke, Antonia, Wilhelm, Lisa, Katja, Fredi und Urs!

Am Ende der Danksagung folgen nun die wichtigsten Menschen in meinem Leben, ohne die natürlich die Doktorarbeit in ihrer heutigen Form nie entstanden wäre, die aber noch vielmehr mein gesamtes Dasein prägen und wohl am meisten abbekommen haben von allen positiven und negativen Gefühlen, die die Promotion hervorgerufen hat. Dies sind meine Eltern Sonja und Lars, die sich stets mit Interesse und Anteilnahme meine Erfahrungen angehört haben und mir das Gefühl gegeben haben, dass die Promotion eben auch „nur Arbeit“ und kein Lebensinhalt ist- eine wichtige Voraussetzung, um unbeschwert und mit Freude der Forschung nachgehen zu können. Mein großer Dank gilt zudem meinem Lebensgefährten Torsten Klinger, der sich jeden Abend meine neuen Erkenntnisse oder Frustrationen des Tages geduldig und voll guten Zuspruchs angehört und mich anschließend durch tausend kleine und größere Dinge, die das Leben lebenswert machen, abgelenkt hat. Das Wissen, dass diese Menschen vollstes Vertrauen in meine Fähigkeiten hatten, eine Promotion zu bewältigen, hat mich in jedem Moment begleitet und mir Kraft und Selbstvertrauen gegeben.